Construction of Nanoscale Coordination Systems by Accumulating Metal-Containing Macrocycles

Masaru Aoyagi

DOCTOR OF PHILOSOPHY

Department of Structural Molecular Science
School of Mathematical and Physical Science
The Graduate University for Advanced Studies

1999

Contents

Chapter 1

Introduction and General Summary

1.1 Introduction

Macrocycles have been playing an important role in the development of host-guest chemistry, molecular recognition chemistry, and supramolecular chemistry in expectation of showing unique abilities for separation, chemical sensing, and catalysis.[1] Despite their potential utilities and abilities, however, these compounds have not been employed in practical use due to synthetic difficulties: i.e., covalent synthesis of macrocycles often requires low yield steps. Recently, macrocyclic frameworks have been constructed quite efficiently through *molecular self-assembly,* which is featured by spontaneous generation of highly ordered structures from well-designed small components under thermodynamic conditions. For the self-assembly process, non-covalent bond such as coordinate bond and hydrogen bond are used for joining subunits. Particularly, coordinate bond is quite effective non-covalent bond for the construction of discrete molecules including macrocycles because of their versatile bond geometry, defined bond angles, and moderate bond strength. In fact, a metal-containing macrocycle, which consists of two Cu(II) and two diketonate ligands and is able to encapsulate guest molecules, was first reported by Maverick in 1984.[2] After that, variety of metal-containing macrocycles have been constructed by molecular self-assembly.[3,4] However, further accumulation of the self-assembled macrocycles have been hardly investigated. Thus, the author paid his special attention to the concept of "*assembly of assemblies*", where self-assembled structures are further converted into more complex systems, and designed the accumulation of macrocyclic complexes into higher ordered structures. The construction of such hierarchical assembled systems by the accumulation of macrocyclic units is the author's basic concept throughout the work in this thesis (Figure 1). Accordingly, the present thesis describes the studies on the construction of various finite and infinite molecular architectures by accumulating metal-containing macrocyclic subunits.

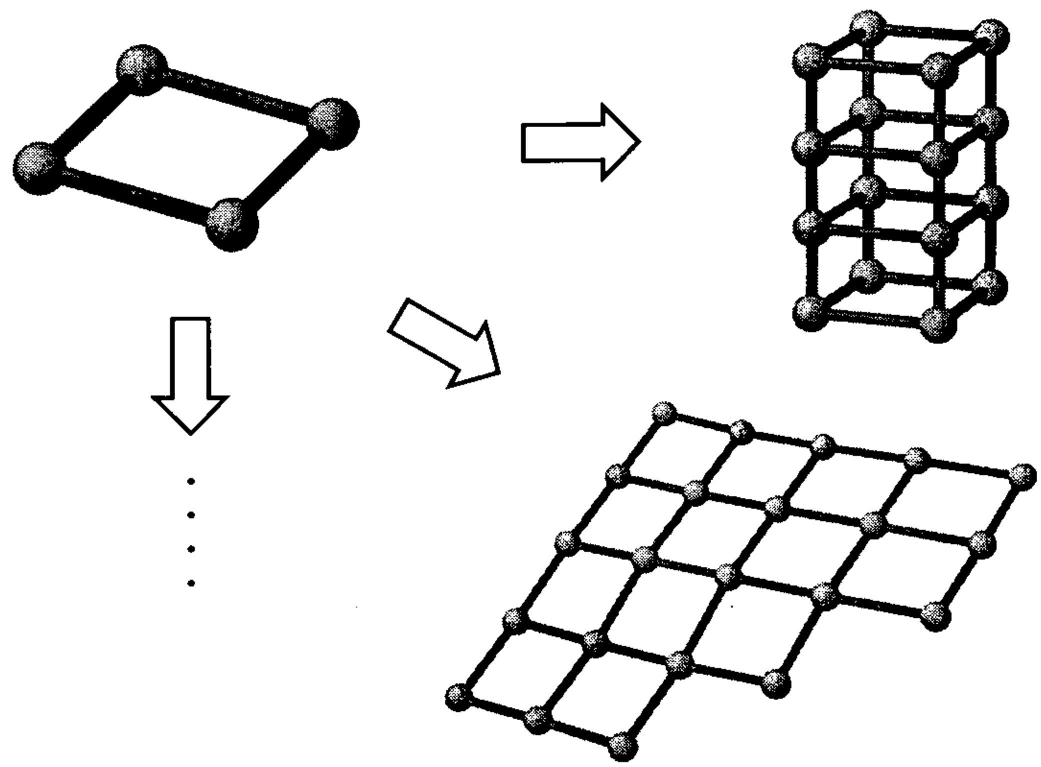

Figure 1. The accumulation of self-assembled macrocyclic units into higher ordered structures: the author's basic concept throughout the thesis.

1.2 Accumulation of M_4L_4 molecular square

Among many metal-containing macrocycles, M_4L_4 (M: metal, L: ligand) square complexes, in which metal provides 90 degree at every corner of the square, are one of the simplest and hence well-studied macrocyclic coordination compounds.[4c,5]

Particularly Pd(II)-(4,4'-bipyridine) square complex **1a** is a prototypical M_4L_4 compound (Figure 2a). The author's first study was focused on this structure, and he planed the accumulation of this square motif into infinite systems. A two-dimensional accumulation of square motif was first observed in an interpenetrated complex **2a** prepared from $Zn(PF_6)_2$ and 4,4'-bipyridine (4,4'-bpy).[6] Later, complexation of $Cd(NO_3)_2$ with

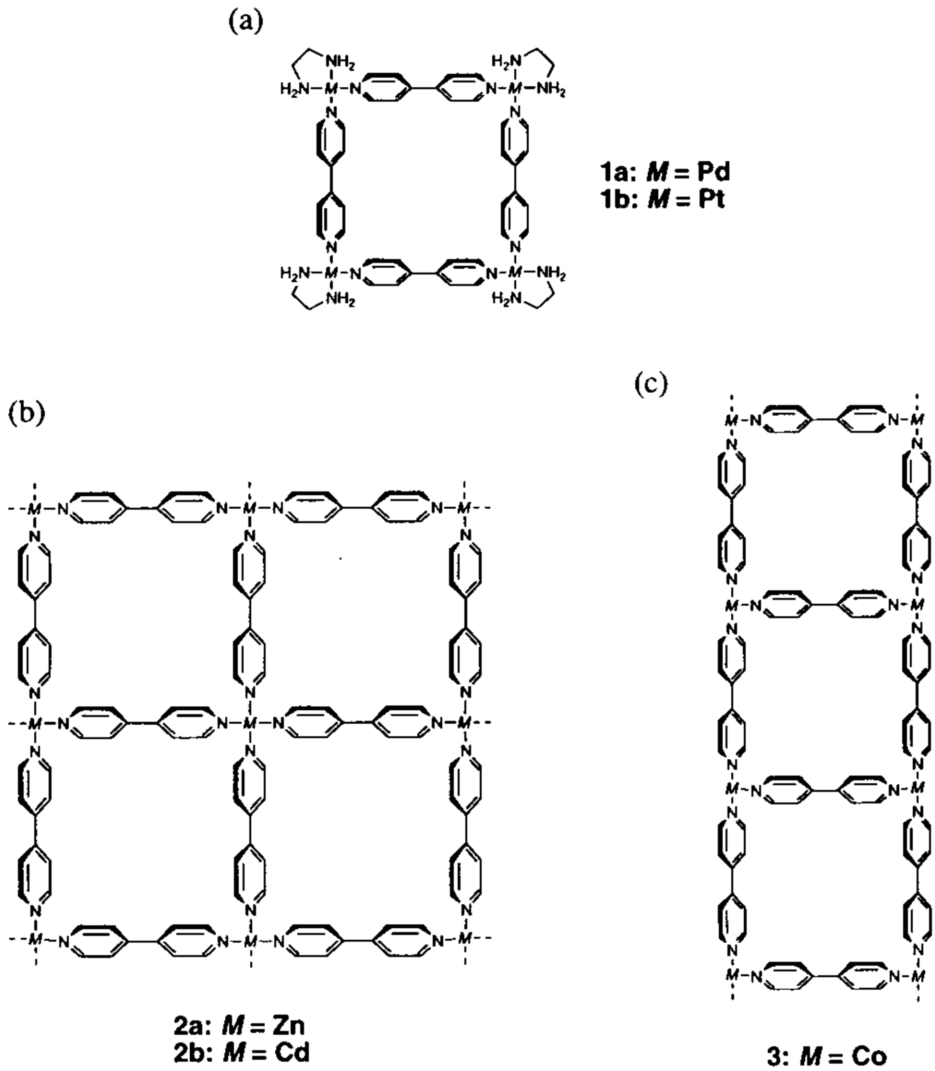

Figure 2. (a) Coordination molecular square 1, and accumulation of the square motif into (b) two-dimensional grid, and (c) one-dimensional ladder.

4,4'-bpy in the presence of an organic guest provided the first example of a non-interpenetrated grid sheet **2b** which accommodates the guest in the square grid cavity (Figure 2b).[7] The square motif also propagated in one-dimension by using cobalt metal center: Co^{2+} ions coordinate to 4,4'-bpy ligands to form the siderails and the rungs of a one-dimensional ladder $[Co(4,4'\text{-bpy})_{1.5}(NO_3)_2]$ (Figure 2c).[8]

Concerning the non-interpenetrated grid **2a**, a question arises if the same grid sheet structure is obtained even in the absence of a guest. The construction of guest-free grid is particularly interesting to develop porous, zeolite-like coordination compounds. Thus, the author first examined accumulation of the square by combining $Cd(NO_3)_2$ and 4,4'-bpy without guest molecules, as described in Chapter 2. As a result, the variation of L/M ratios and concentrations led to the formation of three-different structures: two-dimensional $\{[Cd(4,4'\text{-bpy})_2(H_2O)_2](NO_3)_2{\cdot}4H_2O\}_n$ (**4**), one-dimensional $\{[Cd(4,4'\text{-bpy})_3(H_2O)_2](NO_3)_2{\cdot}2(4,4'\text{-bpy}){\cdot}4.5H_2O\}_n$ (**5**), and zero-dimensional $[Cd_2(4,4'\text{-bpy})_5(H_2O)_4(NO_3)_2](NO_3)_2{\cdot}4H_2O$ (**6**) complexes. The complex **4** possesses a non-interpenetrated fused square grid network in which the cavities are occupied by water and nitrate ions (Figure 3a). The structure of the framework is similar to that of a guest-encapsulated square grid complex **2b**, which is previously reported, except shortened interlayer distance. The one-dimensional polymer **5** and zero-dimensional structure **6** form two-dimensional networks with the assistance of O-H···N hydrogen bonds (Figure 3b, c). The zero-dimensional structure was composed of two Cd^{2+} centers, four monodentate 4,4'-bpy ligands, and a bridging bidentate 4,4-bpy. Whereas ladder and square grid structures are one- and two-dimensional extension of a square structure within a plane.

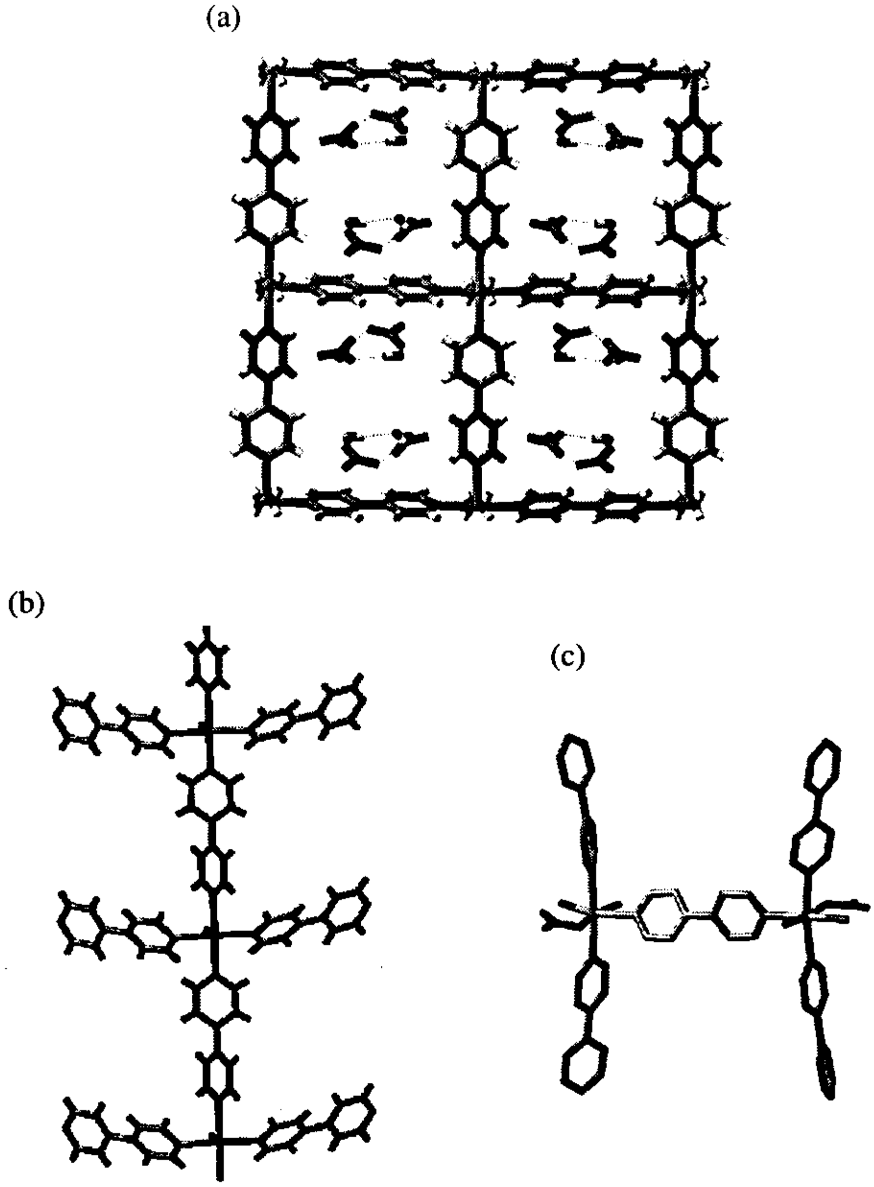

Figure 3. Crystal structure of (a) two-dimensional polymer **4**, (b) one-dimensional polymer **5**, and (c) bimetallic complex **6**.

In Chapter 3, the author studied the accumulation of square complex $\mathbf{1}^{8+}$ along its vertical direction via formation of one-dimensional ···Pt(II)···X-Pt(IV)··· (X: halogen) mixed-valence complexes, that are easily obtained by mixing $Pt(II)L_4$ and $Pt(IV)L_4X_2$ salts and are of special interest because of their specific physical properties.[9] The reaction of $\mathbf{1b}^{8+}$ with cationic Pt(IV) complex, $[PtBr_2(en)_2]^{2+}$ ($\mathbf{7}^{2+}$), afforded a 1:3 complex $\mathbf{1b}\cdot(\mathbf{7})_3{}^{14+}$. Crystallographic analysis of this complex showed that two moieties of $\mathbf{7}^{2+}$ bridged at the cis corner of $\mathbf{1b}^{8+}$ making a stair-like infinite network, whereas another moiety of $\mathbf{7}^{2+}$ was accommodated in the cavity of $\mathbf{1b}^{8+}$ (Figure 4). On the other hand, complexation of **1** with anionic Pt(IV) complex, $PtX_6{}^{2-}$ ($\mathbf{8}^{2-}$; **a**: X = Cl, **b**: X = Br), afforded a 1:4 complex $\mathbf{1}\cdot(\mathbf{8})_4$. UV-vis observations suggested the formation of a linear tube structure, in which each corner of $\mathbf{1}^{8+}$ is bridged by the linear X-Pt-X motif of $\mathbf{8}^{2-}$.

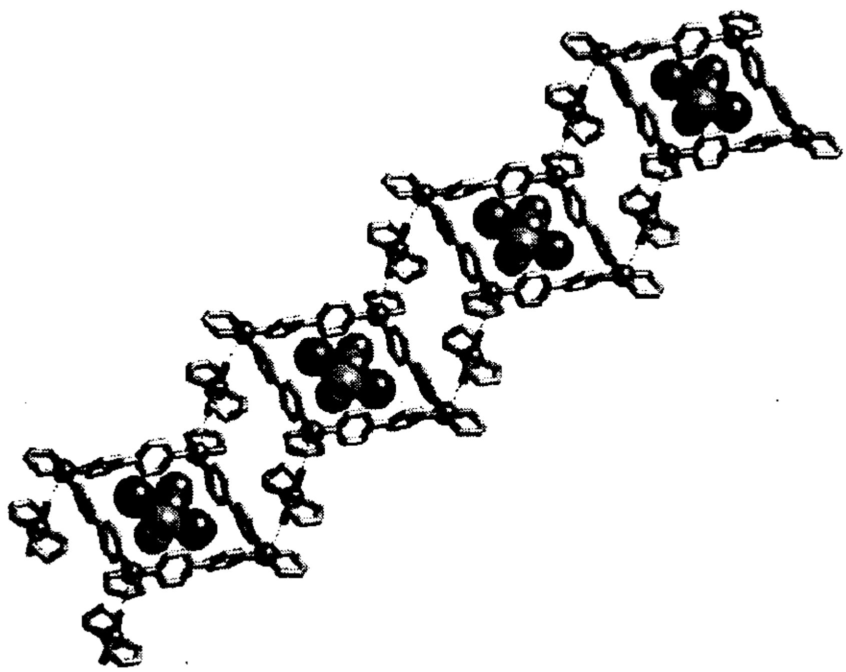

Figure 4. Crystal structure of stair-like infinite network $\mathbf{1b}\cdot(\mathbf{7})_3$.

1.3 Assembly of molecular nanotubes and polytubes

One of the most interesting structures derived from macrocyclic units is tubular assemblies. In fact, tubular polymers, which are capable of ion transportation and catalysis, have been constructed by linking macrocyclic compounds. Cyclodextrin (CD)-

based nanotube was reported by Harada et al.[10] CDs were first assembled into polyrotaxane by threading them on ploy(ethylene glycol) (PEG). The adjacent CD units in polylotaxane were crosslinked to give a molecular tube (Figure 5a). The molecular tube catalyzed formation of I_3^- from KI and I_2 in solution. Another interesting macrocycle-based tubular structure is a peptide nanotube: cyclic D,L-α-peptides and β-peptides were assembled into large tubular aggregates through backbone-backbone hydrogen bonding (Figure 5b).[11] The cyclic peptide bearing appropriate hydrophobic residues formed trans-membrane ion channels on lipid bilayers and transported alkali metal ions and even glucose molecule across the bilayers.[12] However, the degree of polymerization of these tubes are uncertain and, therefor, precise control of the length of tubes have not been realized yet.

(a) (b)

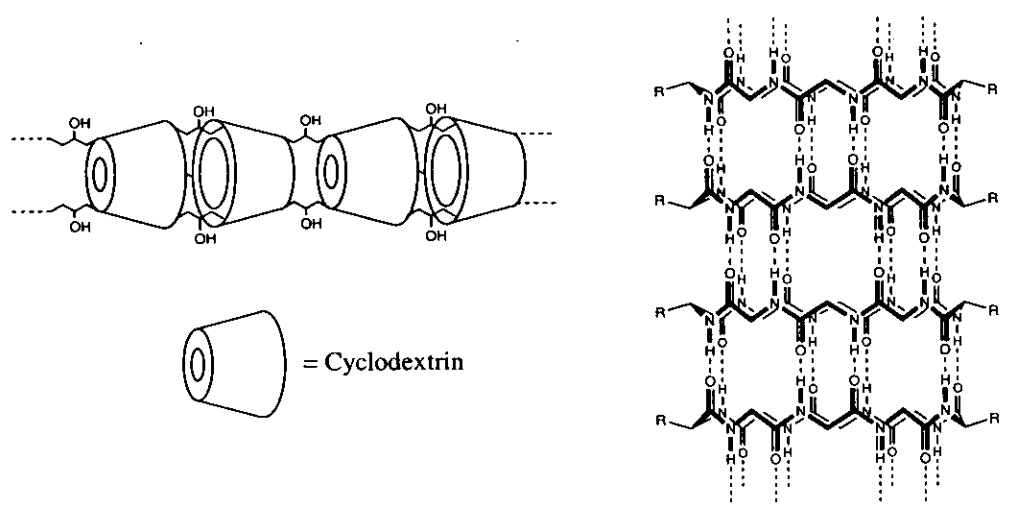

Figure 5. (a) Cyclodextrin nanotube. (b) Peptide nanotube.

In order to control the tube length precisely, the author modified his basic strategy for constructing tubes via assembly of macrocycles. Whereas previous methods all involve the construction of cyclic framework followed by accumulation along the axis of the macrocycle (Figure 6a), the author's new strategy is featured by the initial linking of small units along the axis followed by cyclization (Figure 6b).

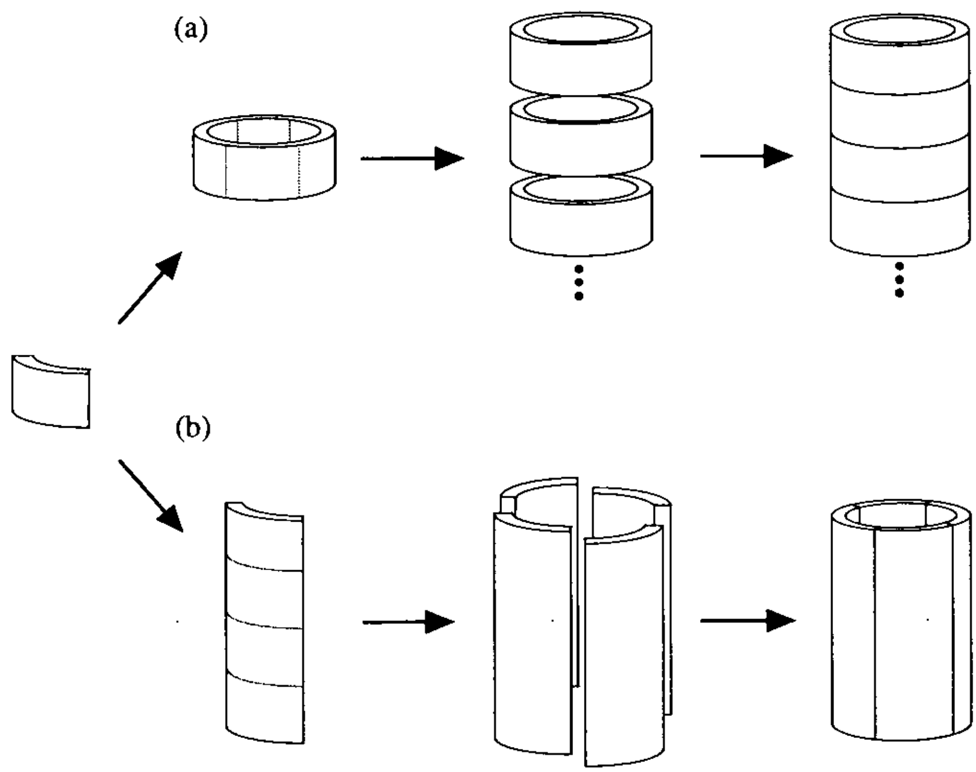

Figure 6. Strategies for constructing nanotubes.

Thus, in Chapter 4, coordination nanotubes, which possess very stable and discrete frameworks, were constructed by linking oligo(3,5-pyridine)s (pentakis: **9a**, tetrakis: **9b**, tris: **9c**) with a cis-protected Pd(II) building block, (en)Pd(NO_3)$_2$ (Figure 7). This transformation was in fact accomplished with the remarkable template effect of biphenyl derivatives. Thus, the reaction of **9** with (en)Pd(NO_3)$_2$ first resulted in the formation of uncharacterizable products. However, the addition of sodium 4,4'-biphenylenedicarboxylate to the solution induced the smooth assembly of nanotubes **10a**-**10c** wherein four molecules of **9** were held together with six to ten Pd(II) units. A nanotube structure **10c** templated by a guest was confirmed by an X-ray crystallographic analysis.

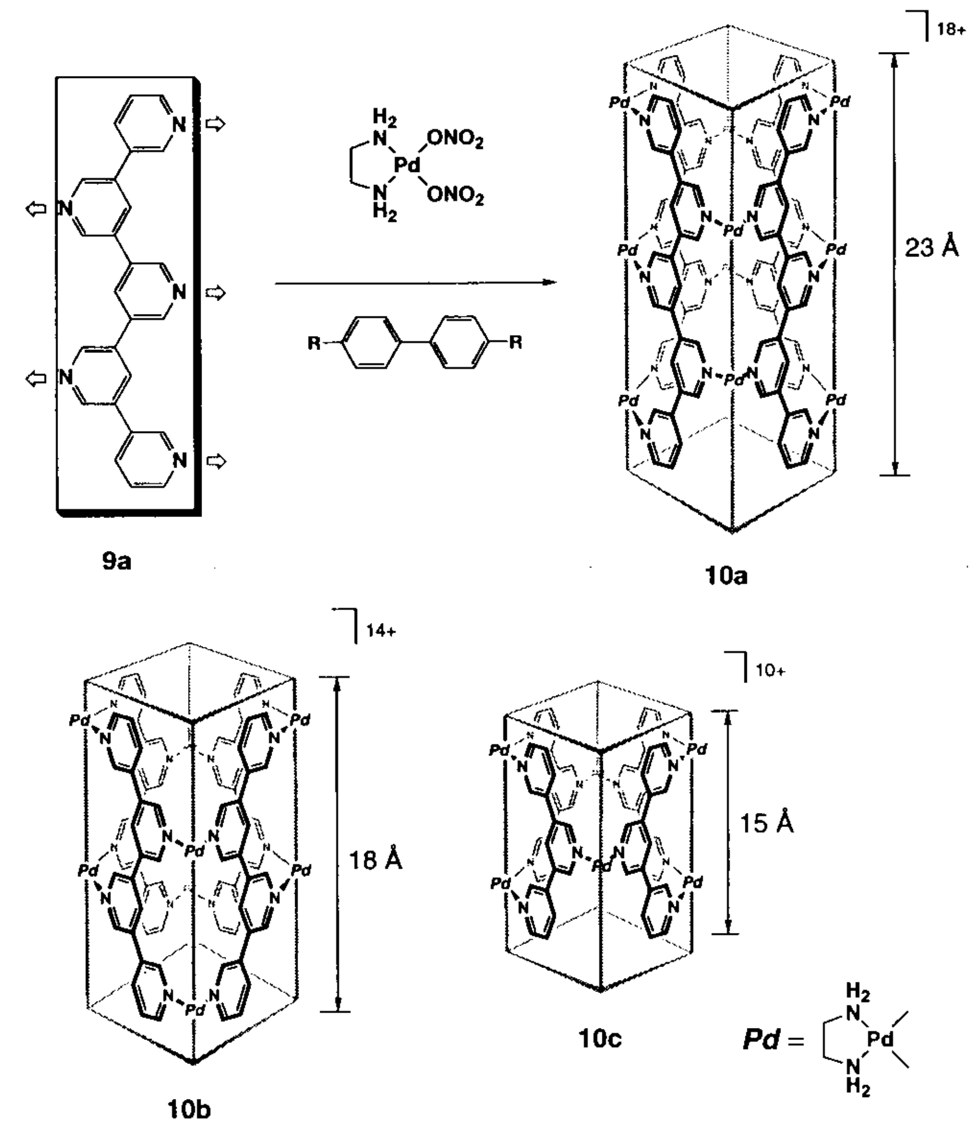

(Template included in the tubes **10a-c** is omitted for clarity.)

Figure 7. Coordination nanotubes **10a-c**.

Reversible guest encapsulation and release process of host-guest complexes is expected to provide application of these complexes to data storage devices[13] and artificial enzymes. In Chapter 5, the dynamics of guest molecule accommodated in the coordination tubes **10a** and **10c** was investigated by variable temperature NMR measurements at different host-guest ratios. As the results, guest molecules were found to shuttle in the tube without flipping at low temperatures, but intermolecularly exchange at elevated temperatures (Figure 8). Coordination nanotube **10b** for which structural isomers can be considerable was isolated as a single isomer by recystallization. The structure of a isomer was confirmed by X-ray crystallography. This single isomer slowly turned into an equilibrium mixture of two structural isomers in aqueous media.

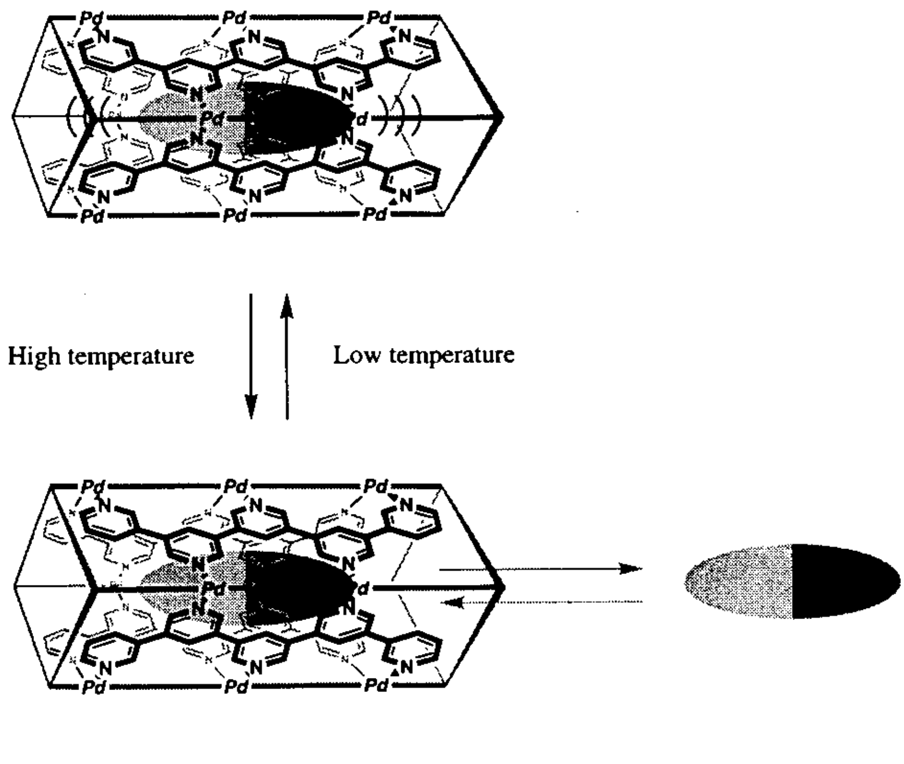

Figure 8. Thermodynamic behavior of guest molecule.

Recently, molecular template synthesis of inorganic[14] and organic-inorganic[15] hybrid porous solid materials were reported as well as that of discrete molecules in solution. To extend the molecular nanotubes into solid materials, in Chapter 6, the formation of the coordination polytubes were examined by combining **9b** and a transition metal (CuI) (Figure 9).

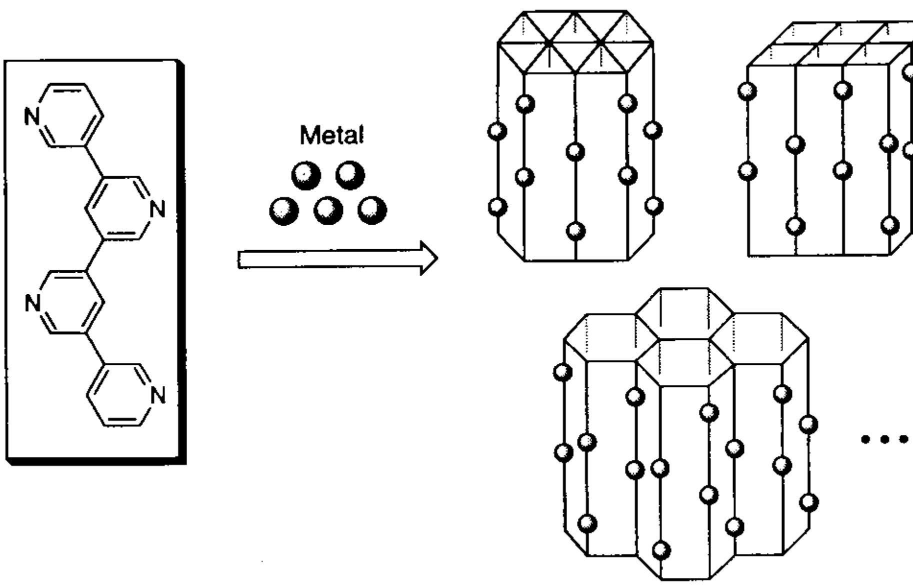

Figure 9. Illustration of polytube assembly.

The X-ray crystallographic analyses showed that two types of non-interpenetration networks that have large porosities were induced by non-aromatic and aromatic guest molecules. A non-aromatic guest CH_3CN induced two-dimensional polytube [**9b**·(Cu_2I_2)]·2G·H_2O (**11**, **G** = CH_3CN) with an accessible porosity of 32% (Figure 10a). On the other hand, aromatic guests such as nitrobenzene or cyanobenzene induced three-dimensional polytube structures [**9b**·(Cu_2I_2)]·2G (**12a**: **G** = nitrobenzene, **12b**: **G** = cyanobenzene) with large accessible porosity of 48% (Figure 10b). The cavities of **11** and **12** were occupied by guest molecules. Thermogravimetric (TG) analysis, IR spectroscopy, and powder X-ray diffraction analysis of **12b** before and after guest removal showed that the polytube framework is kept even after guest removal.

(a)

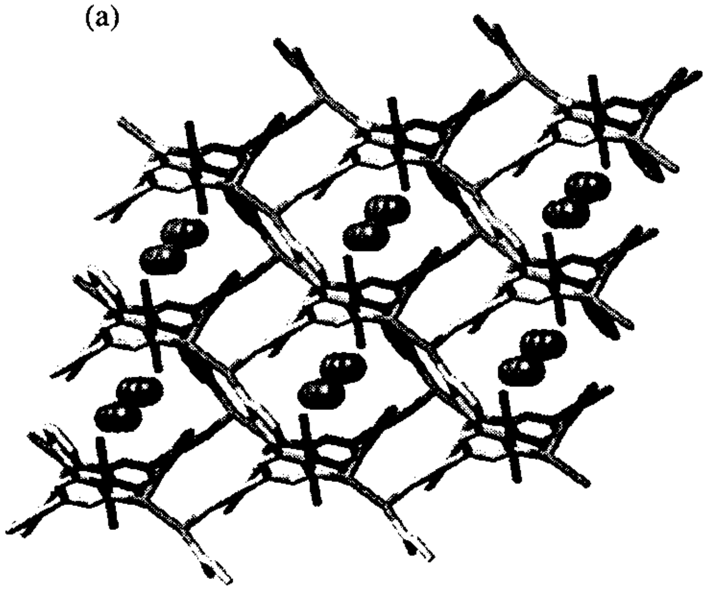

(b)

Figure 10. (a) Crystal structure of the 2D-polytube **11**. (b) Crystal structure of 3D-polytube **12b**.

Reference

(1) *Inclusion Compounds*; Atwood, J. L.; Davies, J. E. D.; MacNicol, D. D., Eds; Academic Press: London, 1991.

(2) Maverick, A. W.; Klavetter, F. E. *Inorg. Chem.* **1984**, *23*, 4129.

(3) (a) Jones, C. J. *Chem. Soc. Rev.* **1998**, *27*, 289. (b) Fujita, M. *Chem. Soc. Rev.* **1998**, *27*, 471.

(4) (a) Schwabacher, A. W.; Lee, J.; Lei, H. *J. Am. Chem. Soc.* **1992**, *114*, 7597. (b) Hunter, C. A.; Sarson, L. D. *Angew. Chem. Int. Ed. Engl.* **1994**, *33*, 2313. (c) Fujita, M.; Yazaki, J.; Ogura, K. *J. Am. Chem. Soc.* **1990**, *112*, 5645. (d) Fujita, M.; Yazaki, J.; Ogura, K. *Chem. Lett.* **1991**, 1031. (e) Fujita, M.; Nagao, S.; Iida, M.; Ogata, K.; Ogura, K. *J. Am. Chem. Soc.* **1993**, *114*, 1574. (f) Houghton, M. A.; Bilyk, A.; Harding, M. M.; Turner, P.; Hambley, T. W. *J. Chem. Soc., Dalton Trans.* **1997**, 2725. (g) Hasenkopf, B.; Lehn, J.-M.; Boumediene, N.; Dupont-Gervais, A.; Dorsselaer, A. V.; Kneise, B.; Fenske, D. *J. Am. Chem. Soc.* **1997**, *119*, 10956.

(5) (a) Stang, P. J.; Cao, D. H. *J. Am Chem. Soc.* **1994**, *116*, 4981. (b) Stang, P. J.; Olenyuk, B. *Acc. Chem. Res.* **1997**, *30*, 502. (c) C. M. Drain, and J.-M. Lehn, *J. Chem. Soc., Chem. Commun.* **1994**, 2313. (d) Rauter, H.; Hillgeris, E. C.; Erxleben, A.; Lippert, B. *J. Am Chem. Soc.* **1996**, *116*, 616. (e) Slone, R. V.; Yoon, D. I.; Calhoum, R. M.; Hupp, J. T. *J. Am Chem. Soc.* **1995**, *117*, 11813.

(6) Gable, R. W.; Hoskins, B. F.; Robson, R. *J. Chem. Soc., Chem. Commun.* **1990**, 1677.

(7) Fujita, M.; Kwon. Y. J.; Washizu, S.; Ogura, K. *J. Am. Chem. Soc.* **1994**, *116*, 1151.

(8) Losier, P.; Zawartko, M. J.; *Angew. Chem., Int. Ed. Engl.* **1996**, *35*, 2779.

(9) (a) Matsumoto, N.; Yamashita, M.; Kida, S. *Bull. Chem. Soc. Jpn.* **1978**, *51*, 2334. (b) Yamashita, M.; Kida, Y.; Hamaue, Y.; Aoki, R. *Inorg. Chim Acta* **1981**, *52*, 43. (c) Papavassilliou, G. C.; Layek, D. *Z. Naturforsch.* **1982**, *37b*, 1406. (d) Yamashita, M.; Ito, H.; Toriumi, K.; Ito, T. *Inorg. Chem.* **1983** *22*,

1566. (e) Yamashita, M.; Murase, I. *Inorg. Chim. Acta* **1985**, *97*, L43. (f) Yamashita, M.; Murase, I.; Ikemoto, I.; Ito, T. *Chem. Lett.* **1985**, 1133. (g) Toriumi, K.; Yamashita, M.; Kurita, S.; Murase, I.; Ito, T. *Chem. Lett.* **1985**, 1133.

(10) Harada, A.; Li, J.; Kamachi, M. *Nature* **1993**, *364*, 516.

(11) (a) Ghadiri, M. R.; Granja, J. R.; Milligan, R. A.; McRee, D. E.; Khazanovich, N. *Nature* **1993**, *366*, 324. (b) Seebabh, D.; Matthews, J. L.; Meden, A.; Wessels, T.; Baerlocher, C.; McCusker, L. B. *Helv. Chim. Acta* **1997**, *80*, 173.

(12) (a) Ghadiri, M. R.; Granja, J. R.; Buehler, L. K. *Nature* **1994**, *369*, 301. (b) Clark, T. D.; Buehler, L. K.; Ghadiri, M. R. *J. Am. Chem. Soc.* **1998**, *120*, 651. (c) Granja, J. R.; Ghadiri, M. R. *J. Am. Chem. Soc.* **1994**, *116*, 10785.

(13) (a) Anelli, P.-L.; Asakawa, M.; Ashton, P. R.; Bissell, R. A.; Clavier, G.; Kaifer, A. E.; Langford, S. J.; Mattelsteg, G.; Menzer, S.; Philip, D.; Slawin, A. M. Z.; Spencer, N.; Stoddart, J. F.; Tolley, M. S.; Williams, D. J. *Chem. Eur. J.* **1997**, *3*, 1113. (b) Benniston, A. C. *Chem. Soc. Rev.* **1996**, *25*, 427. (c) Lane, A. S.; Leigh, D. A.; Marphy, A. *J. Am. Chem. Soc.* **1997**, *119*, 11092.

(14) (a) Ekambaram, S.; Sevov, S. C. *Angew. Chem., Int. Ed. Engl.* **1999**, *38*, 372. (b) Martin, J. D.; Leafblad, B, R. *Angew. Chem., Int. Ed. Engl.* **1998**, *37*, 3318.

(15) (a) Yaghi, O. M.; Li, G.; Li, H. *Nature* **1995**, *378*, 703. (b) Reineke, T. M.; Eddaoudi, M.; O'Keeffe, M.; Yaghi, O. M. *Angew. Chem., Int. Ed. Engl.* **1999**, *38*, 2590.

Chapter 2

Formation of Two, One, and Zero-Dimensional Coordination Polymers from Cd(II) ion and 4,4'-Bipyridine

Abstract: Complexation of $Cd(NO_3)_2$ with 4,4'-bipyridine (4,4-bpy) gave, depending on the L/M ratios and concentrations, two-dimensional, one-dimensional or zero-dimensional coordination polymers, which were characterized by X-ray crystallography. The two dimensional structure was shown to be a non-interpenetrated square grid network in which the square cavities were occupied by water and nitrate ions. The one-dimensional polymer also formed a two-dimensional network with the assistance of O-H···N hydrogen bonds. The zero-dimensional structure was composed of two Cd^{2+} centers, four monodentate 4,4'-bpy, and a bridging bidentate 4,4-bpy. The networks and the packing of these structures were analyzed in terms of coordination and hydrogen bonds.

2.1 Introduction

The coordination polymeric networks of a transition metal-(4,4'-bipyridine) have been studied intnsively during the last decade.[1] Reprts show that the 4,4'-bipyridine (4,4'-bpy) ligand forms various topological networks with/without altering L/M ratios because of its linear and exobidentate nature. Possible 4,4'-bpy networks include 1D chain,[2-4] ladder,[5] square and hexagonal grid,[6,7] bilayer,[8] and diamondoid[9] structures. These networks have large cavities in their framework and the structures possess the potential for including microporous solid materials (including molecular absorption,[8] heterogeneous catalyst). Among all the networks, a square grid **I** is the prototypical infinite framework.[6] The grid **I** could be regarded as polymer version of a molecular square[10] and was first observed in an interpenetrated complex prepared from $Zn(PF_6)_2$ and 4,4'-bpy.[6a] On the other hand, complexation of $Cd(NO_3)_2$ with 4,4'-bpy in the presence of an organic guest provided the first example of a non-interpenetrated grid sheet **I** which accommodates the guest in the square grid cavity.[6b] Although the crystal structure of the clathrate complex, $[Cd(4,4'\text{-bpy})_2](NO_3)_2 \cdot 2o\text{-}C_6H_4Br_2$, has been solved, the question arises of whether Cd(II)-(4,4'-bpy) complex forms a similar non-interpenetrated framework even in the absence of a guest molecule? In order to address this question, the author further examined the synthesis and metal complexes by combining $Cd(NO_3)_2$ and 4,4'-bpy at various L/M ratios.

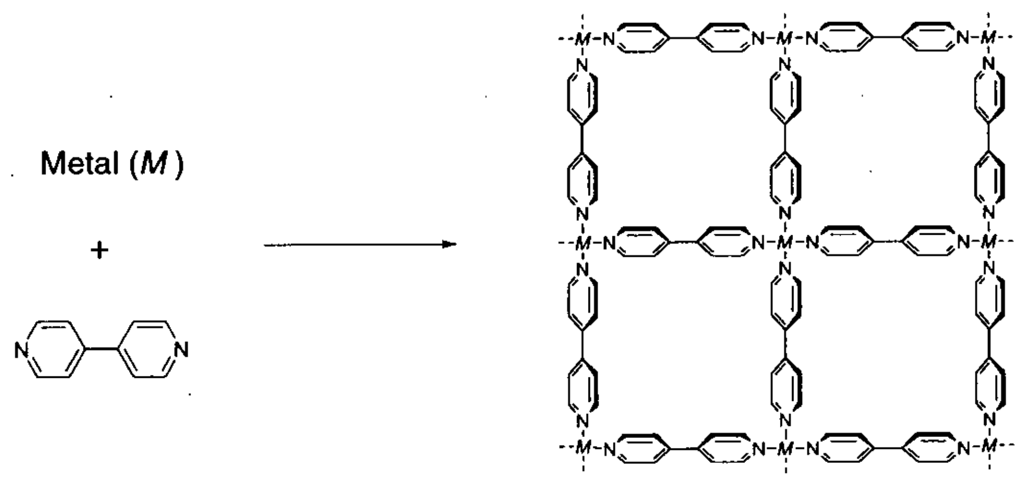

I

Scheme 1. Formation of a square grid from metal ions and 4,4'-bpy.

2.2 Results and Discussion

2.2.1 Reaction of $Cd(NO_3)_2{\cdot}4H_2O$ and 4,4'-bpy

The crystallization experiments have been carried out by increasing the L/M ratio from 1.0 to 4.0 in increments of 0.5 and decreasing the concentration from 200 mM to 20 mM in decrements of 30 mM. The reactions were done by adding aqueous solution of $Cd(NO_3)_2{\cdot}H_2O$ (8 mL) to EtOH solution of 4,4'-bpy (2 mL). Interestingly, the variation of L/M ratios and concentrations led to the formation of three types of structures (Table 1):

$\{[Cd(4,4'\text{-bpy})_2(H_2O)_2](NO_3)_2{\cdot}4H_2O\}_n$ (**1**),

$\{[Cd(4,4'\text{-bpy})_3(H_2O)_2](NO_3)_2{\cdot}2(4,4'\text{-bpy}){\cdot}4.5H_2O\}_n$ (**2**), and

$[Cd_2(4,4'\text{-bpy})_5(H_2O)_4(NO_3)_2](NO_3)_2{\cdot}4H_2O$ (**3**).

Table 1. Selected reaction conditions and products.

	L/M ratio				
[M]	1.0	2.0	2.5	3.0	4.0
200 mM	**1**	**1**	**1**	**1+2**	**1+2**
110 mM	**1**	**1**	**1**	**1+2**	**1+2**
80 mM	**1**	**1**	**1**	**1+2**	**1+2**
50 mM	-	-	**1**	**1+2**	**3**
20 mM	-	-	-	-	-

The structures of the products were characterized by X-ray crystallography. In all three complexes, the Cd-atom has an octahedral coordination, but with different coordination environments. In **1** and **2**, each Cd-atom coordinats four 4,4'-bpy ligands and two water molecules, while in **3**, it coordinates three 4,4'-bpy ligands, one nitrate and two water molecules. The network features and crystal packing will be discussed in the following sections.

2.2.2 Structure of $\{[Cd(4,4'\text{-bpy})_2(H_2O)_2](NO_3)_2 \cdot 4H_2O\}_n$: two-dimensional

The structure of **1** is a two-dimensional layer with no interpenetration and no enclatharation of organic guest molecules (Figure 1a). It has two 4,4'-bpy moieties: one of them sits on the inversion center (labeled as **A**) while the other sits on the glide plane (labeled as **B**). **A** is planar with a 0° interplanar angle between the two pyridine rings, whereas **B** is non-planar with a 40° interplanar angle between the two pyridine rings. Each square cavity of dimension 8 x 8 Å is occupied by two cyclic tetramers that are formed via hydrogen bonding interactions between two nitrates and two solvated water molecules (Figure 1b, O···O: 2.772, 2.774, 2.804, 2.862 Å). Two of these tetramers

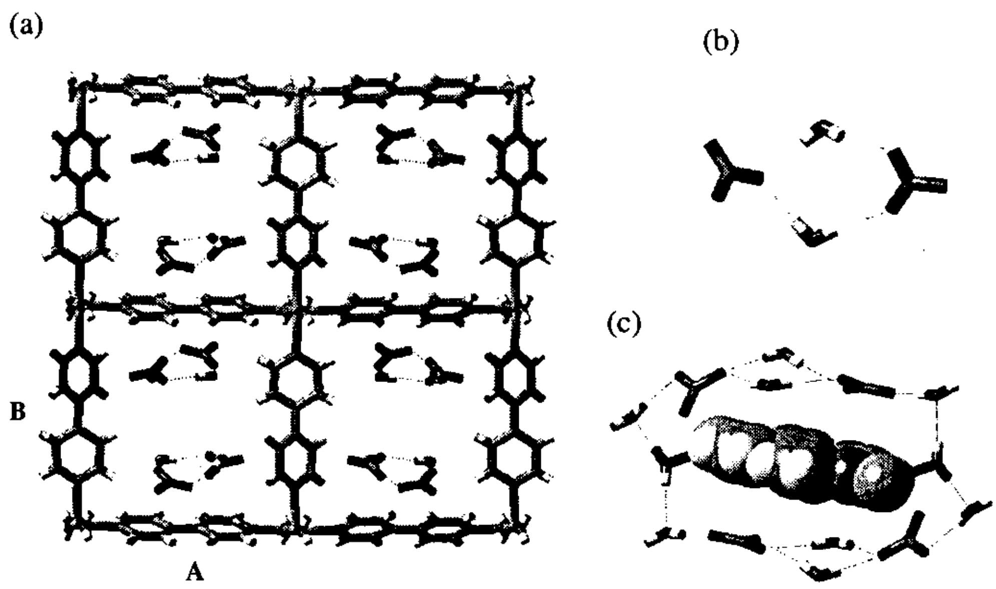

Figure 1. Illustrations for the crystal structure of **1**: (a) Representation of the two-dimensional grid sheet. The nitrate ions and the water molecules in the square cavities. (b) The hydrogen-bonded tetramers of nitrates and water molecules. (c) Representation of the molecular rotaxane via hydrogen bonds. The threading 4,4'-bpy molecule and Cd ions are represented in space filling mode.

further interact with ligated water molecules to form a wheel like hydrogen bonding network around 4,4'-bpy ligand (O···O: 2.678 Å). As a result a rotaxane structure via hydrogen bonds is formed (Figure 1c). Interestingly, the ligated water molecules do not accepted any protons, whereas solvated water molecules accepted one proton.

The 2D layers stack in zigzag (Figure 2a) and slipped (Figure 2b) fashion along the 4,4'-bpy rings **A** and **B**, respectively. Notably, the interlayer separation (4.79 Å) is remarkably smaller than in its clatharate complex (6.30 Å).[6b] The stacking of the grids results in channels that are occupied by the above described nitrate and water tetramers.

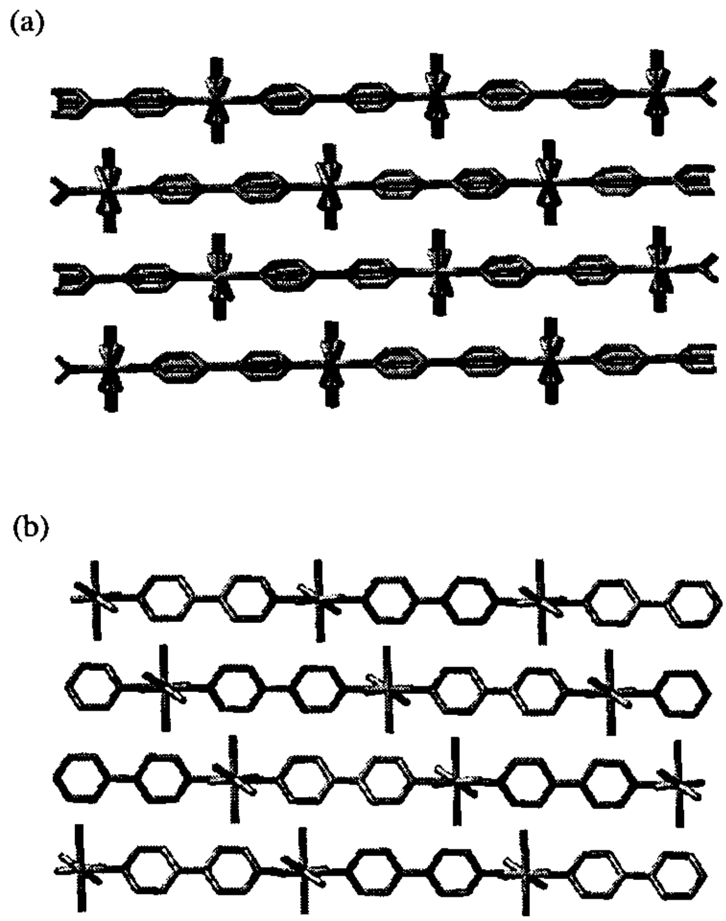

Figure 2. (a) Stacking of grid sheets in zigzag fashion. A view along 4,4'-bpy **B**. (b) Stacking of grid sheets in slipped fashion. A view along 4,4'-bpy **A**.

2.2.3 Structure of {[$Cd(4,4'\text{-}bpy)_3(H_2O)_2](NO_3)_2 \cdot 2(4,4'\text{-}bpy) \cdot 4.5H_2O\}_n$: One-dimensional

The structure **2** has three coordinated and two enclatharated 4,4'-bpy molecules per metal atom. One of the coordinated 4,4'-bpy ligands serves as a bifunctional ligand to form a one-dimensional network, while the other two form side arms for the one-dimensional chain by acting as mono-functional ligands (Figure 3a). This structure could be termed as a molecular antenna, a prototypical structure of the railroad polymer.[2c] The antennas join together via O-H···N hydrogen bonds which are formed between ligated H_2O molecules and uncoordinated N-atoms of 4,4'-bpy (Figure 3b, O···N: 2.795, 2.818 Å). The recurrence of the cyclic ···H_2O-Cd-(4,4'-bpy) ···H_2O-Cd-(4,4'-bpy) ···

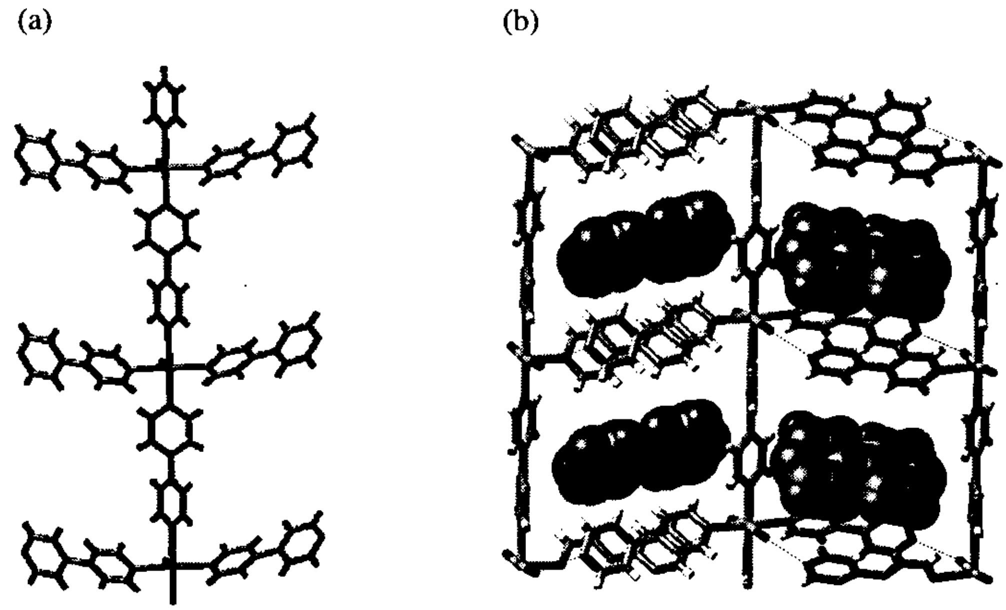

Figure 3. Illustrations for the crystal structure of **2**: (a) Representation of the one-dimensional chain. (b) Representation of the two-dimensional hydrogen bonded network. The guest 4,4'-bpy molecules are represented in space filling mode.

pattern suggests that it can be used as a supramolecular synthon in crystal engineering.[11] As a result of the hydrogen bonding, a two-dimensional layer was formed with the cavities (8 x 9 Å) that are occupied by guest 4,4'-bpy molecules (Figure 2b). These layers stack along the *a*-axis in a zigzag fashion with an interlayer separation of 8.79 Å. The second guest 4,4'-bpy molecule lies in between the layers via a plethora of aromatic interactions.

2.2.4 Structure of $[Cd_2(4,4'\text{-bpy})_5(H_2O)_4(NO_3)_2](NO_3)_2 \cdot 4H_2O$: zero-dimensional

The structure **3** is a bimetallic complex. The two coordinated water molecules have the cis geometry around the Cd-atom (Figure 4a). The asymmetric unit contains two Cd-atoms, five 4,4'-bpy ligands, coordinated and non-coordinated nitrate ions and four water molecules. The Cd-O and Cd-N bond lengths vary from 2.291 to 2.384 Å and from 2.323 to 2.365 Å, respectively.

The bond distances on Cd1 and Cd2 differ only in the second decimal point. The crystal structure lacks, however, an inversion center because of the complexity of the three-dimensional hydrogen bond network. Interestingly, the network contains a one-dimensional chain that is formed by O-H···N hydrogen bonds (O···N: 2.732, 2.757 Å) between the ligated water molecules and the terminal N-atom of 4,4'-bpy (Figure 4b). The 4,4'-bpy ligands also interact via $\pi \cdots \pi$ interactions. These one-dimensional chains form a three-dimensional network by joining each other via tetramers of two water molecules and two nitrates (Figure 4c, O···O: 2.798, 2.803, 2.805, 2.817 Å). This cyclic tetramer composed of 10-atoms, unlike the tetramer in **1** (9-atoms, Figure 1b).

(a) (c)

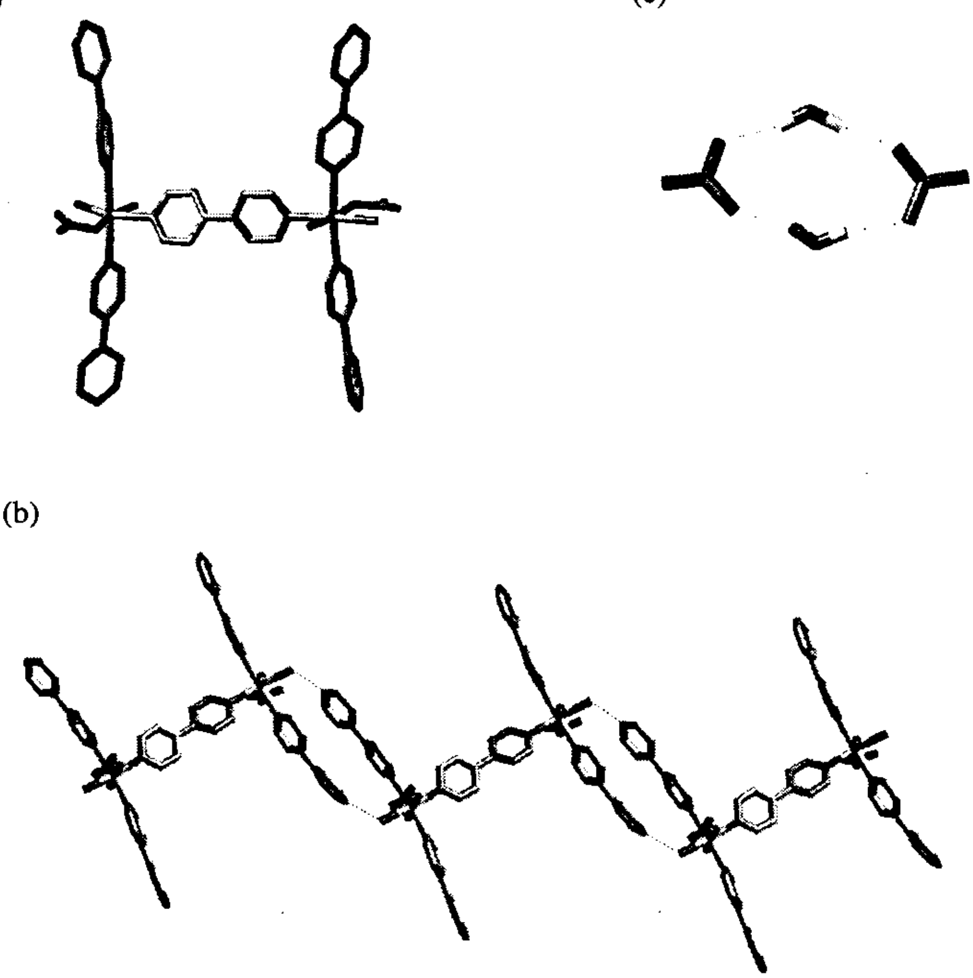

Figure 4. Illustrations for the crystal structure of 3: (a) Representation of the zero-dimensional species. Notice the cis geometry of the coordinated water molecules. (b) One-dimensional hydrogen-bonded network based on the cyclic ···H_2O-Cd-(4,4'-bpy) ···H_2O-Cd-(4,4'-bpy)··· dimers - part of the three-dimentional hydrogen-bonded network. (c) Representation of the hydrogen-bonded tetramer formed by water and nitrates. Compare with Figure 1b.

2.3 Conclusion

L/M ratio and concentration dependence of the formation of three types of coordination assemblies are related to coordination aggregates in the solution. In lower

L/M ratio, the square aggregate consisting of four cadmium and four 4,4'-bpy tends to generate at almost all conditions. The aggregate associates and crystallizes to form 2D network **1**. In the ratio of L/M≥3, however, formation of a 1D-chain aggregate which is caused by excess of ligand competes with formation of the square aggregate. Then, the two types of aggregates associate and crystallize as **1** and **2**, fractionally . On the other hand, in a high L/M ratio and low concentration, a dinuclear complex, which is the lowest degree of aggregation among **1-3,** is favored in the solution, and crystallizes to form the product **3**.

Three types of network **1**, **2**, and **3** are formed from Cd(II) ion and 4,4'-bpy. The network **1** was shown to exist as a non-interpenetrated grid structure even in the absence of aromatic guest molecules. Instead of organic guest, water molecules and nitrate ions located in the cavity and formed a hydrogen bond network. It is important to note that the L/M ratios and concentration of the solutions resulted in three different crystals with different dimensionality of the network. In **2** and **3**, the hydrogen bonding interactions played an important role in forming three-dimensional networks. The motifs observed here could serve as metal-coordinated or hydrogen-bonded synhtons in crystal engineering experiments.

2.4 Experimental Section

General: 4,4'-bpy and $Cd(NO_3)_2{\cdot}4H_2O$ were obtained commercially and used as received. Melting points were determined on a YANACO MP-500V. FTIR spectra were recorded on a SHIMADZU FTIR-8300 spectrometer. Microanalysis were performed by Research Center for Molecular Materials of Institute for Molecular Science.

Preparation and physical data of 1, 2, and 3: Coordination polymers **1**, **2**, and **3** were also prepared under the following methods.

$\{[Cd(4,4'\text{-}bpy)_2(H_2O)_2](NO_3)_2\cdot 4H_2O\}_n$ (1): An aqueous solution (8 mL) of $Cd(NO_3)_2\cdot 4H_2O$ (1 mmol) was combined with an ethanol (2 mL) solution of 4,4'-bpy (2 mmol). The initially formed fine precipitate (small amount) was filtered and the clear filtrate was allowed to stand at room temperature for 3 d to give single crystals of **1** in 70% yield. Mp. > 300 °C. IR (KBr, cm^{-1}) 3394, 1603, 1533, 1491, 1385, 1221, 1074, 1007, 806, 631. Elemental analysis: Calcd for $[Cd(4,4'\text{-}bpy)_2(H_2O)_2]\cdot 4H_2O\cdot 2NO_3$: C, 36.57; H, 4.30; N, 12.79. Found: C, 36.69; H, 4.09; N, 12.86.

$\{[Cd(4,4'\text{-}bpy)_3(H_2O)_2](NO_3)_2\cdot 2(4,4'\text{-}bpy)\cdot 4.5H_2O\}_n$ (2): An aqueous solution (1.6 mL) of $Cd(NO_3)_2\cdot 4H_2O$ (0.28 mmol) was combined with an ethanol (0.4 mL) solution of 4,4'-bpy (1.12 mmol). The initially formed fine precipitate (small amount) was filtered and the clear filtrate was allowed to stand at room temperature for 3 d to give mixture of single crystals of **1** (24%) and **2** (34%). Mp. > 300 °C. IR (KBr, cm^{-1}) 3385, 1600, 1533, 1491, 1384, 1221, 1074, 995, 810, 629, 617, 507. Elemental analysis: Calcd for $[Cd(4,4'\text{-}bpy)_3(H_2O)_2]\cdot 2(4,4'\text{-}bpy)\cdot 2NO_3\cdot 4.5H_2O$: C, 52.94; H, 4.71; N, 14.82. Found: C, 52.72; H, 4.43; N, 14.76.

$[Cd_2(4,4'\text{-}bpy)_5(H_2O)_4(NO_3)_2](NO_3)_2\cdot 4H_2O$ (3): An aqueous solution (12 mL) of $Cd(NO_3)_2\cdot 4H_2O$ (0.5 mmol) was combined with an ethanol (3 mL) solution of 4,4'-bpy (1.5 mmol). The initially formed fine precipitate (very small amount) was filtered and the clear filtrate was allowed to stand at room temperature for 3 d to give single crystals of **3** in 71% yield. Mp. > 300 °C. IR (KBr, cm^{-1}) 3150, 1600, 1530, 1480, 1400, 1380, 1220, 1070, 1000, 820, 625. Elemental analysis: Calcd for $[Cd(4,4'\text{-}bpy)_{2.5}(H_2O)]\cdot 2NO_3$: C, 45.30; H, 3.65; N, 14.79. Found: C, 45.43; H, 3.72; N, 14.67. Because of the loss of water molecules, the formula obtained by elemental analysis dose not corresponding to the formula based on X-ray crystallography.

X-ray crystal structure determinations: Crystal data of **1**: $C_{20}H_{28}CdN_6O_{12}$, M =

656.89; Monoclinic,space group $C2/c$; a = 18.9015(11) Å, b = 11.7948(7) Å, c = 12.1547(7) Å, β = 97.4380(10)°; V = 2687.0(3) Å^3; Z = 4; D_c = 1.624 g/cm^3; $F(000)$ = 1336; μ(Mo Kα) 1.009 mm^{-1}; crystal size = 0.20 x 0.20 x 0.15 mm; temp.= 167 K; 3105 unique reflections out of 8362 with $I > 2\sigma(I)$; final R-factors R_1 = 0.0176; wR_2 = 0.0499. Crystal data of **2**: $C_{50}H_{103}N_{12}CdO_{12.5}$, M = 1184.84; Monoclinic, space group $C2$; a = 17.5815(16) Å, b = 11.7413(11) Å, c = 24.836(2) Å, β = 94.3215(18)°; V = 5112.3(8) Å^3; Z = 4; D_c = 1.539 g/cm^3; $F(000)$ = 2540; μ(Mo Kα) 0.506 mm^{-1}; crystal size = 0.25 x 0.20 x 0.20 mm; temp.= 193 K; 8232 unique reflections out of 13740 with $I > 2\sigma(I)$; final R-factors R_1 = 0.0518; wR_2 = 0.1347. Crystal data of **3**: $C_{25}H_{28}N_7CdO_{10}$, M = 698.95; Monoclinic, space group Pc; a = 12.4725(18) Å, b = 15.195(2) Å, c = 15.390(2) Å, β = 96.625(3)°; V = 2897.2(7) Å^3; Z = 4; D_c = 1.602 g/cm^3; $F(000)$ = 1420; μ(Mo Kα) 0.821 mm^{-1}; crystal size = 0.25 x 0.20 x 0.20 mm; temp.= 173 K; 10014 unique reflections out of 18522 with $I > 2\sigma(I)$; final R-factors R_1 = 0.0221; wR_2 = 0.0541. Single crystal X-ray diffraction data for all the complexes were collected on a Siemens SMART/CCD diffractometer equipped with a low temperature device. Diffracted data were corrected for absorption using the SADABS[12] program. SHELXTL[13] was used for the structure solution and refinement was based on F^2. All non hydrogen atoms were refined anisotropically. The H-atoms of the C-H groups were fixed in calculated positions and refined isotropically with thermal parameters based upon the corresponding C-atoms [U(H) = 1.2 Ueq (C)]. The H-atoms of water molecules in **1** and **3** were located and refined isotropically. In **2**, pyridine rings in the bifunctional ligand and the guest 4,4'-bpy were fixed as regular hexagons, nitrate anions and guest water molecules have a disorder which is unresolved and all these disordered positional atoms were refined isotropically by treating them as carbon atoms. PLATON[14] program was used for detecting inversion centers in complexes **2** and **3**. For **2**, no inversion center was found, whereas for **3**, an approximate inversion center was found but the water molecules did not lie on it. Pertinent crystallographic data will be present in the Appendix.

References

(1) Hagrman, P. J.; Hagrman, D.; Zubieta, J. *Angew. Chem., Int. Ed.* **1999**, *38*, 2638.

(2) Liner chain: (a) Blake, A. J.; Hill, S.J.; Hubberstey, P.; Li, W.-S. *J. Chem. Soc., Dalton Trans.* **1997**, 913. (b) Carlucci, L.; Ciani, G.; Procerpio, D. M.; Sinori, A. *J. Chem. Soc., Dalton Trans.* **1997**, 1801. (c) Yaghi, O. M.; Li, H.; Groy, T. L.; *Inorg. Chem.* **1997**, *36*, 4292.

(3) Zigzag: (a) Blake, A. J.; Hill, S.J.; Hubberstey, P.; Li, W.-S. *J. Chem. Soc., Dalton Trans.* **1998**, 909. (b) Batsanov, A. S.; Begrey, M. J.; Hubberstey, P.; Stroud, J. *J. Chem. Soc., Dalton Trans.* **1996**, 1947.

(4) Helices: Biradha, K.; Corey, C. J.; Zaworotko, M. J. *Angew. Chem., Int. Ed.* **1999**,*38*, 492.

(5) Losier, P.; Zaworotko, M. J. *Angew. Chem., Int. Ed. Engl.* **1996**, *35*, 2779

(6) Square grid: (a) Gable, R. W.; Hoskins, B. F.; Robson, R. *J. Chem. Soc., Chem. Commun.* **1990**, 1677. (b) Fujita, M.; Kwon, Y. J.; Washizu, S.; Ogura, K. *J. Am. Chem. Soc.* **1994**, *116*, 1151. (c) Subramanian, S.; Zawarotko, M. J. *Angew. Chem., Int. Ed. Engl.* **1995**, *34*, 2127. (d) Tong, M.-L.; Ye, J.-W.; Cai, J.-W.; Chen, X.-W, Ng, S. W. *Inorg. Chem.* **1998**, *37*, 2645.

(7) A hexagonal grid: Yaghi, O. M.; Li, H. *Angew. Chem., Int. Ed. Engl.* **1995**, *34*, 207.

(8) Kondo, M.; Yoshitomi, T.; Seki, K.; Matsuzaka, H.; Kitagawa, S. *Angew. Chem., Int. Ed. Engl.* **1997**, *36*, 1725.

(9) (a) Carlucci, L.; Ciani, G.; Proserpio, D. M.; Sinori, A. *J. Chem. Soc., Chem. Commun.* **1994**, 2755. (b) MacGillivray, L. R.; Subramamian, S.; Zaworotko, M. J. *J. Chem. Soc., Chem. Commun.* **1994**, 1325. (c) Lopez, S.; Kahraman, M.; Harmata, M.; Keller, S. W. *Inorg. Chem.* **1997**, *36*, 6138.

(10) (a) Fujita, M.; Yazaki, J.; and Ogura, K. *J. Am Chem. Soc.* **1990**, *112*, 5645. (b) Fujita, M.; Yazaki, J.; Ogura, K. *Tetrahedron Lett.* **1991**, *32*, 5589. (c) Fujita, M.; Yazaki, J.; Ogura, K. *Chem. Lett.* **1991**, 1031. (d) Fujita, M.; Sasaki, O.; Mitsuhashi, T.; Fujita, T.; Yazaki, J.; Yamaguchi, K.; Ogura, K. *J. Chem. Soc.,*

Chem. Commun. **1996**, 1535.

(11) Desiraju, G. R. *Angew. Chem., Int. Ed. Engl.* **1995**, *34*, 2311.

(12) Sheldrick, G. M. *SADABS*: Univ. Gottingen, 1996.

(13) Sheldrick, G. M. *SHELXTL, Release 5.03*; Siemens Analytical X-ray Instruments Inc.: Madison, WIS, 1994.

Chapter 3

Pd(II)- and Pt(II)-linked Tetranuclear Complexes as Assembly Units for Higher Ordered Structures

Bull. Chem. Soc. Jpn. **1999**, *72*, 2603.

Abstract: The formation of ···Pt(II)···Br-Pt(IV)··· mixed-valence complexes was utilized for the assembly of square compounds, $[(en)M(4,4'\text{-bpy})]_4(NO_3)_8$ ($\mathbf{1}\cdot(NO_3)_8$; **a**: M = Pt(II), **b**: M = Pd(II), 4,4'-bpy = 4,4'-bipyridine), into higher ordered infinite complexes. The reaction of $\mathbf{1}^{8+}$ with cationic Pt(IV) complex, $[PtBr_2(en)_2]^{2+}$ ($\mathbf{2}^{2+}$), afforded a 1:3 complex $\mathbf{1a}\cdot(\mathbf{2})_3{}^{14+}$. Crystallographic analysis of this complex showed that two moieties of $\mathbf{2}^{2+}$ bridged at the cis corner of $\mathbf{1a}^{8+}$ making a stair-like infinite network, whereas another moiety of $\mathbf{2}^{2+}$ was accommodated in the cavity of $\mathbf{1a}^{8+}$. On the other hand, complexation of **1b** with anionic Pt(IV) complex, $PtX_6{}^{2-}$ ($\mathbf{3}^{2-}$; **a**: X = Cl, **b**: X = Br), afforded a 1:4 complex $\mathbf{1}\cdot(\mathbf{3})_4$. UV-vis observations suggested the formation of a linear tube structure, in which each corner of $\mathbf{1}^{8+}$ is bridged by the linear X-Pt-X motif of $\mathbf{3}^{2-}$.

3.1 Introduction

Cis protected Pd(II)- and Pt(II)- linked square complexes such as $\mathbf{1}^{8+}$ are prototypical compounds among a family of tetranuclear square complexes in descreat molecular systems. In **1**,[8] the transition metals provide 90 degree angles at every corner of the square.[1] A way of modifying this structure into an organic soluble one has been developed recently.[2a] Introduction of functional groups such as chiral biphenyls, calixarene, porphyrins, nucleic acids, and crown ether units into the square is also reported.[2b,3] A Pd(II)-Re(I) bimetallic square shows luminescent property.[4] As descrived in Chapter 2, formamtion of 4,4'-bpy bridging coordination polymers which have fused suquare ring structure were reported.[5] However, except these reports, the simple square structure has never been employed as a building block for higher dimensional structures. Thus, the author studied the accumulation of square complexes **1**$^{8+}$ into higher ordered infinite complexes via formation of ···Pt(II)···X-Pt(IV)··· (X: halogen) mixed-valence complexes. Mixed-valence one-dimensional materials, easily obtained by mixing $M(II)L_4$ and $M(IV)L_4X_2$ salts, are of special interest because of their specific physical properties such as conductivity and non-linear optical activities.[6]

In this chapter, the author describes how the complexes **1**$^{8+}$ assemble into stair and tubular networks upon complexation with Pt(IV) species **2**$^{2+}$ and **3a**$^{2-}$ or **3b**$^{2-}$, respectively (Chart 1).

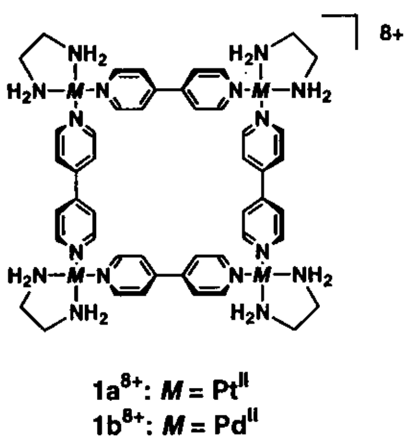

1a^{8+}: *M* = Pt^{II}
1b^{8+}: *M* = Pd^{II}

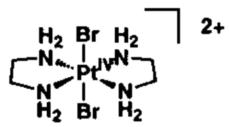

2^{2+}

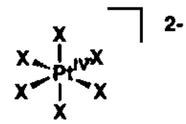

3a^{2-}: X = Cl
3b^{2-}: X = Br

Chart 1.

3.2 Results and Discussion

3.2.1 Reaction of Pt(II) molecular square with Pt(IV) complex $[PtBr_2(en)_2]Br_2$

It is well-known that the reaction of $(en)_2Pt^{2+}$ with $\mathbf{2}^{2+}$ gives mixed-valence one-dimensional $\{[(en)_2Pt][Pt\,Br_2(en)_2]\}_n^{4n+}$. Thus, it is anticipated that $\mathbf{1a}^{8+}$ will react with $\mathbf{2}^{2+}$ in a 1:4 stoichiometry, giving a one-dimensional tubular network. However, when $\mathbf{1a}\cdot(NO_3)_8$ was treated with four equivalents of $\mathbf{2}\cdot Br_2$ in 5 M $NaNO_3$ aqueous solution, these components reacted in a 1:3 stoichiometry, giving complex $[\mathbf{1a}\cdot\mathbf{2}_3](NO_3)_{14}\cdot 6H_2O$ (**4**) as yellow crystals (64% isolated yield). The ratio of molecular components of **4** has been determined by elemental analysis and ^1H NMR. Even the use of larger amount of $\mathbf{2}\cdot Br_2$ (6 equiv.) resulted in the formation of the same product in 91% isolated yield. Solid state UV-vis spectrum of **4** shows a new absorption band at 420 nm which was not observed in solution. Thus, this absorption indicates a possible charge transfer interaction between Pt(II)- Pt(IV) through the halogen atoms.

The X-ray analysis of **4** showed that two moieties of $\mathbf{2}^{2+}$ bridged the cis corner of $\mathbf{1a}^{8+}$ forming a stair-like network. The third moiety of $\mathbf{2}^{2+}$ acted as a guest molecule and occupied the cavity of molecular square $\mathbf{1a}^{8+}$ (Figure 1a, 1b). The geometry of $\mathbf{1a}^{8+}$ was similar to that of the corresponding Pd(II) complex $\mathbf{1b}^{8+}$ whose crystal structure was reported.[1d] The distance of Pt(II)-Br (3.22 and 3.37 Å) was slightly longer than that of typical $[PtBr_2(en)_2][Pt(en)_2](ClO_4)_4$ complex (3.006 Å),[6g] indicating a weaker interaction between Pt(IV) and Pt(II) through bromine atom. As a result of Pt(II)···Br-Pt(IV) interaction, a rectangular grid was formed which has no free space.

(a)

(b)

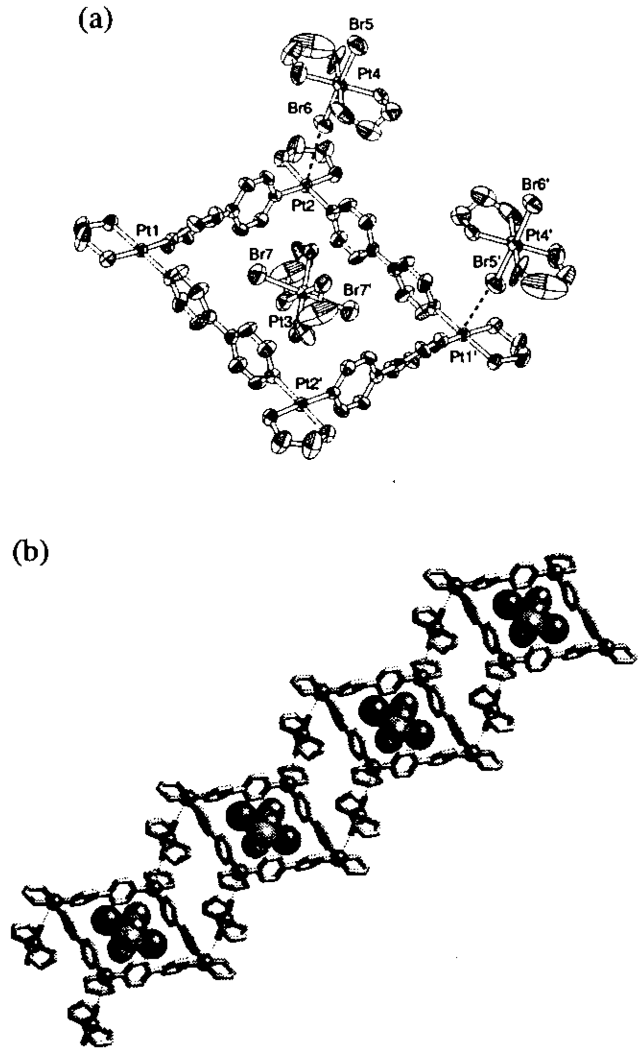

Figure 1. (a) ORTEP drawing of **4**. Pt(1)-Pt(2), 11.09 Å; Pt(1)-Pt(2'), 11.12 Å; Pt(1)-Br(5), 3.22 Å; Pt(2)-Br(6), 3.37 Å; Pt(4)-Br(5), 2.43 Å; Pt(4)-Br(6), 2.44 Å; Pt(3)-Br(7), 2.43 Å. Counter ions and water molecules are omitted for clarity. (b) Stair-like structure of **4**. Encapsulated $PtBr_2(en)_2$ molecules are represented in space filling mode.

Stair-like networks run along *b*-axis and stack such that there was a herringbone pattern of **4** grids (Figure 2). The inter-stair separation in the herringbone layer was 9.7 Å. Counter ions and water molecules were found in between stairs, forming an infinite hydrogen bond networks with NH_2 groups of $\mathbf{2}^{2+}$.

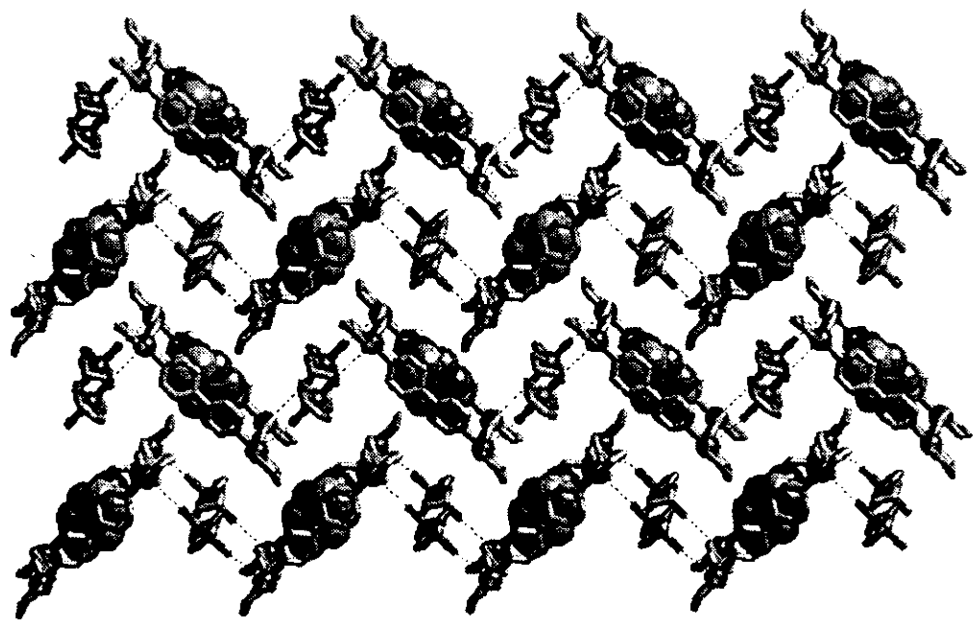

Figure 2. Top view of the layer structure of **4**. NO_3^- and H_2O molecules are omitted because some of them are disordered.

Interestingly, a cationic molecule $\mathbf{2}^{2+}$ was accommodated by cationic host $\mathbf{1a}^{8+}$ (Figure 3). This unusual "cation-in-a-cation" structure may be stabilized by NO_3^- and H_2O networks existing between the layers, though the details remain unclear due to the partial disorder of the counter ions and solvents. The perfect match of their shape and size, as found in Figure 3, should be also important to override unfavorable electrostatic effect.[7] On the other hand, $\mathbf{1a}^{8+}$ and $\mathbf{2}^{2+}$ dissociated in the solution. The NMR measurement showed that the chemical shifts of $\mathbf{1a}^{8+}$ and $\mathbf{2}^{2+}$ prepared by dissolving crystal of **4** in D_2O were identical to those of sole compounds.

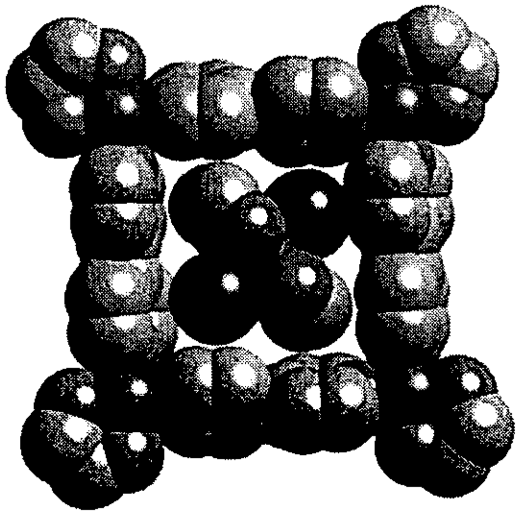

Figure 3. Top view of the molecular square $1a^{8+}$ with encapsulated cationic guest 2^{2+}.

3.2.2 Reactions of Pt(II) and Pd(II) molecular squares with $PtCl_6^{2-}$ and $PtBr_6^{2-}$

Reactions of 1^{8+} and anionic Pt(IV) complexes such as $PtCl_6^{2-}$ (**3a**$^{2-}$) and $PtBr_6^{2-}$ (**3b**$^{2-}$) were also attempted. An aqueous solution of **1**$\cdot(NO_3)_8$ and an aqueous solution of potassium salts of 3^{2-} were mixed in 1:5 ratio. Immediately, colored insoluble powder precipitated. Elemental analysis of the product showed the formula of **1**$\cdot$(**3**)$_4$, and yields of product were 92-97%. Even the use of large excess of 3^{2-} (16 equiv.) resulted in the formation of the same products. The products were characterized by UV-vis and elemental analysis. The UV-vis spectrum showed new absorption bands which indicate the existence of interaction of Pd(II) and Pt(IV) (e.g., 390 and 490 nm for **1b**$\cdot$(**3a**)$_4$) (Figure 4), suggesting that each corner of 1^{8+} is bridged by the linear X-Pt(IV)-X motif of 3^{2-}. From these observations, the author proposes the assembly of square 1^{8+} into polytube structures such as **5** and **6** or their hybrid that involve one-dimensional Pt(II)···X-Pt(IV)-X··· chains (Chart 2).

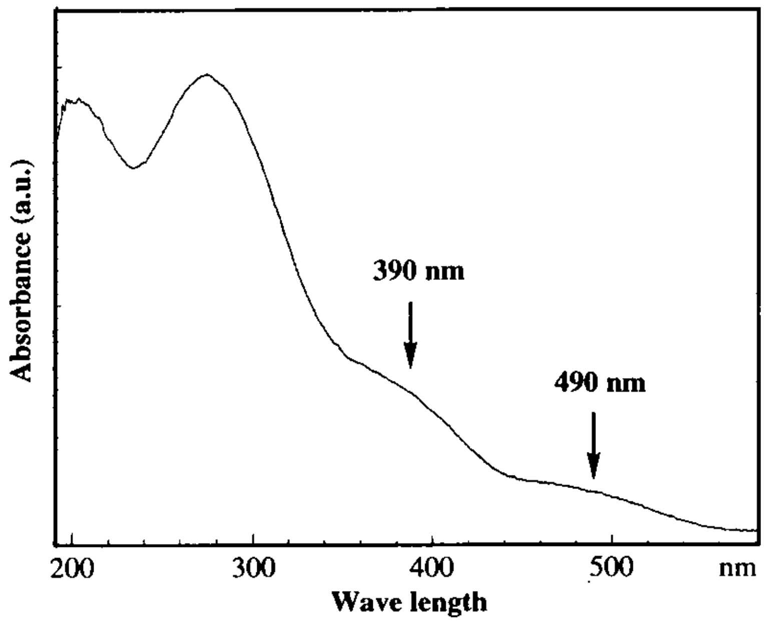

Figure 4. UV-vis spectrum of **1b**·(**3a**)$_4$.

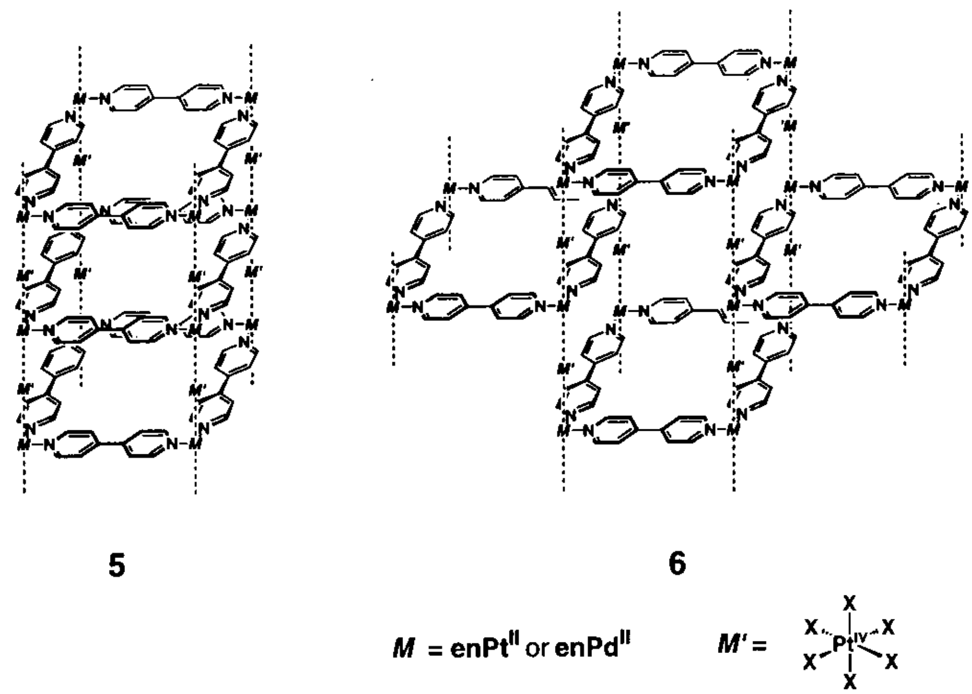

Chart 2.

3.3 Conclusion

Novel stair-like and tubular structures were prepared by two stage self-assembly process. In the first stage, $M(NO_3)_2(en)$ (M: Pt or Pd) and 4,4'-bpy are assembled into square complexes $\mathbf{1}^{8+}$. In the second stage, the square $\mathbf{1}^{8+}$ and $Pt^{IV}L_4X_2$ are assembled into higher dimensional supramolecular structure through M(II)···halogen-Pt(IV) interaction. Moreover, the present report demonstrated that formation of halogen-bridged mixed valence complex can be used for aggregation of metal containing supramolecules.

3.4 Experimental Section

General: Compound **1a**·$(NO_3)_8$[1a], **1b**·$(NO_3)_8$[1c] and **2**·Br_2[6a] were prepared according to reported procedures. Potassium salts of $\mathbf{3a}^{2-}$ and $\mathbf{3b}^{2-}$ were obtained commercially and used as received. Melting points were determined on a YANACO MP-500V. UV-vis spectra were measured on a SHIMADZU MultiSpec-1500 spectrometer or a SHIMADZU UV-3100PC spectrometer. FTIR spectra were recorded on a SHIMADZU FTIR-8300 spectrometer. ^{1}H NMR spectra were recorded on a JEOL JNM-LA500 (500 MHz) spectrometer. Microanalysis were performed by Research Center for Molecular Materials of Institute for Molecular Science.

Preparation of 4: An aqueous solution (1 mL) of **1a**·$(NO_3)_8$ (0.05 mmol) and **2**·Br_2 (0.2 mmol) was treated with $NaNO_3$ (425 mg) at room temperature. A trace amount of insoluble material was filtrated and the clear yellow solution was allowed to stand for 1d. Yellow crystals which appeared were collected and dried *in vacuo* to give **4** in 64% yield. Mp. 224-227 °C (decomp.). ^{1}HNMR (500 MHz, D_2O, TMS as an external standard) δ = 8.90 (d, J = 5.6 Hz, 16H, Py*Ha*), 7.86 (d, J = 5.6 Hz, 16H, Py*Hb*), 3.11(t, J = 13.7 Hz, 24H, $-CH_2-$), 2.86 (s, 16H, $-CH_2-$). IR (KBr) 3449, 3045, 1618, 1385, 1173, 1138, 1053, 826 cm^{-1}. Elemental analysis: Calcd for $C_{60}H_{124}Br_6N_{42}O_{42}Pt_7 \cdot 6H_2O$: C, 17.81; H, 3.09; N, 14.54. Found: C, 17.78; H, 3.05; N, 14.43.

X-ray Crystallographic Analysis of 4: Single crystals of **4** were obtained by slow diffusion of the aqueous solution (1 mL) of **1a**·$(NO_3)_8$ (25 mM) and **2**·Br_2 (100 mM) into an aqueous solution of $NaNO_3$ (10 M, 1 mL) at room temperature for 3 d. X-ray data for **4:** $C_{60}H_{124}Br_6N_{44}O_{42}Pt_7 \cdot 12H_2O$, M = 4190.80, monoclinic, space group $P2_1/c$; a = 20.648(4), b = 16.205(3), c = 19.397(3) Å, β = 111.031(11), V = 6057.8(18) $Å^3$; D_C = 2.278 g/cm^3, Z = 2; $F(000)$ = 3956; $\mu(MoK\alpha)$ = 10.134 mm^{-1}; crystal size = 0.4 x 0.25 x 0.25 mm; temp. 293 K; 25113 reflections collected, 10175 ($I>2\sigma(I)$) reflections observed; R_1 = 0.0434; wR_2 = 0.1185. The data were collected on a Siemens SMART/CCD diffractometer. Diffraction data were corrected for absorption using the SADABS[8] program. SHELXTL[9] was used for the structure solution and refinement was based on F^2. All non-hydrogen atoms were refined anisotropically. Hydrogen atoms were fixed in calculated positions and refined isotropically with thermal parameters based upon the corresponding C-atoms [U(H) = 1.2 Ueq (C)]. Crystallographic data have been deposited at the CCDC, 12 Union Road, Cambridge CB2 1EZ, UK and the deposition number of the data is 134340.

Preparation of 1a·(3a)$_4$, 1a·(3b)$_4$, 1b·(3a)$_4$ and 1b·(3b)$_4$: An aqueous solution (1.0 cm^3) of **1** (0.02 mmol) was added into an aqueous solution (10 cm^3) of **3** (0.1 mmol) at room temperature. Colored products were collected by filtration and dried *in vacuo*. The ratios of water were calculated from elemental analysis data. **1a·(3a)$_4$**: Brown solid, 95%, mp. >300 °C. IR (KCl, cm^{-1}) 3202, 1616, 1421, 1221, 1047, 820, 665. Elemental analysis: Calcd for $C_{48}H_{64}N_{16}Cl_{24}Pt_8 \cdot 13H_2O$: C, 16.42; H, 2.58; N, 6.38. Found: C, 16.40; H, 2.58; N, 6.38. **1a·(3b)$_4$**: Dark brown solid, 92%, mp. 288-291 °C (decomp). IR (KBr, cm^{-1}) 3198, 1614, 1420, 1217, 1047, 816, 667. Elemental analysis: Calcd for $C_{48}H_{64}N_{16}Br_{24}Pd_4Pt_4 \cdot 20H_2O$: C, 12.26; H, 2.23; N, 4.76. Found: C, 12.32; H, 2.01; N, 4.81. **1b**·(**3a**)$_4$: Yellow powder, 96%, mp. 284-287 ℃ (decomp). IR (KCl, cm^{-1}) 3213, 1612, 1418, 1219, 1059, 816, 658. Elemental analysis: Calcd for $C_{48}H_{64}N_{16}Cl_{24}Pd_4Pt_4 \cdot 13H_2O$: C, 18.27; H, 2.87; N, 7.10. Found: C, 18.14; H, 2.73; N, 7.12. **1b**·(**3b**)$_4$: Orange powder, 97%, mp. 234-237 ℃ (decomp). IR (KBr, cm^{-1}) 3205, 1611, 1418, 1218, 1057, 814, 659. Elemental analysis: Calcd for $C_{48}H_{64}N_{16}Br_{24}Pd_4Pt_4 \cdot 14H_2O$: C, 13.59; H, 2.19; N, 5.28. Found: C, 13.28; H, 1.82; N, 5.32.

References

(1) (a) Fujita, M.; Yazaki, J.; and Ogura, K. *J. Am Chem. Soc.* **1990**, *112*, 5645. (b) Fujita, M.; Yazaki, J.; Ogura, K. *Tetrahedron Lett.* **1991**, *32*, 5589. (c) Fujita, M.; Yazaki, J.; Ogura, K. *Chem. Lett.* **1991**, 1031. (d) Fujita, M.; Sasaki, O.; Mitsuhashi, T.; Fujita, T.; Yazaki, J.; Yamaguchi, K.; Ogura, K. *Chem. Commun.* **1996**, 1535.

(2) (a) Stang, P. J.; Cao, D. H. *J. Am Chem. Soc.* **1994**, *116*, 4981. (b) Stang, P. J.; Olenyuk, B. *Acc. Chem. Res.* **1997**, *30*, 502.

(3) (a) Drain, C. M.; Lehn, J.-M. *J. Chem. Soc., Chem. Commun.* **1994**, 2313. (b) Rauter, H.; Hillgeris, E. C.; Erxleben, A.; Lippert, B. *J. Am Chem. Soc.* **1996**, *116*, 616.

(4) Slone, R. V.; Yoon, D. I.; Calhoum, R. M.; Hupp, J. T. *J. Am Chem. Soc.* **1995**, *117*, 11813.

(5) (a) Gable, R. W.; Hoskins, B. F.; Robson, R. *J. Chem. Soc., Chem. Commun.* **1990**, 1677. (b) Fujita, M.; Kwon, Y. J.; Washizu, S.; Ogura, K. *J. Am. Chem. Soc.* **1994**, *116*, 1151. (c) Subramanian, S.; Zaworotko, M. J. *Angew. Chem., Int. Ed. Engl.* **1995**, *34*, 2127. (d) Losier P.; Zaworotko, M. J. *Angew. Chem., Int. Ed. Engl.* **1996**, *35*, 2779.

(6) (a) Matsumoto, N.; Yamashita, M.; Kida, S. *Bull. Chem. Soc. Jpn.* **1978**, *51*, 2334. (b) Yamashita, M.; Kida, Y.; Hamaue, Y.; Aoki, R. *Inorg. Chim. Acta* **1981**, *52*, 43. (c) Papavassilliou, G. C.; Layek, D. *Z. Naturforsch* **1982**, *37b*, 1406. (d) Yamashita, M.; Ito, H.; Toriumi, K.; Ito, T. *Inorg. Chem.* **1983**, *22*, 1566. (e) Yamashita, M.; Murase, I. *Inorg. Chim. Acta*, **1985**, *97*, L43. (f) Yamashita, M.; Murase, I.; Ikemoto, I.; Ito, T. *Chem. Lett.* **1985**, 1133. (g) Toriumi, K.; Yamashita, M.; Kurita, S.; Murase, I.; Ito, T. *Chem. Lett.* **1985**, 1133.

(7) There are several examples of metal linked cyclic receptors encapsulating anions and electron rich molecules. (a) Hasenknopf, B.; Lehn, J.-M.; Boumediene, N.; Dpont-Gervais, A.; Dorsselaer, A. V.; Kneisel, B.; Fenske, D. *J. Am Chem. Soc.* **1997**, *119*, 10956. (b) Schnebeck, R.-D.; Freisinger, E.; Lippert, B. *Angew. Chem., Int.*

Ed. **1999**, *38*, 168. (c) Schwabacher, A. W.; Lee, J.; Lei, H. *J. Am Chem. Soc.* **1992**, *114*, 7597. (d) Fujita, M.; Nagao, S.; Iida, M; Ogata, K.; Ogura, K. *J. Am Chem. Soc.* **1993**, *115*, 1574. See also ref. 1c.

(8) Sheldrick, G.M. *SADABS*: Univ. Gottingen, 1996.

(9) Sheldrick, G.M. *SHELXTL, Release 5.03*; Siemens Analytical X-ray Instruments Inc.: Madison, WIS, 1994.

Chapter 4

Quantitative Formation of Coordination Nanotubes Templated by Rod-like Guests

J. Am. Chem. Soc. **1999**, *121*, 7457.

Abstract: Coordination nanotubes were constructed by linking oligo(3,5-pyridine)s with a cis-protected Pd(II) building block, (en)Pd(NO_3)$_2$ (en = ethylenediamine). This transformation was, in fact, accomplished with the remarkable template effect of biphenyl derivatives. Thus, the reaction of oligo(3,5-pyridine)s with (en)Pd(NO_3)$_2$ first resulted in the formation of uncharacterizable products. However, the addition of sodium 4,4'-biphenylenedicarboxylate to the solution induced the smooth assembly of nanotubes wherein four oligo(3,5-pyridine) molecules were held together with six to ten Pd(II) units. A nanotube structure templated by a guest was confirmed by an X-ray crystallographic analysis.

4.1 Introduction

Molecular-based tubular structures have attracted considerable current interest because of their potential abilities for selective inclusion and transportation of ions and molecules and catalysis for specific chemical transformations, by exploiting the interior space of the tubes.[1-5] For constructing nanotube structures, non-covalent syntheses using hydrophobic interaction[2,5] and hydrogen bonding[3,4] have been shown quite effective, though the precise control of tube lengths remains unrealized yet. Herein reported is a coordination approach to nanotubes possessing very stable, discrete frameworks. The author designed the assembly of oligo(3,5-pyridine)s (**1**) into tubular structures by linking them with transition metal components.

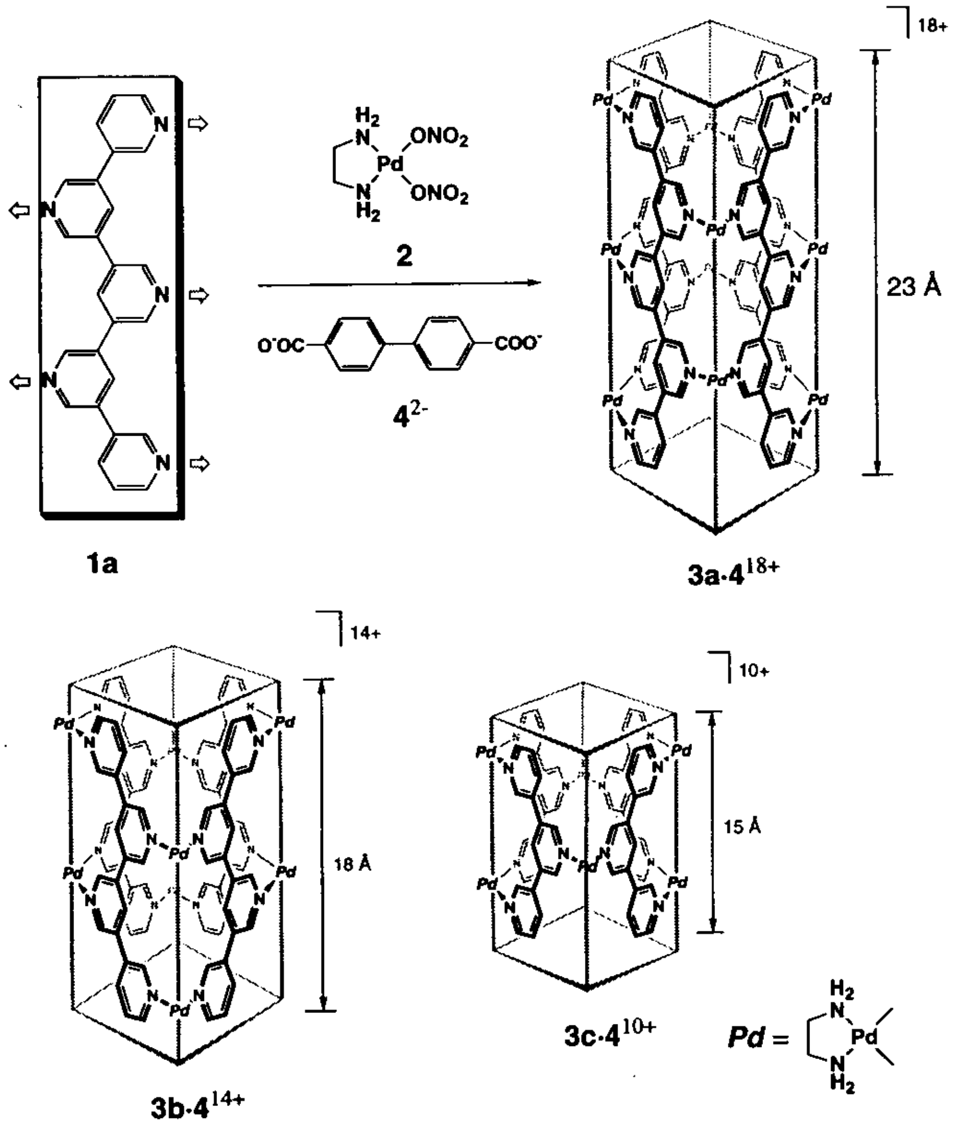

(Template 4^{2-} included in the tubes **3a-3c** is omitted for clarity.)

Scheme 1.

The strategy for the construction of the tube structures is summarized in Scheme 1. Pentakis(3,5-pyridine) ligand **1a**,[6] for example, should take a coplanar conformation due to the dipole repulsion among pyridine nuclei. Thus, when this ligand is linked together with Pd(II) building block **2** which provides 90 degree turn into the assembled structure,[7] coordination nanotube **3a** is expected to assemble from four molecules of **1a** and ten molecules of **2**. Moreover, **3a** has orthorhombic hydrophobic cavity in which guest molecules can be encapsulated. Similar coordination tubes **3b** and **3c** are also designed.

4.2 Results and Discussion

4.2.1 The assembly of a coordination nanotube

The reaction of **1a** with **2** in D_2O first resulted in the formation of uncharacterized products (Figure 1a). Surprisingly, the addition of sodium 4,4'-biphenylene-dicarboxylate (Na·**4**) to the solution induced the assembly of a single product (Figure 1b), which smoothly turned into a sole product after the solution was heated at 60 °C for 1 h (Figure 1c). The NMR spectrum showed nine proton signals which stemmed from half the framework of **1a** in the product. Furthermore, a NOESY experiment supported the coplanar conformation of the ligand framework.[8] From these observations, the product was assigned as coordination nanotube **3a**. Actually, the formula of **3a**·**4** was confirmed by coldspray ionization mass spectrometry (CSI-MS)[9] measurement (*m/z* 699 $[M-6(NO_3)]^{6+}$; 852 $[M-5(NO_3)]^{5+}$; 1080 $[M-4(NO_3)]^{4+}$). From the aqueous solution, the host-guest complex (**3a**·**4**, nitrate salt) was isolated as a colorless precipitate in 81% yield by adding large amount of acetone. Elemental analysis was consistent with the formula of **3a**·**4**$(NO_3)_{18}\cdot 25H_2O$.

The template effect of **4** for the assembly of tube **3a** has been obviously revealed by the following results. First, the protons of guest **4** were highly up-field shifted in ^1H NMR by 2.6 ppm indicating the accommodation of the guest in the nanotube. Second, other rod-like molecules such as unsubstituted biphenyl and *p*-terphenyl were effective, whereas large molecules such as adamantane carboxylate did not show any template effect.[10] Third, in the absence of **4**, tube **3a** was not assembled effectively even after one week at 60 °C.

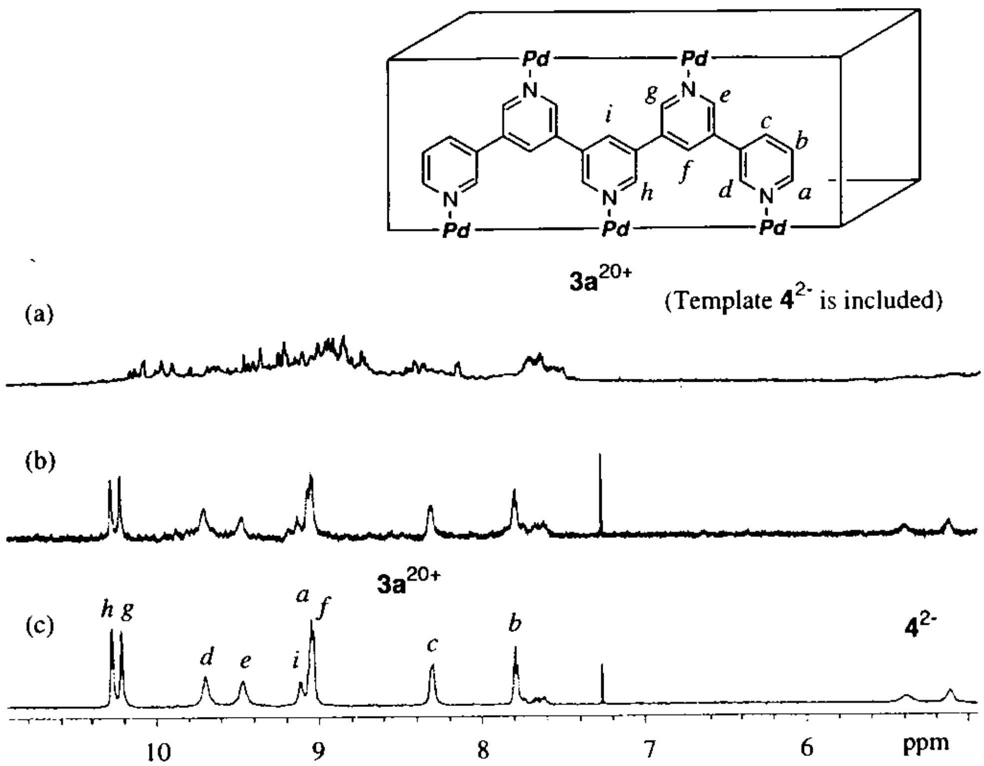

Figure 1. The ^1H NMR observation of the guest-templated formation of **3a·4** (500 MHz, D_2O, 25 °C, TMS as an external standard). Spectra were obtained after the following procedures. (a) Ligand **1a** (0.01 mmol) was treated with **2** (0.025 mmol, 1 mL) in D_2O (1 mL) for 5 min. at 60 °C. (b) To this solution was added a D_2O solution of Na·**4** (25 mM, 0.12 mL) and the mixture was stirred for 1 h at room temperature. (c) Then, the mixture was stirred for additional 1 h at 60 °C.

4.2.2 VT NMR study of the coordination nanotube

The template molecule was strongly bound within the interior of the tube and even unsubstituted biphenyl could not be extracted with $CHCl_3$ from an aqueous solution of **3a**·biphenyl at room temperature. Only at high temperatures (>70 °C), biphenyl was slowly extracted with $CHCl_3$ from the aqueous solution. Interestingly, the guest-templated assembly of tube **3a** is a complete reversible process: i.e., when the guest biphenyl was extracted into $CHCl_3$ phase at 70 °C, once assembled **3a** easily turned into an oligomer mixture, which regenerated tube **3a** upon the addition of the template molecule to the mixture again.

The dynamic behavior of the guest molecule in the cavity, revealed by variable temperature NMR measurement, is particularly interesting (Figure 2). At 25 °C, broad guest signals appeared at δ 5.39 and δ 5.12. Upon heating, the signals became much broader and disappeared around 60 °C. Surprisingly, the signals reappeared at 80 °C at slightly down-field shifted positions. This unusual behavior is well explained by the shuttle movement of the guest in the nanotube: the guest stays at a fixed position of the tube, shuttles on the NMR time scale at 60 °C, and rapidly moves or partially goes out from the tube above 60 °C.

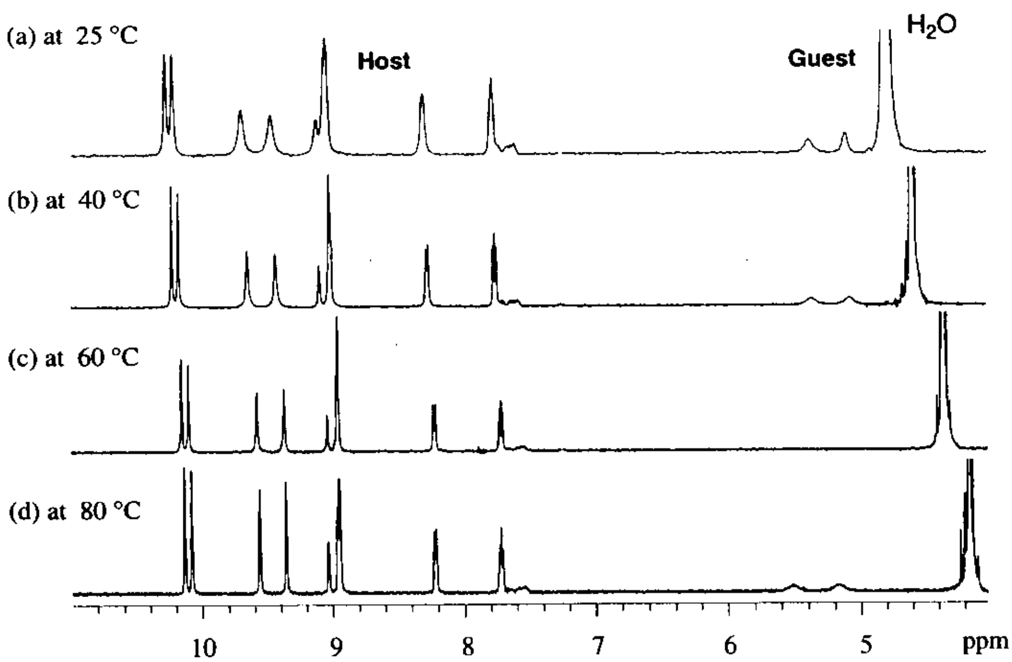

Figure 2. The VT-^{1}H NMR observation of **3a·4** (500 MHz, D_2O, TMS as an external standard): A slight excess amount of **4** (1.2 equiv.) was employed to template the assembly of **3a**. (a) At 25 °C; (b) At 40 °C; (c) At 60 °C; (d) At 80 °C.

4.2.3 The assembly of other coordination nanotubes

Tetrakis(3,5-pyridine) ligand **1b** and tris(3,5-pyridine) ligand **1c** were also assembled into coordination nanotube **3b·4** and **3c·4**, respectively. The assemblies were confirmed by 1D and 2D NMR measurements and the molecular formula of **3b·4**$(NO_3)_{14}$ and **3c·4**$(NO_3)_{14}$ were confirmed by elemental analysis and CSI-MS with series of $[M-(NO_3)_n]^{n+}$ (n = 3-6) peaks.

The tubular structure enclathrating the template molecule was confirmed by the X-ray crystallographic analysis of complex **3c** assembled from tris(3,5-pyridine) ligand **1c**, Pd(II) complex **2**, and template **4**. Again, the treatment of **1c** with **2** afforded a complex mixture which, however, turned into **3c** upon addition of **4** and heating at 70 °C. Single crystals were obtained by diffusing isopropyl alcohol into an aqueous solution of **3c** and **4** (1:2) at room temperature for 2 d. The crystal structure (Figure 3a) displays the tubular structure of **3c** which is efficiently assembled around template **4**. As expected, each ligand takes almost coplanar conformation and dihedral angles between adjacent pyridine rings are less than 28 degree. The top view of this complex (Figure 3b) shows strong π-π

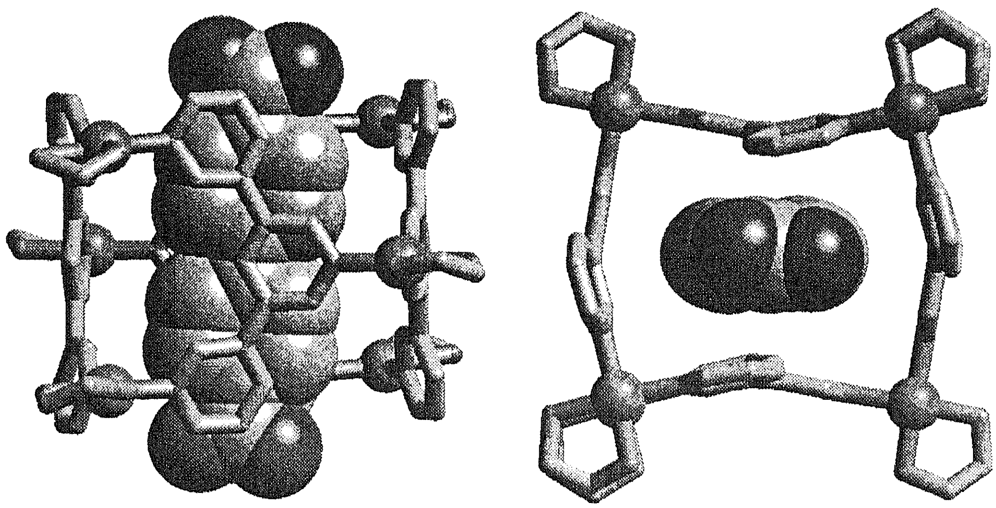

Figure 3. Crystal structure of **3c**·(**4**)$_2(NO_3)_8$ (left: Side view, right: top view). For clarity, H atoms and NO_3^- ions are omitted.

and CH-π interactions between **3c** and **4**. Namely, the shape from the top view, which should be square ideally, is significantly distorted in such a way that two ligands are stacked on the π-face of **4** with π-π interaction distances (3.5-3.6 Å) and two other ligands are orthogonally interacted with **4** in CH-π interaction distances (2.9-3.0 Å). Interestingly, another biphenyl carboxylate is located outside and stacked between the tubes, though it is omitted for clarity.

4.3 Conclusion

Coordination nanotube **3a**, **3b**, and **3c** assembled *with the aid of the remarkable template effect of a rod-like template molecule.*[11-13]. The π–π and CH-π interactions between host and guest was responsible for the template effect. Moreover, the tube assembly and dissociation process was reversible upon addition and remove of guest molecule. The guest selective assembly and reversible assembling-dissociation process of the coordination nanotubes suggests their posses potential abilities for application to not only separation materials but also phase transfer catalysis for specific chemical transformations.

4.4 Experimental Section

General: Compound **2**[14] and 3-tributylstanyl pyridine[6] were prepared according to reported procedures. Sodium salt of **4**$^-$ were prepared by combining sodium hydroxide and biphenyl dicarboxylicacid which were obtained commercially. Thin layer chromatography (TLC) was performed on precoated silica plates (Merck, Kieselgel 60 F_{254} 2 mm). Column chromatography was performed on silicagel (Merck, Kieselgel 60, 70-230 mesh). Melting points were determined on a YANACO MP-500V. FTIR spectra were recorded on a SHIMADZU FTIR-8300 spectrometer. ^{1}H NMR spectra were recorded on a JEOL JNM-LA500 (500 MHz) spectrometer. ^{13}C NMR spectra were recorded on a JEOL JNM-LA500 (125 MHz) spectrometer. Microanalysis were performed by Research Center for Molecular Materials in Institute for Molecular Science. Mass spectra were recorded on a SHIMADZU GCMS-QP5050A (for low-resolution EIMS) spectrometer or a SHIMADZU/KRATOS CONCEPT IS (for high-resolution EIMS and FABMS) spectrometer or a JEOL Type JMS-7000 (for CSIMS) spectrometer.

Preparation of 5-bromo-3,3'-bipyridine: A mixture of 3,5-dibromopyridine (9.92 g, 41.9 mmol), 3-tributylstannylpyridine (10.28 g, 27.9 mmol, see ref. 6 of the text), $PdCl_2(PPh_3)_2$ (0.98 g, 1.40 mmol) and lithium chloride (5.92 g, 140 mmol) in dry toluene (200 mL) was refluxed for 48 h under argon. The reaction mixture was filtered and the solution was evaporated. The crude product was purified by column chromatography (silicagel, $CHCl_3$/ethyl acetate 1/2) to give 5-bromo-3,3'-bipyridine as colorless crystals (4.35 g, 66%). Mp. 101-102 °C. ^1H NMR (500 MHz, $CDCl_3$) δ = 8.84 (d, J = 2.0 Hz, 1H), 8.76 (d, J = 2.0 Hz, 1H), 8.73 (d, J = 2.0 Hz, 1H), 8.70 (dd, J = 4.7, 1.5 Hz, 1H), 8.04 (t, J = 2.0 Hz, 1H), 7.88 (ddd, J = 8.0, 2.5, 2.0 Hz, 1H), 7.45 (dd, J = 8.0, 4.7 Hz, 1H); ^{13}C NMR (125 MHz, $CDCl_3$) δ = 150.3, 149.8, 148.1, 146.2, 136.9, 135.0, 134.6, 132.1, 123.9, 121.1. IR (KBr, cm^{-1}) 3449(br), 3026, 1435, 1391, 1113, 1009, 889, 802, 714, 706, 687, 619. MS m/z 234 (M^+). Elemental analysis: Calcd for $C_{10}H_7N_2Br$: C, 51.09; H, 3.00; N, 11.92. Found: C, 50.76; H, 2.89; N, 11.83.

Preparation of 5-tributylstanyl-3,3'-bipyridine: Under argon, n-butyllithium (6 mmol, 1.53 M in hexane) was slowly added to a THF solution of 5-bromo-3,3'-bipyridine (1.175 g, 5 mmol) at -78 °C. After 2 h, n-Bu_3SnCl was added dropwise. The mixture was stirred at -78 °C for 2 h and 0 °C for 1 h. After the solvent was evaporated, the residue was poured into water (50 mL) and extracted with $CHCl_3$ (50 mL x 3). The organic phase was dried over Na_2SO_4 and evaporated. The crude product was purified by clumn chromatography (silicagel, $CHCl_3$/ethyl acetate 1/1) to give 5-tributylstanyl-3,3'-bipyridine as a brown oil (1.228 g,, 55%). ^{1}H NMR (500 MHz, $CDCl_3$) δ = 8.76 (dd, J = 2.5, 0.8 Hz, 1H), 8.65 (d, J = 2.5 Hz, 1H), 8.57 (dd, J = 4.8, 1.7 Hz, 1H), 8.56 (d, J = 4.8, 1.5 Hz, 1H), 7.84 (dd, J = 2.5, 1.5 Hz, 1H), 7.80 (ddd, J = 7.80, 2.45, 1.7 Hz, 1H), 7.33 (ddd, J = 7.8, 4.9, 0.8 Hz, 1H), 1.52-1.46 (m, 2H), 1.31-1.23 (m, 2H), 1.07 (t, J = 8.1 Hz, 2H), 0.82 (t, J = 7.3 Hz, 2H); ^{13}C NMR (125 MHz, CDCl3) δ = 155.4, 149.0, 148.2, 147.5, 142.2, 137.2, 134.3, 134.0, 133.2, 123.6, 28.8, 27.2, 13.5, 9.6. IR (neat, cm^{-1}) 3018, 2955, 2924, 2853, 2870, 1458, 1402, 1385, 1022, 1013, 806, 718. MS m/z 444 (M^+). Elemental analysis: Calcd for $C_{22}H_{34}N_2Sn$: C, 59.35; H, 7.70; N, 6.29. Found: C, 59.27; H, 7.95; N, 6.42.

Preparation of 3,3':5',3'':5'',3''':5''':3''''-pentapyridine (1a): A mixture of 3,5-dibromopyridine (0.325 g, 1.37 mmol), 5-tributylstannyl-3,3'-bipyridine (1.83g, 4.1 mmol), $PdCl_2(PPh_3)_2$ (0.096 g, 0.137 mmol) and lithium chloride (0.581 g, 1.37 mmol) in dry toluene (40 mL) was refluxed for one week under argon. The mixture was concentrated in vacuo. After soxhlet extraction with $CHCl_3$ and methanol, solvent was evaporated. The crude product was purified by column chromatography (silicagel, $CHCl_3$/methanol 15/1) to give **1a** as colorless crystals (90 mg, 17%). Mp. >300 °C. ^{1}H NMR (500 MHz, $CDCl_3$) d = 8.97 (d, J = 2.3 Hz, 2H), 8.89 (d, J = 2.3 Hz, 2H), 8.84 (d, J = 2.3 Hz, 2H), 8.83 (dd, J = 2.3, 0.8 Hz, 2H), 8.60 (dd, J = 4.9, 1.8 Hz, 2H), 8.22 (t, J = 2.3 Hz, 1H), 8.17 (t, J = 2.3 Hz, 2H), 7.99 (ddd, J = 8.1, 2.3, 1.8 Hz, 2H), 7.47 (ddd, J = 8.1, 4.9, 0.8 Hz, 2H). IR (KBr, cm^{-1}) 3422(br), 3038, 1398, 1389, 1340, 1020, 1009, 887, 804, 716, 660, 631. HRMS (EI): Calcd for $C_{25}H_{17}N_5$: 387.14840. Found: 387.14775.

Preparation of ligand 3,3':5',3'':5'',3'''-quaterpyridine (1b): A zinc powder (0.882 g, 13 mmol) was added to a DMF solution of $NiCl_2 \cdot 6H_2O$ (3.068 g, 13 mmol) and triphenylphosphine (13.2 g, 40 mmol) under argon and the mixture was stirred for 1

h. To this mixture 5-bromo-3,3'-bipyridine (3.0 g, 13 mmol) was added and the resulting mixture was refluxed for 2 d. After solvent was evaporated, the residue was poured into $CHCl_3$ and extracted with aqueous HCl. The aqueous phase was neutralized by NaOH and extracted with $CHCl_3$. The organic layer was dried over Na_2SO_4 and evaporated to give a crude product, which was purified by column chromatography (silicagel, $CHCl_3$/methanol 30/1) to give **1b** as colorless crystals (0.70 g, 35%). Mp. 261-263 °C. ^{1}H NMR (500 MHz, $CDCl_3$) δ = 8.93 (d, J = 2.3 Hz, 2H), 8.92 (d, J = 0.90 Hz, 2H), 8.91 (d, J = 2.3 Hz, 2H), 8.70 (dd, J = 4.9, 1.8 Hz, 2H), 8.10 (t, J = 2.3 Hz, 2H), 7.95 (ddd, J = 8.0, 2.3, 1.8 Hz, 2H), 7.45 (ddd, J =8.0, 4.9, 0.9 Hz, 2H); ^{13}C NMR (125 MHz, $CDCl_3$) δ = 149.8, 148.3, 148.0, 147.7, 134.6, 134.0, 133.4, 133.0, 133.0, 123.9. IR (KBr, cm^{-1}) 3408(br), 3032, 1406, 1391, 1342, 1018, 1005, 893, 800, 716, 708, 629. MS *m/z* 310 (M^+). Elemental analysis: Calcd for $C_{20}H_{14}N_4$: C, 77.40; H, 4.55; N, 18.05. Found: C, 77.56; H, 4.28; N, 18.17.

Preparation of ligand 3,3'-5',3"-terpyridine (1c): A mixture of 3,5-dibromopyridine (1.422 g, 6.0 mmol), 3-tributylstannylpyridine (6.63 g, 18 mmol), $PdCl_2(PPh_3)_2$ (0.421 g, 0.60 mmol) and lithium chloride (2.544 g, 60 mmol) in dry toluene (120 mL) was refluxed for 11 h under argon. The mixture was filtered and the solvent was evaporated. The crude product was purified by column chromatography (silicagel, ethyl acetate/methanol 10/1) to give **1c** as colorless crystals (1.217 g, 87%). Mp. 160-161 °C. ^{1}H NMR (270 MHz, $CDCl_3$) δ = 8.99 (d, J = 2.3 Hz, 2H), 8.92 (dd, J = 2.3, 0.7 Hz, 2H), 8.71 (dd, J = 5.0, 1.7 Hz, 2H), 8.06 (d, J = 2.3 Hz, 1H), 7.96 (ddd, J = 7.9, 2.3, 1.7 Hz, 2H), 7.46 (ddd, J = 7.9, 5.0, 0.7 Hz, 2H); ^{13}C NMR (75 MHz, $CDCl_3$) δ = 149.7, 148.3, 147.7, 134.6, 133.8, 133.1, 132.9, 123.9. IR (KBr, cm^{-1}) 3423 (br), 3040, 1481, 1400, 1340.4, 1025, 1005, 903, 799, 710, 625. MS *m/z* 233 (M^+). Elemental analysis: Calcd for $C_{15}H_{11}N_3$: C, 77.23; H, 4.75; N, 18.01. Found: C, 77.30; H, 4.44; N, 17.91.

Preparation and physical properties of 3a·4$(NO_3)_{18}$: Ligand **1a** (0.04 mmol) and **2** (0.1 mmol) were combined in H_2O (1.5 mL) and stirred for 5 h at 70 °C. To this solution, aqueous solution (0.5 mL) of Na·**4** (0.01 mmol) was added and the mixture was stirred at 70 °C for 9 h. After filtration, addition of acetone (10 mL) to the solution precipitated a colorless powder which was collected and dried under reduced pressure to give **3a·4** in 81% yield. Mp. 256-258 °C (decomp.). ^1H NMR (500 MHz, D_2O, 60 °C, TMS as an external standard) δ = 10.12 (s, 8H, Py*H*α), 10.06 (s, 8H, Py*H*α), 9.55 (brs, 8H, Py*H*α), 9.34 (brs, 8H, Py*H*α), 8.98 (s, 4H, Py*H*γ), 8.94 (d, *J* = 6.4 Hz, 8H, Py*H*α), 8.91 (s, 8H, Py*H*γ), 8.21 (d, *J* = 7.7 Hz, 8H, Py*H*γ), 7.70 (t, *J* = 6.4 Hz, 8H, Py*H*β), 5.32 (brs, 4H, **4**·Ar*H*), 4.99 (brs, 4H, **4**·Ar*H*), 3.0-2.8 (m, 40H, CH_2); ^{13}C NMR (125 MHz, D_2O, 60 °C, TMS as external standard) δ = 153.2 (*C*H), 151.5 (*C*H), 151.3 (*C*H), 151.2 (*C*H), 150.0 (*C*H), 139.4 (*C*H), 135.6 (*C*H and *Cq*), 134.2 (*Cq*), 133.7 (*Cq*), 133.5 (*C*H), 133.3 (*Cq*), 129.1 (**4**·*C*H), 128.2 (*C*H), 122.7 (**4**·*C*H), 48.1 (*C*H_2), 48.0 (*C*H_2), 47.9 (*C*H_2). This NMR characterization was based on the 2D NMR measurements such as HH-COSY, NOESY, CH-COSY. These spectra will be present in the Appendix at the end of this thesis. IR (KBr, cm^{-1}) 1589, 1385, 1059, 704. Elemental analysis: Calcld for $C_{134}H_{156}N_{58}O_{58}Pd_{10}\cdot25H_2O$: C, 32.05; H, 4.13; N, 16.18. Found: C, 32.24; H, 3.98; N, 15.97

Preparation and physical properties of 3b·4$(NO_3)_{14}$: Ligand **1b** (0.15 mmol) and Pd(II) complex **2** (0.075 mmol) were combined in H_2O (1.0 mL) and stirred for 10 min at 70 °C. To this solution, aqueous solution (0.19 mL) of Na·**4** (0.019 mmol) was added and the mixture was stirred at 70 °C for 2 h. After filtration, addition of acetone (5 mL) to the solution precipitated a colorless powder which was collected and dried under reduced pressure to give **3b·4**$(NO_3)_{14}$ in 85% yield. Mp. 263-265 °C (decomp.). ^1H NMR (500 MHz, D_2O, 60 °C, TMS as an external standard) for isomer **A**, δ = 10.09 (s, 8H, Py*H*a), 9.63 (s, 8H, Py*H*a), 9.39 (s, 8H, Py*Ha*) 8.96 (d, *J* = 5.8 Hz, 8H, Py*H*a), 8.86 (s, 8H, Py*H*g), 8.25 (d, *J* = 8.1 Hz, 8H, Py*H*g), 7.71 (t, *J* = 6.6 Hz, 8H, Py*H*b), 5.40 (d, *J* = 6.9 Hz, 8H, Ar*H*), 4.99 (d, *J* = 6.9 Hz, 8H, Ar*H*) 2.9-2.8 (m, 32H, CH_2); for isomer **B**, δ = 10.09 (s, 4H, Py*H*a), 10.07 (s, 4H, Py*H*a), 9.66 (s, 4H, Py*H*a), 9.47 (s, 8H, Py*H*a), 9.34 (s, 4H, Py*H*a), 8.93 (d, *J* = 5.8 Hz, 4H, Py*H*a), 8.89 (d, *J* = 5.8 Hz, 4H, Py*H*a), 8.88 (s, 4H, Py*H*g), 8.74 (s, 4H, Py*H*g), 8.39 (d, *J* = 8.1 Hz, 4H, Py*H*g), 8.15 (d, *J* = 8.1 Hz, 4H, Py*H*g), 7.82 (d, *J* = 6.6 Hz, 4H, Py*H*b), 7.55 (t, *J* = 6.6 Hz, 4H, Py*H*b), 5.46 (brs, 4H, Ar*H*), 4.93 (brs, 4H, Ar*H*), 2.9-2.8 (m, 32H, CH_2). This NMR characterization was based on the HH-COSY measurement. This specturm will be present in the Appendix. IR (KBr) 3406, 3072, 1591,1385,1138, 1059, 891, 812, 702, 453 cm^{-1}. Elemental analysis: Calcd for $C_{110}H_{128}N_{46}O_{46}Pd_8 \cdot 18H_2O$: C, 32.98; H, 4.13; N, 16.08. Found: C, 32.96; H, 3.99; N, 15.96. CSI-MS: *m/z* 511 $[M-6(NO_3)]^{6+}$; 674 $[M-5(NO_3)]^{5+}$; 858 $[M-4(NO_3)]^{4+}$; 1165 $[M-4(NO_3)]^{3+}$.

Preparation and physical properties of 3c·4$(NO_3)_{14}$: Complex **3c·4** for NMR measurement was prepared by reaction of **1c**, **2** and **4** in D_2O in ratio of 4:6:1. ^1H NMR (500 MHz, D_2O, 25 °C, TMS as external standard) δ = 9.88 (d, *J* = 2.0 Hz, 8H, Py*H*α), 9.56 (d, *J* = 1.5 Hz, 8H, Py*H*α), 9.06 (dd, *J* = 5.8, 1.0 Hz, 8H, Py*H*α), 8.92 (s, 4H, Py*H*γ), 8.21 (d, *J* = 8.2 4H, Py*H*γ), 7.68 (dd, *J* = 8.2, 5.8 Hz, 8H, Py*H*β), 5.57 (d, *J* = 8.2 Hz, 4H, **4**·Ar*H*) , 5.01 (d, *J* = 8.2 Hz, 4H, **4**·Ar*H*), 3.0-2.9 (m, 24H, CH_2); ^{13}C NMR (125 MHz, D_2O, 25 °C, TMS as external standard) δ = 170.4 (*Cq*), 153.4 (*C*H), 150.2 (*C*H), 149.8 (*C*H), 138.5 (*C*H), 137.6 (**4**·*Cq*), 137.5 (**4**·*C*q), 135.4 (*C*H), 134.7 (*Cq*), 132.9 (*Cq*), 129.5 (**4**·*C*H), 128.3 (*C*H), 122.2 (**4**·*C*H), 47.8 (CH_2), 47.7 (CH_2). This NMR characterization was based on the 2D NMR measurements such as HH-COSY, CH-COSY, and HMBC. These spectra will be present in the Appendix. Although the formation of 1:1 complex (**3c·4**) was confirmed by NMR, crystallization always gave 1:2 complex **3c·(4)**$_2$. Isolation and physical properties of **3c·(4)**$_2$ (nitrate salt): Compound Na·**4** (0.018 mmol) was added to a solution of **1c** (0.035 mmol) and **2**

(0.052 mmol) in H_2O (0.5 mL). The mixture was heated at 70 °C for 1 d and filtered. Slow diffusion of ethanol into the solution for 4 d precipitated a colorless powder, which was collected and dried under reduced pressure to give **3c**·(**4**)$_2$ (nitrate salt) in 95% yield (based on **4**). Mp. 226-227 °C (decomp.). IR (KBr, cm^{-1}) 1583, 1539, 1385, 1057, 702. Elemental analysis: Calcd for $C_{100}H_{108}N_{32}O_{32}Pd_6 \cdot 15H_2O$: C, 37.78; H, 4.38; N, 14.10. Found: C, 37.74; H, 4.26; N, 14.16. CSI-MS: *m/z* 469 $[M-6(NO_3)]^{6+}$; 639 $[M-5(NO_3)]^{5+}$; 868 $[M-4(NO_3)]^{4+}$.

X-ray crystallographic analysis of 3c·(4)$_2$(NO$_3$)$_8$: A mixture of **1c** (46.6 mg, 0.2 mmol), **2** (87.2 mg, 0.3 mmol) and **4** (26.3 mg, 0.1 mmol) was stirred for 1 h at 70 °C and cooled to room temperature. After filtration, *i*-propyl alcohol slowly diffused into the solution for 2 d to give X-ray quality crystals. X-ray data for $C_{100}H_{108}N_{32}O_{32}Pd_6 \cdot 26H_2O$: M = 3377.58, monoclinic, space group *P21/n*; a = 17.429(3), b = 14.785(3), c = 27.061(5) Å, β = 101.555(4), V = 6832(2) Å^3; D_C = 1.642 g/cm^3, z = 2; $F(000)$ = 3448; $\mu(MoK\alpha)$ = 0.876 mm^{-1}; temp. = 293 K; 28290 reflections collected, 11995 ($I>2\sigma(I)$) reflections observed; R_1 = 0.0812; wR_2 = 0.2110. The data for **3c** was collected on a Siemens SMART/CCD diffractometer. Diffracted data were corrected for absorption using the SADABS[15] program. SHELXTL[16] was used for the structure solution and refinement was based on F^2. All non-hydrogen atoms were refined anisotropically. Hydrogen atoms were fixed in calculated positions and refined isotropically with thermal parameters based upon the corresponding C-atoms [U(H) = 1.2 Ueq (C)]. Pertinent crystallographic data will be present in the Appendix.

References

(1) Iijima, S. *Nature* **1991**, *354,* 56.

(2) (a) Harada, A.; Li, J.; Kamachi, M. *Nature* **1992**, *356,* 325. (b) Harada, A. J. Li, M. Kamachi, *Nature* **1993**, *364,* 516. (c) For a review: A. Harada, in *Modular Chemistry*, Michl, J. Ed.; Kluwer Academic Publishers: Dordrecht, The Netherlands, *1997*; p.361.

(3) (a) Ghadiri, M. R.; Granja, J. R.; Milligan, R. A.; McRee, D. E.; Khazanovich, N. *Nature* **1993**, *336,* 324. (b) For a review: Hartgerink, J. D.; Clark, T. D.; Ghadiri, M. R. *Chem. Eur. J.* **1998**, *3,* 1367.

(4) Shimizu, T.; Kogiso, M.; Masuda, M. *Nature* **1996**, *383*, 487.

(5) Kimizuka, N.; Kawasaki, T.; Hirata, K.; Kunitake, T. *J. Am. Chem. Soc.* **1995**, *117*, 6360.

(6) Ligand **1a** was prepared by Pd(0)-catalyzed cross-coupling reaction of 3,5-dibromopyridine and 5-tributylstannyl-3,3'-bipyridine: Fujita, M.; Oka, H.; Ogura, K. *Tetrahedron Lett.* **1995**, *36,* 5247.

(7) (a)Fujita, M.; Yazaki, J.; Ogura, K. *J. Am. Chem. Soc.* **1990**, *112*, 5645. (b) Fujita, M. *Acc. Chem. Res.* **1999**, *32,* 5 (c) Fujita, M. in *Comprehensive Supramolecular Chemistry*, Sauvage, J.-P., Hosseini, M. W., Eds.; Pergamon Press: Oxford, 1995; Vol. 9, Chap. 7.

(8) NOE cross peaks were observed between H_c-H_e, H_d-H_f, H_f-H_h and H_g-H_i in **3a**, indicating the coplanar, zigzag conformation of ligand **1a**.

(9) Sakamoto, S.; Fujita, M.; Kim, K.; Yamaguchi, K. *Tetrahedron* in press.

(10) Since these guests were insoluble in water, experiments were carried out in a D_2O-Hexane two-phase system: an aqeous solution prepared from **1a** and **2** was combined with a hexane solution of a guest and the mixture was stirred at 70 °C for several hours. ^{1}H NMR of the aqueous phase showed the quantitative formation of **3a·G** (**G**= biphenyl or *p*-terphenyl).

(11) Organic templating: (a) Anderson, S.; Anderson, H. L.; Sanders, J. K. M. *Acc. Chem. Res.* **1993**, *26*, 469. (b) Fujita, M.; Nagao, S.; Ogura, K. *J. Am. Chem.*

Soc. **1995**, *117*, 1649. (c) Bilyk A.; Harding, M. M. *J. Chem. Soc., Chem. Commun.* **1995**, *1995*, 1697. (d) Ibukuro, F.; Kusukawa, T.; Fujita, M. *J. Am. Chem. Soc.* **1998**, *120*, 8561.

(12) Metal-ion templating: (a) Dietrich-Buchecker, C. O.; Sauvage, J.-P.; Kintzinger, J.-P. *Tetrahedron Lett.* **1983**, *24*, 5095. (b) For a review: Dietrich-Buchecker, C. O.; Sauvage, J.-P. *Chem. Rev.* **1987**, *87*, 795.

(13) Anion templating: (a) Müller, A.; Penk, M.; Rohlfing, R.; Krickemeyer, E.; Döring, J. *Angew. Chem., Int. Ed. Engl.* **1990**, *29*, 926. (b) Yamase, T.; Ohtaka, K. *J. Chem. Soc., Dalton Trans.* **1994**, 2599. (c) Müller, A.; Reuter, H.; Dillinger, S. *Angew. Chem., Int. Ed. Engl.* **1995**, *34*, 2328. (d) Hansenknopf, B.; Lehn, J.-M.; Knesel, B. O.; Baum, G.; Fenske, D. *Angew. Chem., Int. Ed. Engl.* **1996**, *35*, 1838. (e) Fleming J. S.; Mann, K. L. V.; Carraz, C.-A.; Psillakis, E.; Jeffery, J. C.; MacCleverty, J. A.; Ward, M. D. *Angew. Chem., Int. Ed.* **1998**, *37*, 1279.

(14) Drew, H.D. K.; Pinkard, F. W.; Treston, G. H.; Wardlaw, W. *J. Chem. Soc.* **1932**, 1895.

(15) Sheldrick, G. M. *SADABS*: Univ. Gottingen, 1996.

(16) Sheldrick, G. M. *SHELXTL, Release 5.03*; Siemens Analytical X-ray Instruments Inc.: Madison, WIS, 1994.

Chapter 5

Dynamic Behavior of Rod-Like Guest Molecules in Self-Assembled Coordination Nanotubes

Abstract: The dynamics of guest molecule accommodated in the coordination nanotubes which were described in the previous chapter was investigated by variable temperature NMR measurements. Guest molecules are found to shuttle in the tube without flipping at low temperatures, but intermolecularly exchange at elevated temperatures. The tube assembled from tetrakis(3,5-pyridine) was isolated as a single isomer by recystallization. The structure of this isomer was confirmed by X-ray crystallography. The single isomer slowly turned into an equilibrium mixture of two structural isomers in aqueous media.

5.1 Introduction

Studies on the dynamic behavior of guest molecules accommodated in the host framework are rapidly growing recently because host-guest complexes possess potential for data storage devices[1] and artificial enzymes. Particularly, in tubular shaped host, guests are expected to move only in a one-dimensional direction within a tightly fitted tubular space. Such a restricted guest motion would lead to novel functions of tubular molecules: e.g., shape-selective molecular transportation and (catalytic) chemical transformation.[2, 3] This chapter describes NMR studies on the dynamic motion of rod-like guests accommodated in coordination nanotubes $\mathbf{2a}^{20+}$ and $\mathbf{2c}^{12+}$.[4] Dynamics of the interconversion between the two isomers of $\mathbf{2b}^{16+}$ will also be discussed.

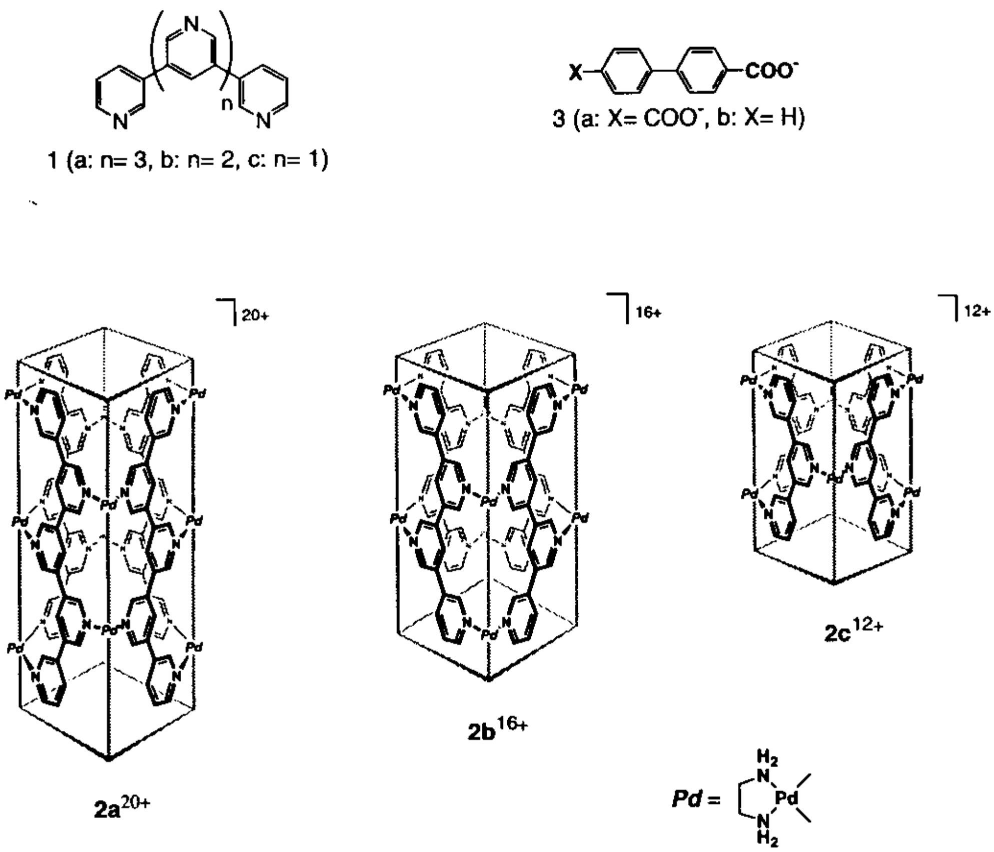

Chart 1.

5.2 Results and Discussion

5.2.1 The motion of a guest molecule accommodated in coordination nanotubes

In Chapter 4, temperature dependence of coordination nanotube $\mathbf{2a}^{20+}\cdot\mathbf{3a}^{2-}$ in ^{1}H NMR spectra has been described. By the temperature dependency, mobility of the guest molecule $\mathbf{3a}^{2-}$ within the tube $\mathbf{2a}^{20+}$ can be discussed. Thus, in order to address the guest motion within the tube, asymmetric biphenyl derivative $\mathbf{3b}^{-}$ was used as a template instead of $\mathbf{3a}^{2-}$. When enPd$(NO_3)_2$, **1a** , and Na·**3b** were combined in H_2O in a 10:4:1

molar ratio, tube structure $\mathbf{2a}^{20+}\cdot\mathbf{3b}^{-}$ was assembled. The ^{1}H NMR spectra of this product was also temperature dependent. At low temperature, the signals of H*d*, H*d'*, H*e*, and H*e'* were observed independently (δ = 9.47, 9.40, 9.27, 9.16 ppm respectively) because of asymmetric $\mathbf{3b}^{-}$ made each end of the tube different environment. The spectrum indicates that $\mathbf{3b}^{-}$ shuttles in the tube at low temperature. However, upon heating, those signals became broader and coalesced into two singlets because the guest molecules started moving on the NMR timescale and the motion became rapid on the spectrum timescale (Figure 1).

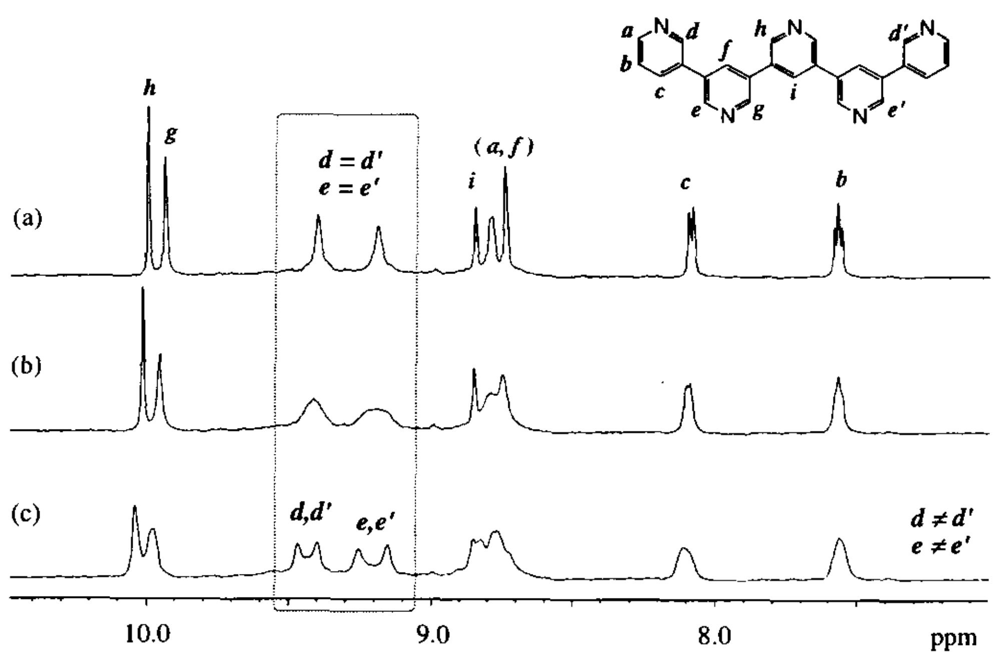

Figure 1. Variable-temperature ^{1}H NMR spectra recorded in D_2O at (a) 55 °C, (b) 41 °C, and (c) 25 °C.

The rate constant kc = 113 s^{-1}, and activation energy, $\Delta G^{\#}(Tc)$ = 15.5 kcal/mol were calculated by using following equations:[5] $kc = 2^{-0.5}\pi\Delta\nu$, $\Delta G^{\#}(Tc)$ =

$RTc[22.96+\ln(Tc/\Delta v)]$, where Tc (= 41 °C) is coalescence temperature and Δv (= 51 Hz) is separation in Hz between the two signals.

In order to obtain further information of the motion of the guest molecule, variable temperature NMR spectra were recorded at different host-guest concentration ratio. Interestingly, when two equivalents of **3b**$^-$ was used, Tc was decrease by 28 °C (corresponding to 1.5 kcal/mol in $\Delta G^{\neq}_c$). The dependence of Tc upon host-guest ratio can be ascribed to the deference in the guest exchange mechanism. When H:G = 1:2, the guest exchange takes place without emptying the tube via an SN2-like transition state (or intermediate) with lower activation energy (Figure 2a). On the other hand, when H:G = 1:1, the guest has to exchange via an SN1-like transition state (or intermediate) with higher energy involving the empty host (Figure 2b).

^{1}H NMR studies for **2c**$^{12+}$·**3b**$^-$ also showed similar temperature and molar ratio dependence. When H:G = 1:1, the signals of H*d*, H*d'*, H*e*, and H*e'* (Scheme 2) were observed independently (δ = 9.40, 9.60, 9.51, 9.84 ppm, respectively) at low temperature. Upon heating, these signals coalesced into two singlets at 29 °C (Δv = 50.5 Hz, kc = 112 s^{-1}, $\Delta G^{\neq}_c$ = 14.8 kcal/mol). However, at a H/G ratio of 1:2 ([**2c**$^{12+}$]:[**3b**$^-$]), the signals did not coalesce even at 5 °C.

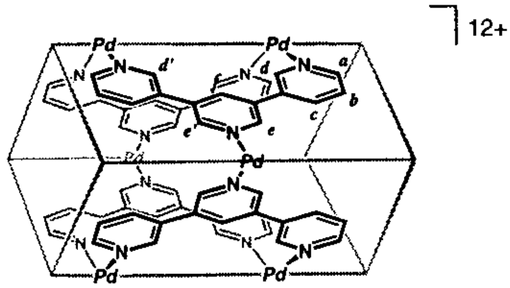

2c^{12+}

Chart 2.

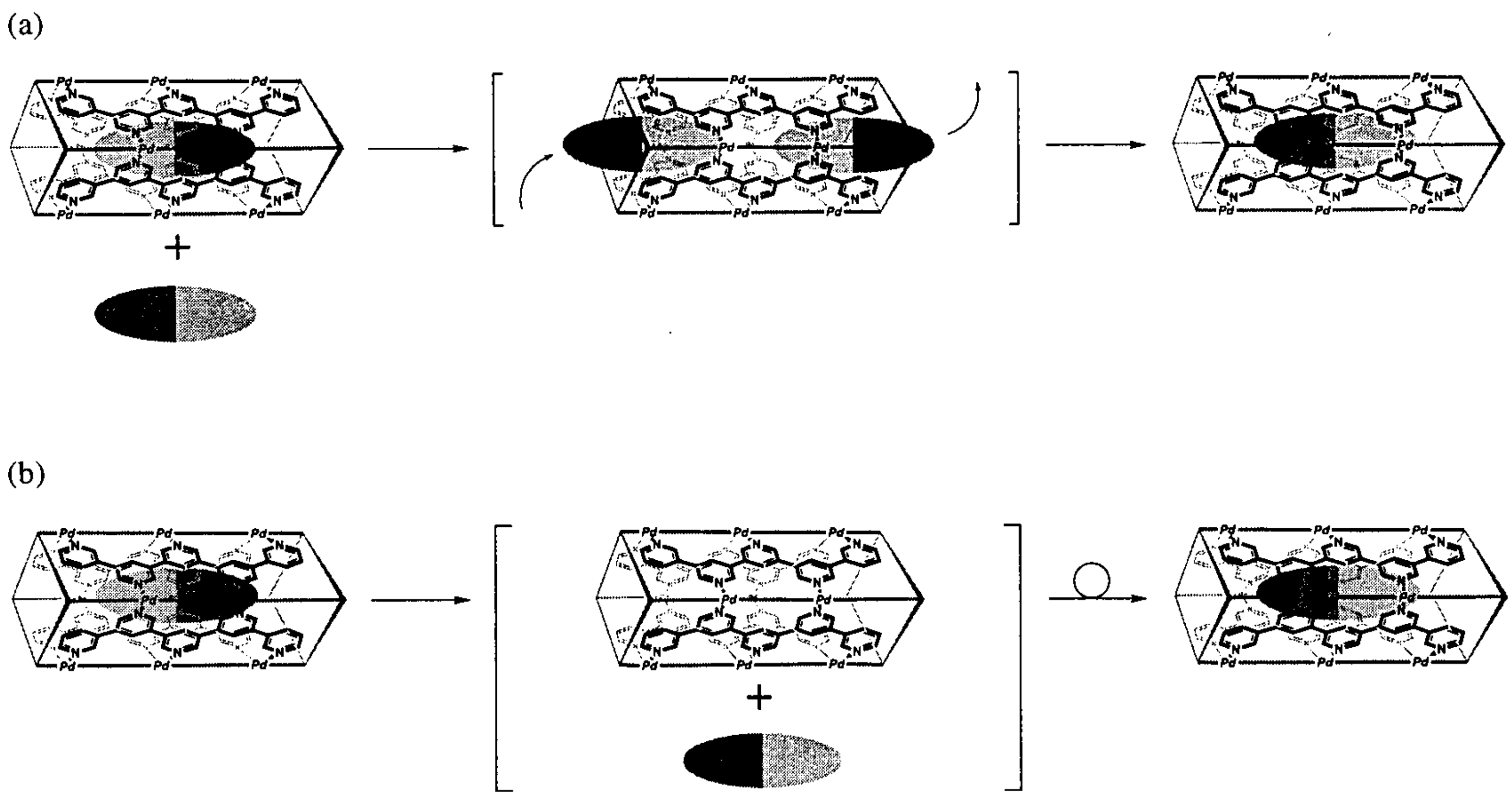

Figure 2. Illustration for the mechanism of guest exchange (a) at [H]:[G]=1:2, (b) at [H]:[G]=1:1.

5.2.2 The interconversion of a nanotube between two isomers

For coordination nanotube $\mathbf{2b}^{16+}$ which assembles from tetrakis(3,5-pyridine) ligand **1b**, structural isomers **A** and **B** can be considered as depicted in Figure 3. In isomer **A**, the C_2-symmetric situation of each ligand is broken and 14 protons of **1b** framework should be independently observed in ^{1}H NMR. In contrast, each ligand is placed on a C_2-symmetric environment in isomer **B** and only seven protons corresponding to half of the framework of **1b** should be observed in ^{1}H NMR. Indeed, ^{1}H NMR spectrum of the crude reaction solution showed approximately 1:1 mixture of isomer **A** and **B**, although some of the signals were overlapped.

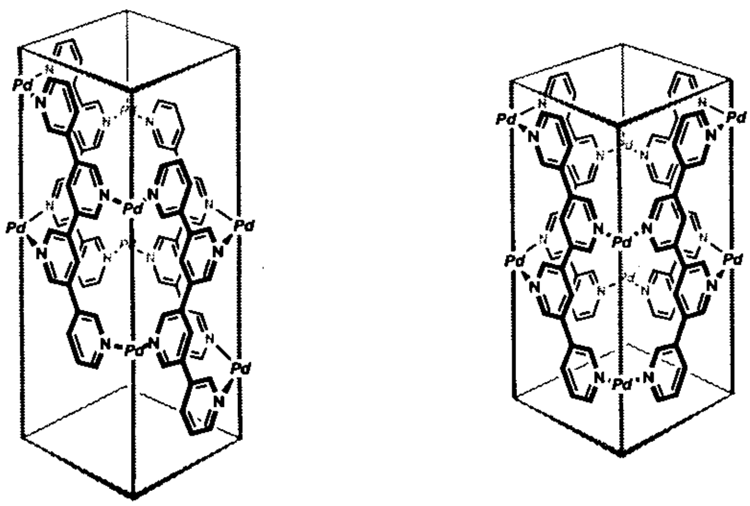

A B

Figure 3. (a) Schematic presentation of the structural isomers of **2b** (isomers **A** and isomer **B**).

Interestingly, slow diffusion of ethyl alcohol into aqueous solution of the isomer mixture of $\mathbf{2b}^{16+}\cdot\mathbf{3a}^{2-}$ ([$\mathbf{2b}^{16+}$]:[$\mathbf{3a}^{2-}$] = 1:2) crystallized isomer **A** from the solution. After the crystals were dissolved in D_2O without heating, ^{1}H NMR spectrum was recorded within 1 h. The spectrum showed only isomer **A** encapsulating **3a**$^{2-}$ and one equivalent of free **3a**$^{2-}$.[6] This observation shows that isomer **A** has considerable kinetic stability and dose not isomerized into **B** within 1h. However, when the solution was kept at room temperature, the signals of isomer **B** appeared in the ^{1}H NMR spectrum. After 13 days, ratio of **A**:**B** was almost equilibrated at approximately 6:4 (Figure 4). At 70 °C, an equilibrium mixture was obtained within 1h, whereas no isomerization was observed below 5 °C.

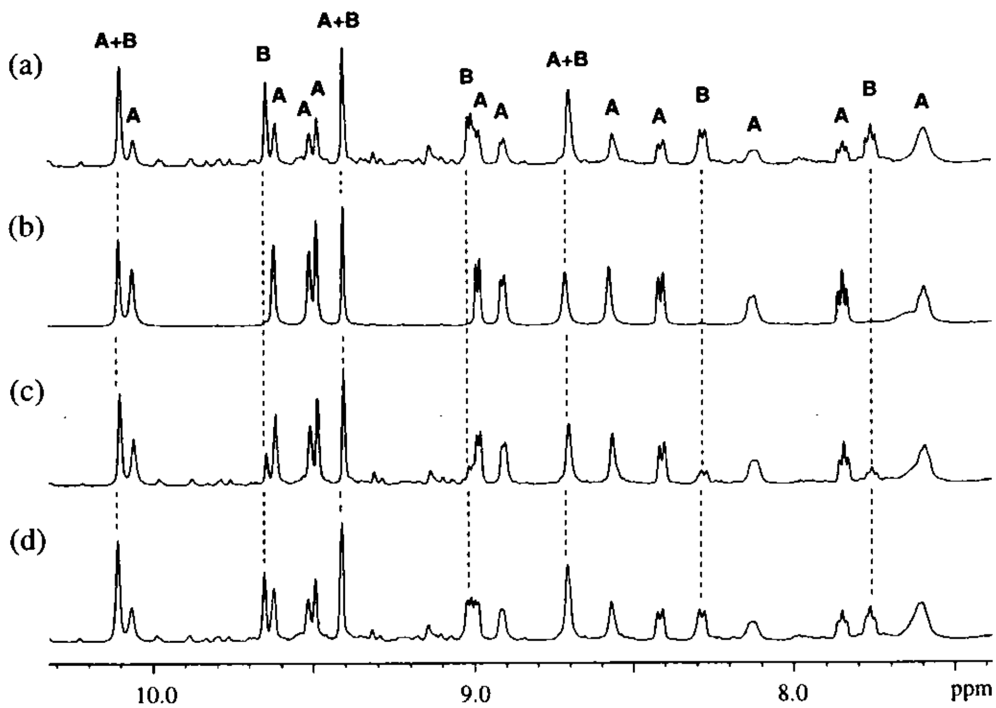

Figure 4. (a) Spectroscopic observation of isomerism of **2b** recorded in D_2O. (a) Crude mixture. (b) At 1 h after the precipitates dissolved. (c) After 5 d. (d) After 13 d.

The structure of isomer **A** finally also confirmed by crystallographic analysis. The rod-like guest was surrounded by four ligands which were connected by eight enPd(II) units (Figure 5). The connectivity of ligands completely agrees with NMR finding. The tube has distorted square shape cavity. In the cavity, quite efficient π-π and CH-π interactions[7,8] between the tube and guest were observed as they were in the crystal structure of $\mathbf{2c}^{12+}\cdot\mathbf{3a}^{2-}$.[4] Another moiety of $\mathbf{3a}^{2-}$, nitrate ions, and water molecules located out side of $\mathbf{2b}^{16+}$.

(a) (b)

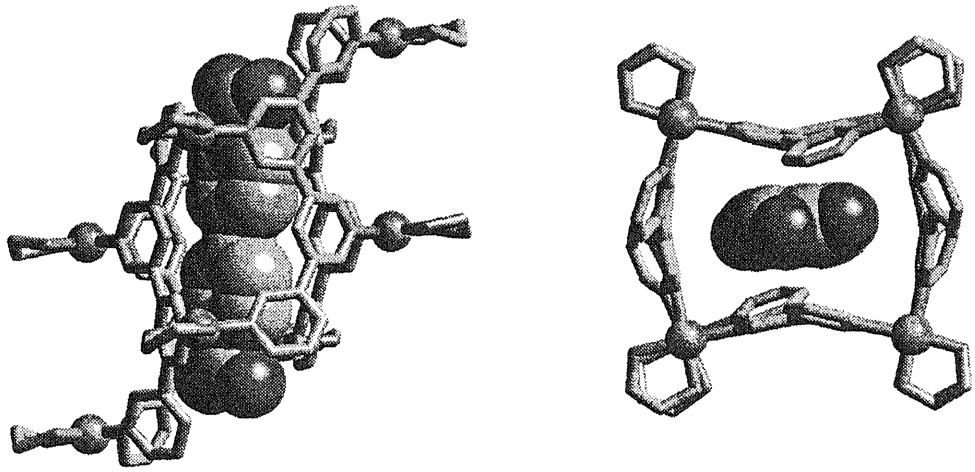

Figure 5. (a) Crystal structure of $\mathbf{2b}^{16+}\cdot\mathbf{3a}^{2-}$ (isomer **A**). (b) Top view. For clarity, H atoms, water molecules, NO_3^- ions, and **3a** located outside are omitted.

5.3 Conclusion

The dynamics of an asymmetric guest in coordination nanotubes were studied by variable temperature NMR measurements. The guest allowed to move in a one-dimensional way and exchange only at high temperature via SN1 or SN2 mechanism.

Since cavity of **2a** is long enough to accommodate more than two guest molecules, one can expect the tube to include more than two guests, and, hence provide novel functions such as catalysis and stabilization of guests.[9, 10]

5.4 Experimental Section

General: $enPd(NO_3)_2$ was prepared according to reported procedures.[11] The sodium salt of $\mathbf{3a}^{2-}$ and $\mathbf{3b}^{-}$ were prepared by combining sodium hydroxide and corresponding carboxyacids which were obtained commercially. Variable temperature ^1H NMR, HH-COSY, and NOESY spectra were recorded on a JEOL JNM-LA500 (500 MHz) spectrometer.

Preparation and physical properties of $\mathbf{2a}^{20+}\cdot\mathbf{3b}^{-}$: $enPd(NO_3)_2$ (0.1 mmol) and **1a** (0.04 mmol) were combined in D_2O (2.0 mL) and stirred for 5 h at 70 °C. To this solution, aqueous solution (0.1 mL) of Na·**3b** (0.01 mmol) was added and the mixture was stirred at 70 °C for 9 h. ^1H NMR (500 MHz, D_2O, 55 °C, TMS as an external standard) δ = 10.42 (s, 8H, Py*H*α), 10.36 (s, 8H, Py*H*α), 9.82 (s, 8H, Py*H*α), 9.61 (s, 8H, Py*H*α), 9.27 (s, 4H, Py*H*γ), 9.21 (s, J = 6.4 Hz, 8H, Py*H*α), 9.16 (s, 8H, Py*H*γ), 8.51 (d, J = 7.7 Hz, 8H, Py*H*γ), 7.99 (t, J = 6.4 Hz, 8H, Py*H*β), 5.32 (brs, 4H, **3b**·Ar*H*), 4.99 (brs, 4H, **3b**·Ar*H*), 3.0-2.8 (m, 40H, CH_2).

Preparation and physical properties of $\mathbf{2c}^{12+}\cdot\mathbf{3b}^{-}$: $enPd(NO_3)_2$ (0.15 mmol) and **1c** (0.1 mmol) were combined in D_2O (3.0 mL) and stirred for 1 h at 70 °C. To 0.6 mL of this solution, aqueous solution (0.05 mL) of Na·**3b** (0.005 mmol) was added and the mixture was stirred at 70 °C for 4 h. ^1H NMR (500 MHz, D_2O, 15 °C, TMS as an external standard) δ = 9.94 (s, 4H, Py*H*α), 9.84 (s, 4H, Py*H*α), 9.60 (s, 4H, Py*H*α), 9.51 (s, 4H, Py*H*α), 9.08 (s, 8H, Py*H*α), 8.91 (s, 4H, Py*H*γ), 8.27 (s, 8H, Py*H*γ), 7.72 (s, 8H, Py*H*β), 5.93 (brs, 1H, **3b**·Ar*H*), 5.53 (brs, 2H, **3b**·Ar*H*), 5.14 (brs, 2H, **3b**·Ar*H*), 5.01 (brs, 2H, **3b**·Ar*H*), 3.0-2.9 (m, 24H, CH_2); ^{13}C NMR (125 MHz, D_2O, 25 °C, TMS as an external standard) δ = 169.183 (**3b**·*Cq*), 152.7 (*C*H), 149.7 (*C*H), 149.5 (*C*H), 149.0 (*C*H), 139.3 (**3b**·*Cq*), 138.5 (*C*H), 138.3 (**3b**·*Cq*), 137.7 (*C*H), 135.1 (*C*H), 134.2 (*Cq*), 133.9 (*Cq*), 132.6 (*Cq*), 132.4 (*Cq*), 130.1 (**3b**·*C*H), 128.7 (**3b**·*C*H), 128.2 (**3b**·*C*H), 127.6 (*C*H), 127.5 (*C*H), 122.0 (**3b**·*C*H),), 121.6 (**3b**·*C*H), 46.9 (CH_2), 46.8 (CH_2).

Recrystallization of $\mathbf{2b^{16+}\cdot(3a^{2-})_2}$: A mixture of **1b** (23.3 mg, 0.075 mmol), $enPd(NO_3)_2$ (43.6 mg, 0.15 mmol) and Na_2·**3a** (10.7 mg, 0.038 mmol) was stirred for 1 h at 70 ℃ and cooled to room temperature. After filtration, ethyl alcohol slowly diffused into the solution for 3 weeks to give crystals. NOESY spectrum of the product showed several NOE cross corresponding to isomer **A**. The spectra of the NOESY and relational HH-COSY will be presented in the Appendix at the end of this thesis. X-ray crystallographic data was collected by using this crystal.

X-ray crystallographic analysis of $\mathbf{2b\cdot(3a)_2\cdot(NO_3)_{12}}$: X-ray data for $C_{124}H_{216}N_{47}O_{93}Pd_8$: M = 4704.64, triclinic, *P*-1; a = 17.549(2), b = 20.344(3), c = 29.840(4) Å, α = 107.231(3), β = 91.243(3), γ = 114.438(3) °, V = 9133 Å^3, Z = 2; D_c = 1.711 g/cm^3; $F(000)$ = 4802; μ(Mo$K\alpha$) = 0.884 mm^{-1}; temp. = 153 K; 31565 reflections collected, 21432 ($I>2\sigma(I)$) reflections observed; R_1= 0.1299; wR_2 = 0.3168. The data for **2b**·(**3a**)$_2$·$(NO_3)_{12}$ was collected on a Siemens SMART/CCD diffractometer. Diffracted data were corrected for absorption using the SADABS[12] program. SHELXTL[13] was used for the structure solution and refinement was based on F^2. All non-hydrogen atoms were refined isotropically. Hydrogen atoms were fixed in calculated positions and refined isotropically with thermal parameters based upon the corresponding C-atoms [U(H) = 1.2 Ueq (C)]. Pertinent crystallographic data will be present in the Appendix.

References

(1) (a) Anelli, P.-L.; Asakawa, M.; Ashton, P. R.; Bissell, R. A.; Clavier, G.; Kaifer, A. E.; Langford, S. J.; Mattelsteg, G.; Menzer, S.; Philip, D.; Slawin, A. M. Z.; Spencer, N.; Stoddart, J. F.; Tolley, M. S.; Williams, D. J. *Chem. Eur. J.* **1997**, *3*, 1113. (b) Benniston, A. C. *Chem. Soc. Rev.* **1996**, *25*, 427. (c) Lane, A. S.; Leigh, D. A.; Marphy, A. *J. Am. Chem. Soc.* **1997**, *119*, 11092.

(2) (a) Harada, A.; Li, J.; Kamachi, M. *Nature* **1992**, *356*, 325. (b) Harada, A;. Li, J.; Kamachi, M. *Nature* **1993**, *364*, 516. (c) For a review: A. Harada, in *Modular Chemistry*, Michl, J. Ed.; Kluwer Academic Publishers: Dordrecht, The Netherlands, 1997; p.361.

(3) (a)Ghadiri, M. R.; Granja, J. R.; Milligan, R. A.; McRee, D. E.; Khazanovich, N.; *Nature* **1993**, *336*, 324. (b) For a review: Hartgerink, J. D.; Clark, T. D.; Ghadiri, M. R. *Chem. Eur. J.* **1998**, *3*, 1367.

(4) Aoyagi, M.; Biradha, K.; Fujita, M. *J. Am. Chem. Soc.* **1999**, *121*, 7457.

(5) Braun, S.; Kalinowski, H.-O.; Berger, S. *100 and More Basic NMR Experiment*; VCH, Weinheim, 1996.

(6) The assignment of the signals of isomer **A** based on COSY and NOESY NMR spectra.

(7) (a) Jorgensen, W. L.; Severance, D. L. *J. Am. Chem. Soc.* **1990**, *112*, 4768. (b) Hunter, C. A.; Sanders, L. K. M. *J. Am. Chem. Soc.* **1990**, *112*, 5525.

(8) (a) Gould, R. O.; Gray, A. M.; Taylor, P.; Walkinshaw, M. D. *J. Am. Chem. Soc.* **1985**, *107*, 5921. (b) Burley, S. K.; Petsko, G. A. *J. Am. Chem. Soc.* **1986**, *108*, 7995.

(9) (a) Heinz, T.; Rudkevich, D. M.; Rebeck, J., Jr. *Nature* **1998**, *394*, 764. (b) Heinz, T.; Rudkevich, D. M.; Rebeck, J., Jr. *Angew. Chem., Int. Ed.* **1999**, *38*, 1136. (c) Kusukawa, T.; Fujita, M. *J. Am. Chem. Soc.* **1999**, *121*, 1397. (d) Kusukawa, T.; Fujita, M. *Angew. Chem., Int. Ed.* **1998**, *37*, 3142.

(10) (a) Kang, J.; Samtamaria, J.; Hilmersson, G.; Rebek, J. Jr. *J. Am. Chem. Soc.* **1998**, *120*, 3650. (b) Kang, J.; Samtamaria, J.; Hilmersson, G.; Rebek, J. Jr. *J.*

Am. Chem. Soc. **1998**, *120*, 7389. (c) Kang, J.; Rebek, J. Jr. *Nature* **1997**, *385*, 50.

(11) Drew, H. D. K.; Pinkard, F. W.; Treston, G. H.; Wardlaw, W. *J. Chem. Soc.* **1932**, 1895.

(12) Sheldrick, G. M. *SADABS*: Univ. Gottingen, 1996.

(13) Sheldrick, G. M. *SHELXTL, Release 5.03*; Siemens Analytical X-ray Instruments Inc.: Madison, WIS, 1994.

Chapter 6

Two- and Three-dimensional Coordination Polytubes Templated by Non-aromatic and Aromatic molecules

J. Am. Chem. Soc. **2000**, *122*, 2397-2398.

Abstract: The formation of the coordination polymers were examined by combining 3,3':5',3":5",3"'-quaterpyridine (**1**) and CuI. The X-ray crystallographic analyses showed that two types of non-interpenetration networks were induced by non-aromatic and aromatic guest molecules in the reaction media. A non-aromatic guest CH_3CN induced two-dimensional polytube $[\mathbf{1}\cdot(Cu_2I_2)]\cdot 2(CH_3CN)\cdot H_2O$ (**2**) with an accessible porosity of 32%. On the other hand, aromatic guests such as nitrobenzene or cyanobenzene induced three-dimensional polytube structures $[\mathbf{1}\cdot(Cu_2I_2)]\cdot 2\mathbf{G}$ (**3a**: **G** = nitrobenzene, **3b**: **G** = cyanobenzene) with large accessible porosity of 48%. The cavities of **2** and **3** were occupied by guest molecules.

6.1 Introduction

Porous coordination polymers are of interest due to their potential for precise and rational design, through control of the shape, size and function of the pores.[1,2] Such polymers generally have open two-dimensional or three-dimensional framework. Despite numerous studies on the porous coordination polymers, there still remains difficulty in predicting cavities in these frameworks because of the frequent occurrence of interpenetration of the networks.[2] This problem can be, in principle, solved by designing organic lignads which disfavor the interpenetration. In this sense, panel-like ligands oligo(3,5-pyridine)s are applicable to construct non-interpenetrate coordination polymers. These ligands assembled into molecular tubes in solution with convergent (en)Pd^{2+} building block.[3] In this chapter, this analogy was extended for construction of polytube structures by connecting divergent metal building block. The polytube structures (Scheme 1) have no possibility of interpenetration. Interestingly, the polytube structures are templated by the guest molecules: i.e., two polytubes possessing different conectivities with the accessible porosity of ca 32 and 48% have been obtained by using different organic guests. The thermal stability of the polymer will be also discussed.

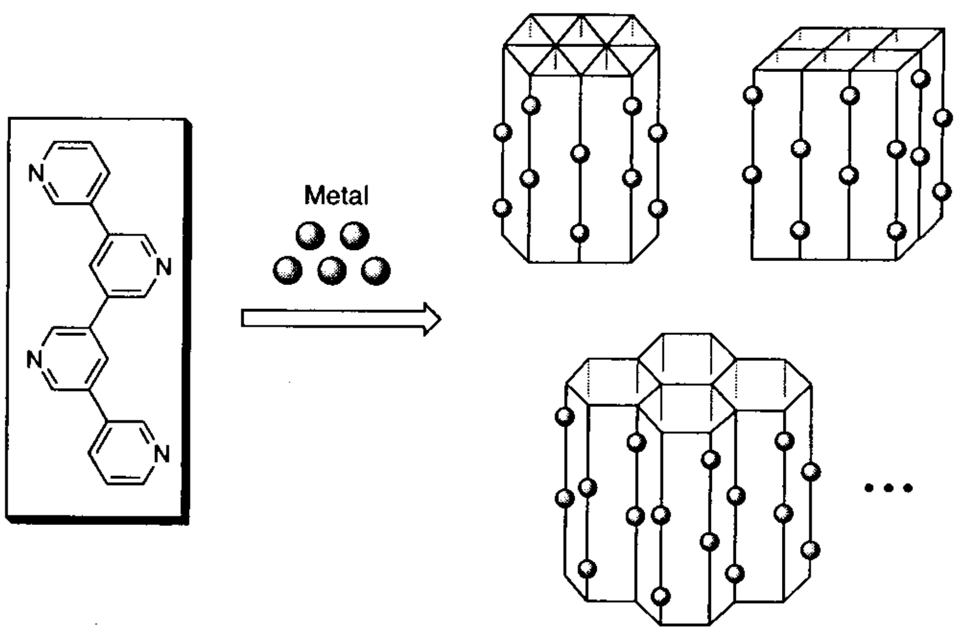

Scheme 1. Schematic illustration for the assembly of polytubes.

6.2 Results and Discussion

6.2.1 Formation of coordination polytubes

After several combination of oligo-(3,5-pyridine) ligands and transition metals were examined, tetrapyridine ligand **1** and CuI were found to be effective for the formation of polytube structures. In the presence of guest molecules, the reaction of CuI in $CHCl_3$ and **1** in nitrobenzene and cyalnobenzene gave guest inclusion complexes [**1**·(Cu_2I_2)]·2(CH_3CN)·H_2O (**2**) or [**1**·(Cu_2I_2)]·2(**G**) (**3a**: **G** = $C_6H_4NO_2$, **3b**: **G** = C_6H_4CN) as single crystals, respectively. The products were characterized by X-ray crystallography. Interestingly, two types of polytube possessing different connectivities were induced by non-aromatic and aromatic guest molecules. In the absence of an aromatic guest, CH_3CN induced two-dimensional polytube structure **2**. On the other hand, aromatic guests, nitrobenzene and cyanobenzene induced three-dimensional polytube structures **3**. In addition, both in **2** and **3**, CuI dimerized into Cu_2I_2 having four binding sites.[4]

6.2.2 Structure of two-dimensional polytube

The X-ray crystallographic structure of **2** revealed a polytube structure by the interconnection of the ligand **1** with Cu_2I_2 units (Figure 1). The conformation of ligand **1** in the network is helicated with interplanar angles, between adjacent pyridine rings, of 5.7°, 46.3° and 44.9°. As a result, the polytube structure is more complicated than those expected from coplanar conformation. Three of the binding sites from each unit point inwards while the remaining points outwards of the tube. Each tube is self-assembled by six units of **1** (24 binding sites) and six units of Cu_2I_2 (24 binding sites). In effect, 18 Cu-N bonds are engaged in assembling one tube. The remaining 12 binding sites, six each from **1** and Cu_2I_2, propagate the tube structure in two dimensions (Figure 1a). The approximate diameter and length of the tube are 8 Å and 7 Å, respectively. Two CH_3CN molecules occupy the cavities in head-to-tail packing. The 2D layers pack on each other in the crystallographic *ab*-plane such that there is a channel formation along *c*-axis (Figure 1b). The accessible porosity of **2** is calculated to be 32%.[6]

(a)

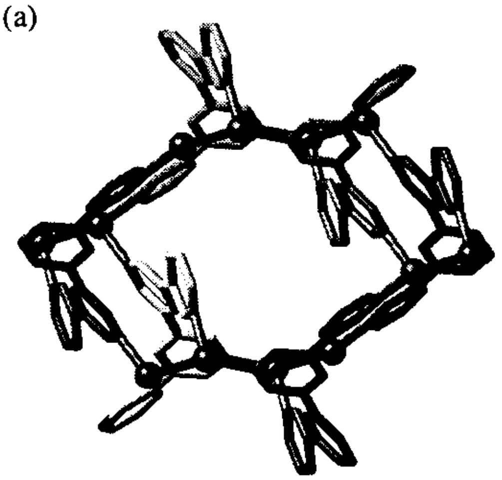

(b)

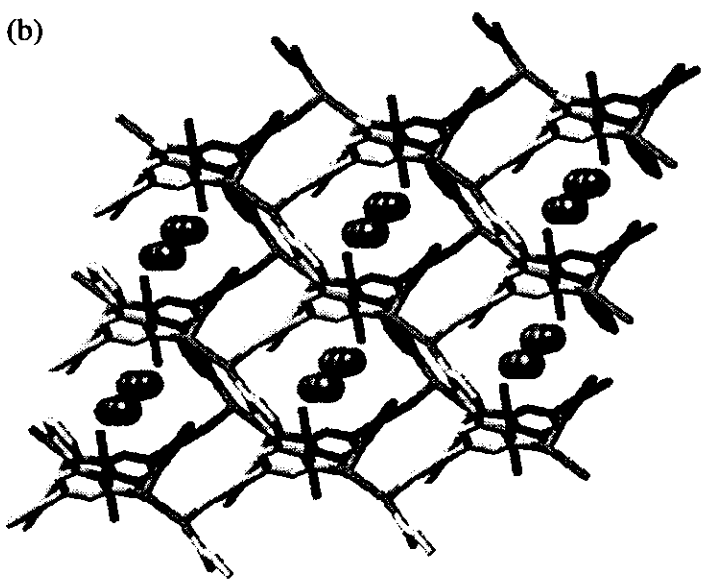

Figure 1. (a) Top view of the 2D-polytube in the crystal structure of **2**. The channels are occupied by the guest, which are omitted for clarity. (b) Representation of the packing of the tubes along crystallographic *c*-axis in **2**. The guest molecules are represented in a space filling mode and a cylinder mode (disordered).

6.2.3 Structures of three-dimensional polytube

The X-ray analysis showed that polytubes **3a** and **3b** accommodated aromatic guest molecules which induced a 3D-network with the large accessible porosity of 48% of the crystal volume (Figure 2). This volume is equivalent to that of the most zeolite open structures such as faujasite, paulingite, and zeolite A families.[8,1n] In both **3a** and **3b**, each polytube is comprised of a 1D-helical network along the crystallographic *a*-axis with the pitch length of 14 Å and with an approximate diameter of 10 Å (Figure 2a). These helices are formed by the interconnection of Cu_2I_2 units with the terminal and middle

(a)

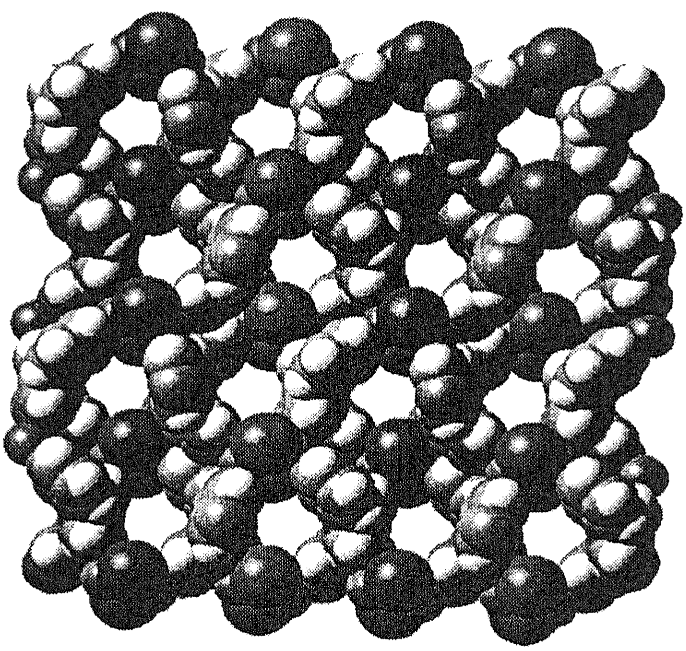

(b)

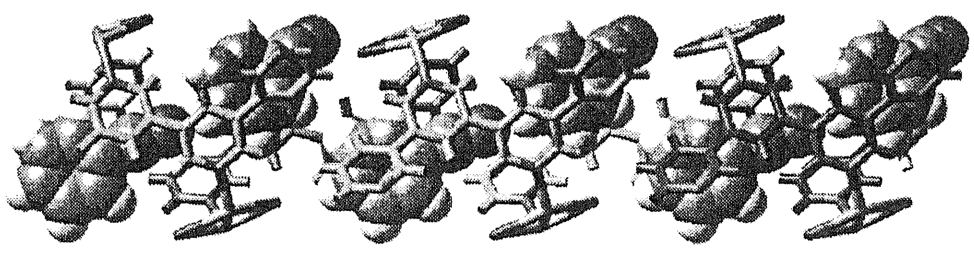

Figure 2. (a) Top view of the space filling drawing of the 3D-polytube in the crystal structure of **3b**. The channels are occupied by guest molecule. (b) Representation of the polytube observed in the crystal structure of **3b**. The guest molecules are represented in a space filling mode.

pyridines of **1** alternately (Figure 2b). As a result, each helix tube is formed by half of the binding sites while the other half extends this tube network in the crystallographic *bc*-plane. In **3a**, the $-NO_2$ group of nitrobenzene is disordered over the two sites with 0.5 occupancy, whereas in **3b**, cyanobenzene has been found without disorder in non-centrosymmetric space group. They form a dimer via C-H···N (H···N: 2.383 Å; C···N; 3.197 Å; C-H···N 146.1°) hydrogen bonds which is further sandwiched between two ligands of **1** via aromatic face-to-face interactions.[9] These interactions cause the formation of a different network structure from **2**. Importantly, although the network is centrosymmetric, the poles of cyanobenzenes are aligned in one direction and resulted in a non centrosymmetric space group.

Thermal stability of **3b** was examined by Thermogravimetric (TG) analysis, IR spectroscopy, and powder X-ray diffraction. In TG analysis, weight loss due to the guest removal at 145 °C was 26%, but above this temperature, the framework was shown to be stable up to 300 °C. The X-ray powder pattern of guest-removed **3b** showed sharp diffraction peaks. Comparing of IR spectra before and after guest removal showed no change except disappearance of guest absorption. These results show that the polytube framework is kept even after guest removal.[10]

Some interesting features are found by comparing the structures of the 2D net **2** and the 3D-net **3**. In both complexes, two of terminal pyridines on ligands A and A' and two of middle pyridines on ligands B and B' are coordinated by a Cu_2I_2 unit. Although the coordination environment of the basic building blocks of **2** and **3** is the same (Figure 3), the network topologies are completely different. In **2**, the ligands A and A' are attached to Cu_2I_2 unit in trans configuration, whereas B and B' are attached in cis configuration. On the other hand, in **3**, both couple of ligands A and A' and B and B' attached to Cu_2I_2 in trans configuration. The Cu-atoms have distorted tetrahedral coordination geometry. The Cu_2I_2 unit is noncoplanar in **2** with the torsion angle of I-Cu-I-Cu is 30° whereas it is coplanar in **3** with the torsion angle of I-Cu-I-Cu is 0°. The Cu-Cu and Cu-I distances ranges between 2.56 and 2.64 Å and 2.64 and 2.70 Å, respectively.

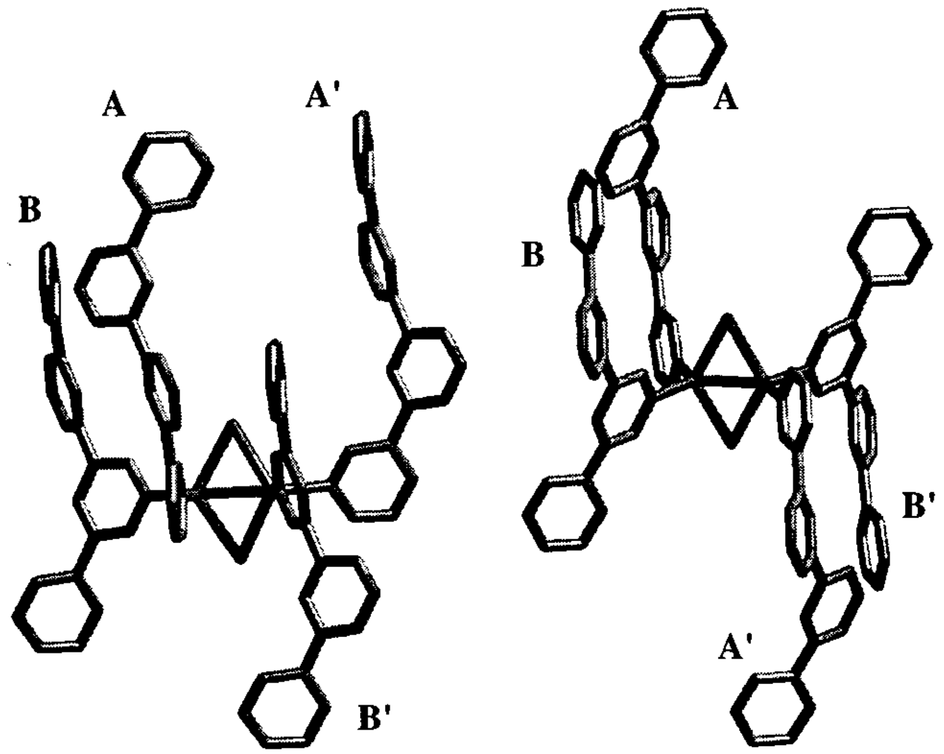

Figure 3. The basic building blocks of **2** (left) and **3b** (right).

6.3 Conclusion

Two-dimensional and three-dimensional coordination polytubes were induced by non-aromatic and aromatic templates, respectively. After removal of guest molecules, the polymer kept its framework and large cavities appeared in the framework. Recently, molecular templated synthesis of inorganic[11] and organic-inorganic hybrid[10] porous materials were reported. But, the point is, the network dimension and pore shape of the polytubes are changeable by template molecules. The template synthesis of the polytubes described in this chapter shows ability to design and produce pore structures with shape and size made to order.

6.4 Experimental Section

General: All of chemicals were obtained commercially and used as received. FTIR spectra were recorded on a SHIMADZU FTIR-8300 spectrometer. TG data was recorded on a TA instrument Thermal Analyst 2100. Powder X-ray diffraction data was corrected on a Mac Science MXP^{3}VA.

Preparation of single crystals of 2, 3a, and 3b: The complex **2**: The CH_3CN solution (10 mL) of CuI (0.098 g, 0.5 mmol) was layered onto a $CHCl_3$ solution (20 mL) of **1** (0.31 g, 1.0 mmol). The solution was allowed to stand for several days to give **2** as yellow crystals. The complexes **3a** and **3b**: The CH_3CN solution (10 mL) of CuI (0.098 g, 0.5 mmol) was layered onto the solution of **1** (0.31 g, 1.0 mmol) in the corresponding guest molecule (20 mL). The solution was allowed to stand for several days to give **3a** and **3b** as yellow crystals. IR for **3b** (KBr, cm^{-1}): before guest removal: 3047, 2226, 1483, 1447, 1408, 1389, 1345, 1026, 887, 800, 758, 708, 688, 548; after guest removal: 3047, 1483, 1412, 1387, 1344, 1016, 883, 808, 710. (cf. cyanobenzene (neat, cm^{-1}): 2230, 1491, 1447, 758, 689, 548)

X-ray Crystal Structure Determinations: Crystal Data of **2**: Triclinic, *P*-1; a = 9.715(1) Å, b = 10.978(2) Å, c = 13.880(2) Å, a = 84.976(3)°, b = 83.800(4)°, γ = 67.496(3)°; V = 1357.8(4) Å^3; Z = 2; D_c = 1.936 g cm^{-3}; 4437 unique reflections out of 5782 with $I > 2\sigma(I)$, final R-factors R_1 = 0.056; wR_2 = 0.090. Crystal Data of **3a**: Monoclinic, *C2/c*, a = 14.081(3) Å, b = 14.413(3) Å, c = 16.420(3) Å, β = 97.814(4)°, V = 3301.4(12) Å^3, Z = 4, D_c = 1.882 g cm^{-3}, 3896 unique reflections out of 10046 with $I > 2\sigma(I)$, final R-factors R_1 = 0.0429; wR_2 = 0.0568. Solving the structure in *Cc* space group resulted in same disordered guest molecule as in *C2/c* space group. Crystal Data of **3b**: Monoclinic, *Cc*, a = 13.975(1) Å, b = 14.563(1) Å, c = 16.437(2) Å, β = 98.576(2)°, V = 3307.7(5) Å^3, Z = 4, D_c = 1.802 g cm^{-3}, 5525 unique reflections out of 10383 with $I > 2\sigma(I)$, final R-factors R_1 = 0.0314; wR_2 = 0.0669. This structure also solved and refined in the *C2/c* space group. However, it resulted in the disordered guest molecule but same *R*-value. Single crystal X-ray diffraction data for all the complexes were collected on a Siemens SMART/CCD diffractometer equipped at 193 K. Diffracted data were corrected for absorption using the SADABS[12] program. SHELXTL[13] was used for the structure solution and refinement was based on F^2. Non hydrogen atoms were refined anisotropically and hydrogen atoms were fixed at calculated positions and refined using a riding model.

References

(1) (a) *Comprehensive Supremolecular Chemistry*; Lehn, J. -M., Ed; Pergamon Press: Oxford, 1996; Vol. 6. (b) Iwamoto, T. (Chapter 2); Lipowski, J. (Chapter 3); Hanotier, J.; Radzizky, P. de (Chapter 4) In *Inclusion Compounds*; Atwood, J. L., Davies, J. E. D., MacNicol, D. D., Eds.; Academic Press: London, 1984; Vol. 1, Chapters 2-4, pp 29-134. (c) Iwamoto, T. *Inclusion Compounds*; Atwood, J. L., Davies, J. E. D., MacNicol, D. D., Eds.; Academic Press: London, 1991; Vol. 5, Chapter 2-4, pp 177-212. (d) Robson, R.; Abrahams, B. F.; Batten, S. R.; Gable, R. W.; Hoskins, B. F.; Liu, J. *Supramolecular Architecture*; Bein, T., Ed.; ACS Symposium Series 499; American Chemical Society: Washington D. C., 1992; Chapter 19. (e) Fujita, M.; Kwon, Y. J.; Washizu, S.; Ogura, K. *J. Am. Chem. Soc.* **1994,** *116,* 1151. (f) Yaghi, O. M.; Davis, C. E.; Li, G; Li, H. *J. Am. Chem. Soc.* **1997**, *119*, 2861. (g) Li, H.; Davis, C. E.; Groy, T. L.; Kelley, D. G.; Yaghi, O. M. *J. Am. Chem. Soc.* **1998**, *120*, 2186. (h) Hennigar, T. L.; MacQuarrie, D. C.; Losier, P.; Rogers, R. D.; Zaworotko, M. J. *Angew. Chem., Int. Ed. Engl.* **1997**, *36*, 972. (i) Janiak, C. *Angew. Chem. Int. Ed. Engl.* **1997**, *36*, 1431 and references therein. (j) Kondo, M.; Yoshitomi, T.; Seki, K.; Matsuzaka, H.; Kitagawa, S. *Angew. Chem., Int. Ed.* **1997**, *36*, 1725. (k) MacGillivary, L. R.; Groeneman, R. H.; Atwood, J. L. *J. Am. Chem. Soc.* **1998**, *120*, 2676. (l) Li, H.; Eddaoudi, M.; Groy, T. L.; Yaghi, O. M. *J. Am. Chem. Soc.* **1998**, *120*, 8571. (m) Choi, H. J.; Suh, M. P. *J. Am. Chem. Soc.* **1998**, *120*, 10622. (n) Chui, S. S.-Y.; Lo, S. M.-F.; Charmant, J. P. H.; Orpen, A. G.; Williams, I. D. *Science* **1999**, *283*, 1148. (o) Gudbjartson, H.; Biradha, K.; Poirier, K. M.; Zaworotko, M. J. *J. Am. Chem. Soc.* **1999**, *121*, 2599. (p) Kepert, C. J.; Rosseinsky, M. J. *Chem. Commun.* **1999**, 375. (q) Kondo, M.; Okubo, T.; Asami, A.; Noro, S.; Yoshitomi, T.; Kitagawa, S.; Ishii, T.; Matsuzaka, H.; Seki, K. *Angew. Chem., Int. Ed.* **1999**, *38*, 140. (r) Tadokoro, M.; Isobe, K.; Uekusa, H.; Ohashi, Y.; Toyoda, J.; Tashiro, K.; Nakasuji, K. *Angew. Chem., Int. Ed.* **1999**, *38*, 95.

(2) (a) Batten, S. R.; Robson, R. *Angew. Chem., Int. Ed.* **1998**, *37*, 1460 and references therein. (b) Blake, A. J.; Champness, N. R.; Chung, S. S. M.; Li, W.-S.; Schröder, M. *Chem. Commun.* **1997**, 1005. (c) Blake, A. J.; Champness, Khlobystov, A. N.; Lemenovskii, D. A.; Li, W.-S.; Schröder, M. *Chem. Commun.* **1997**, 1339. (d) Carlucci, L; Ciani, G.; Macchi, P.; Proserpio, D. M. *Chem. Commun.* **1998**, 1837. (e) Evans, O. R.; Xiong, R.-G.; Wang, Z.; Wong, G. K.; Lin, W. *Angew. Chem., Int. Ed.* **1999**, *38*, 536.

(3) Aoyagi, M.; Biradha, K.; Fujita, M. *J. Am. Chem. Soc.* **1999**, *121*, 7457.

(4) A network structure with a -Cl analog: Yaghi, O. M.; Li, G. *Angew. Chem., Int. Ed.* **1995**, *34*, 207.

(6) Spek, A. L.; 1999, PLATON; A Multi Purpose Crystallographic Tool; Utrecht University, Utrecht, The Netherlands.

(8) Hölderich, W.; Hesse, M.; Näumann, F. *Angew. Chem., Int. Ed. Engl.* **1988**, *27*, 226.

(9) (a) Steiner, T.; Desiraju, G.R. *Chem. Commun.* **1998**, 891. (b) Mascal, M. *Chem. Commun.* **1998**, 303.

(10) (a) Yaghi, O. M.; Li, G.; Li, H. *Nature* **1995**, *378*, 703. (b) Reineke, T. M.; Eddaoudi, M.; O'Keeffe, M.; Yaghi, O. M. *Angew. Chem., Int. Ed.* **1999**, *38*, 2590.

(11) (a) Ekambaram, S.; Sevov, S. C. *Angew. Chem., Int. Ed.* **1999**, *38*, 372. (b) Martin, J. D.; Leafblad, B, R. *Angew. Chem., Int. Ed.* **1998**, *37*, 3318.

(12) Sheldrick, G. M. *SADABS*: Univ. Gottingen, 1996.

(13) Sheldrick, G. M. *SHELXTL, Release 5.03*; Siemens Analytical X-ray Instruments Inc.: Madison, WIS, 1994.

Appendix

X-ray data and NMR data

Chapter 2

Table 1. Crystal data and structure refinement for complex **1**.

Identification code	**1**	
Empirical formula	C20 H28 Cd N6 O12	
Formula weight	656.89	
Temperature	167(2) K	
Wavelength	0.71073 Å	
Crystal system	Monoclinic	
Space group	C2/c	
Unit cell dimensions	a = 18.9015(11) Å	α= 90°.
	b = 11.7948(7) Å	β= 97.4380(10)°.
	c = 12.1547(7) Å	γ = 90°.
Volume	2687.0(3) $Å^3$	
Z	4	
Density (calculated)	1.624 Mg/m^3	
Absorption coefficient	0.884 mm^{-1}	
F(000)	1336	
Crystal size	0.20 x 0.20 x 0.15 mm^3	
Theta range for data collection	2.04 to 27.93°.	
Index ranges	-20<=h<=24, -14<=k<=15, -15<=l<=15	
Reflections collected	8362	
Independent reflections	3105 [R(int) = 0.0138]	
Completeness to theta = 27.93°	96.2 %	
Max. and min. transmission	0.8789 and 0.8431	
Refinement method	Full-matrix least-squares on F^2	
Data / restraints / parameters	3105 / 0 / 185	
Goodness-of-fit on F^2	1.009	
Final R indices [I>2sigma(I)]	R1 = 0.0176, wR2 = 0.0499	
R indices (all data)	R1 = 0.0184, wR2 = 0.0503	
Largest diff. peak and hole	0.445 and -0.300 e.$Å^{-3}$	

Table 2. Atomic coordinates (x 10^4) and equivalent isotropic displacement parameters ($Å^2$x 10^3) for 1. U(eq) is defined as one third of the trace of the orthogonalized U^{ij} tensor.

	x	y	z	U(eq)
Cd(1)	0	2588(1)	7500	14(1)
O(11)	711(1)	2598(1)	9196(1)	24(1)
N(11)	-1000(1)	2529(1)	8500(1)	18(1)
N(21)	0	4592(1)	7500	18(1)
N(31)	0	602(1)	7500	17(1)
C(11)	-1640(1)	2153(1)	8038(1)	26(1)
C(12)	-2235(1)	2120(1)	8595(1)	26(1)
C(13)	-2186(1)	2494(1)	9689(1)	17(1)
C(14)	-1516(1)	2864(1)	10172(1)	24(1)
C(15)	-947(1)	2872(1)	9560(1)	22(1)
C(21)	-524(1)	5184(1)	7881(1)	21(1)
C(22)	-540(1)	6358(1)	7912(1)	20(1)
C(23)	0	6972(2)	7500	16(1)
C(31)	-198(1)	12(1)	8356(1)	19(1)
C(32)	-207(1)	-1160(1)	8387(1)	19(1)
C(33)	0	-1770(2)	7500	16(1)
N(1A)	-2696(1)	4570(1)	7726(1)	32(1)
O(1A)	-2653(1)	4192(2)	6768(1)	55(1)
O(2A)	-3235(1)	4346(1)	8174(1)	43(1)
O(3A)	-2202(1)	5146(1)	8212(1)	41(1)
O(1W)	1574(1)	4396(1)	9561(1)	45(1)
O(2W)	1334(1)	637(1)	9876(1)	37(1)

Table 1. Crystal data and structure refinement for complex **2**.

Identification code	**2**	
Empirical formula	C50 H103 Cd N12 O12.50	
Formula weight	1184.84	
Temperature	193(2) K	
Wavelength	0.71069 Å	
Crystal system	Monoclinic	
Space group	C2	
Unit cell dimensions	a = 17.5815(16) Å	α= 90.0000(16)°.
	b = 11.7413(11) Å	β= 94.3215(18)°.
	c = 24.836(2) Å	γ = 90.000(2)°.
Volume	5112.3(8) $Å^3$	
Z	4	
Density (calculated)	1.539 Mg/m^3	
Absorption coefficient	0.506 mm^{-1}	
F(000)	2540	
Crystal size	0.25 x 0.20 x 0.20 mm^3	
Theta range for data collection	1.64 to 25.00°.	
Index ranges	-11<=h<=20, -12<=k<=13, -29<=l<=28	
Reflections collected	13740	
Independent reflections	8232 [R(int) = 0.0237]	
Completeness to theta = 25.00°	99.6 %	
Refinement method	Full-matrix least-squares on F^2	
Data / restraints / parameters	8232 / 143 / 553	
Goodness-of-fit on F^2	1.088	
Final R indices [I>2sigma(I)]	R1 = 0.0518, wR2 = 0.1347	
R indices (all data)	R1 = 0.0636, wR2 = 0.1400	
Absolute structure parameter	0.00	
Largest diff. peak and hole	0.791 and -0.587 e.$Å^{-3}$	

Table 2. Atomic coordinates (x 10^4) and equivalent isotropic displacement parameters ($Å^2$x 10^3) for **2**. U(eq) is defined as one third of the trace of the orthogonalized U^{ij} tensor.

	x	y	z	U(eq)
Cd(1)	0	7749(1)	5000	22(1)
Cd(2)	0	5626(1)	0	26(1)
C(100)	2425(4)	4565(7)	50(3)	39(2)
C(101)	-2332(9)	9018(15)	5012(6)	120(5)
C(102)	-2334(7)	11466(12)	4698(5)	95(3)
C(103)	-2633(6)	8325(9)	4589(4)	70(3)
C(104)	-2479(10)	10609(17)	4906(7)	147(6)
C(105)	-2803(7)	8387(11)	2298(5)	92(3)
C(106)	-4022(8)	8032(13)	2357(6)	114(4)
C(107)	-3119(11)	8075(18)	4093(8)	165(7)
C(108)	-3350(9)	8464(14)	3610(6)	113(4)
C(109)	-3997(8)	8437(12)	3495(5)	92(4)
C(110)	-3175(7)	8949(11)	3363(5)	87(3)
C(111)	-4123(5)	8417(9)	2919(4)	62(2)
C(112)	-4352(6)	8483(9)	3743(4)	59(3)
C(113)	-3025(10)	7963(15)	1175(7)	118(5)
C(114)	-2733(8)	8217(13)	1722(6)	111(4)
C(115)	-3561(8)	7717(13)	1220(5)	101(4)
C(116)	-2581(10)	7878(16)	915(7)	112(5)
C(117)	-2446(15)	8670(20)	1124(10)	206(10)
C(118)	-2613(12)	7550(20)	608(8)	167(8)
N(41)	0	7620(12)	0	34(3)
N(22)	0	5739(9)	5000	18(2)
O(11)	-1194(3)	7608(6)	4566(2)	36(1)
N(42)	0	3623(10)	0	30(3)
N(20)	0	9696(9)	5000	29(3)
O(21)	1242(3)	5770(6)	374(2)	41(2)
N(11)	482(2)	7798(4)	4136(1)	26(1)
C(10)	1089(2)	7099(4)	4026(1)	30(2)
C(11)	1263(2)	6925(4)	3495(2)	30(2)
C(12)	829(3)	7450(4)	3075(1)	22(2)
C(13)	222(2)	8149(4)	3185(1)	26(2)
C(14)	48(2)	8323(4)	3716(2)	25(2)

C(15)	1000(3)	7185(4)	2492(1)	23(2)
C(16)	1417(3)	6222(4)	2375(2)	36(2)
C(17)	1550(3)	5972(3)	1843(2)	43(2)
N(12)	1265(3)	6685(4)	1428(1)	36(2)
C(19)	849(3)	7648(4)	1546(1)	31(2)
C(18)	716(2)	7898(3)	2078(2)	28(2)
C(20)	518(5)	10322(7)	4763(3)	29(2)
C(21)	536(4)	11489(7)	4743(3)	24(2)
C(22)	0	12151(11)	5000	20(3)
C(23)	-641(5)	5147(7)	4960(3)	29(2)
C(24)	-669(4)	3979(7)	4958(3)	25(2)
C(25)	0	3376(11)	5000	18(3)
N(31)	-465(2)	5527(4)	872(1)	28(2)
C(30)	-973(3)	6358(4)	1019(2)	34(2)
C(31)	-1138(3)	6466(4)	1556(2)	31(2)
C(32)	-795(3)	5742(5)	1945(1)	32(2)
C(33)	-288(3)	4911(4)	1798(2)	33(2)
C(34)	-123(2)	4803(4)	1262(2)	32(2)
C(35)	-947(3)	5915(4)	2548(1)	30(2)
C(36)	-1502(3)	6688(4)	2680(2)	37(2)
C(37)	-1623(2)	6890(4)	3218(2)	41(2)
N(32)	-1190(3)	6319(5)	3624(1)	44(2)
C(39)	-635(3)	5546(4)	3492(2)	54(2)
C(38)	-514(3)	5344(4)	2954(2)	39(2)
C(40)	658(5)	8214(7)	76(3)	29(2)
C(41)	682(5)	9401(8)	79(3)	32(2)
C(42)	0	10014(14)	0	35(4)
C(43)	-625(5)	3067(7)	141(4)	37(2)
C(44)	-647(5)	1910(7)	135(3)	32(2)
C(45)	0	1317(11)	0	30(3)
N(61)	-400(4)	10271(6)	1238(2)	97(3)
C(60)	14(3)	11040(6)	1570(3)	92(3)
C(61)	-190(3)	11240(5)	2091(2)	68(2)
C(62)	-810(3)	10671(5)	2281(2)	50(2)
C(63)	-1225(3)	9903(5)	1950(2)	60(2)
C(64)	-1020(4)	9703(5)	1429(2)	87(3)
C(65)	-1021(3)	10911(5)	2851(2)	48(2)
C(66)	-660(3)	11778(5)	3154(2)	78(3)

C(67)	-856(4)	11989(5)	3676(2)	88(3)
N(62)	-1413(4)	11333(5)	3896(2)	81(2)
C(69)	-1774(3)	10466(5)	3594(2)	66(2)
C(68)	-1578(3)	10255(4)	3071(2)	52(2)
N(51)	2629(4)	9062(7)	1081(2)	101(3)
C(50)	2906(4)	8265(6)	1461(3)	103(4)
C(51)	2781(4)	8412(6)	2002(3)	81(3)
C(52)	2379(4)	9356(6)	2164(2)	73(2)
C(53)	2103(4)	10153(5)	1785(3)	84(3)
C(54)	2228(4)	10006(6)	1243(2)	107(4)
C(55)	2221(3)	9556(5)	2753(2)	62(2)
C(56)	2660(3)	8975(5)	3153(3)	69(2)
C(57)	2544(3)	9157(6)	3693(2)	77(3)
N(52)	1988(4)	9920(6)	3834(2)	82(2)
C(58)	1549(3)	10501(5)	3434(3)	85(3)
C(59)	1665(3)	10319(5)	2894(2)	71(2)

Table 1. Crystal data and structure refinement for complex **3**.

Identification code	**3**	
Empirical formula	C25 H28 Cd N7 O10	
Formula weight	698.94	
Temperature	173(2) K	
Wavelength	0.71073 Å	
Crystal system	Monoclinic	
Space group	Pc	
Unit cell dimensions	a = 12.4725(18) Å	α= 90°.
	b = 15.195(2) Å	β= 96.625(3)°.
	c = 15.390(2) Å	γ = 90°.
Volume	2897.2(7) $Å^3$	
Z	4	
Density (calculated)	1.602 Mg/m^3	
Absorption coefficient	0.821 mm^{-1}	
F(000)	1420	
Crystal size	0.25 x 0.25 x 0.20 mm^3	
Theta range for data collection	1.64 to 28.10°.	
Index ranges	-16<=h<=13, -17<=k<=19, -18<=l<=19	
Reflections collected	18522	
Independent reflections	10014 [R(int) = 0.0173]	
Completeness to theta = 28.11°	96.4 %	
Refinement method	Full-matrix least-squares on F^2	
Data / restraints / parameters	10014 / 2 / 791	
Goodness-of-fit on F^2	0.953	
Final R indices [I>2sigma(I)]	R1 = 0.0221, wR2 = 0.0541	
R indices (all data)	R1 = 0.0251, wR2 = 0.0553	
Absolute structure parameter	0.00	
Largest diff. peak and hole	0.707 and -0.322 e.$Å^{-3}$	

Table 2. Atomic coordinates (x 10^4) and equivalent isotropic displacement parameters ($Å^2$x 10^3) for **3**. U(eq) is defined as one third of the trace of the orthogonalized U^{ij} tensor.

	x	y	z	U(eq)
Cd(1)	358(1)	504(1)	1273(1)	21(1)
Cd(2)	-1789(1)	-5552(1)	5519(1)	20(1)
O(1W)	830(2)	1756(2)	563(1)	42(1)
O(2W)	1410(3)	-444(2)	582(2)	34(1)
O(3W)	-2798(2)	-6400(1)	6386(1)	24(1)
O(4W)	-2873(2)	-4488(1)	6148(2)	27(1)
O(5W)	5322(2)	5350(2)	1666(2)	32(1)
O(6W)	3258(2)	208(2)	104(2)	40(1)
O(7W)	5001(4)	6565(3)	2926(3)	93(2)
O(8W)	3360(3)	1683(3)	-965(2)	79(1)
N(1A)	-958(3)	2258(2)	1938(2)	38(1)
O(1A)	-863(2)	1426(2)	1933(2)	30(1)
O(2A)	-522(3)	2716(2)	1411(2)	70(1)
O(3A)	-1519(3)	2591(2)	2456(2)	53(1)
N(1B)	-592(2)	-7113(2)	4817(2)	26(1)
O(1B)	-486(2)	-6270(1)	4791(2)	28(1)
O(2B)	-1337(2)	-7409(2)	5217(2)	42(1)
O(3B)	16(2)	-7576(2)	4447(2)	43(1)
N(1C)	2502(3)	2187(2)	-3189(2)	32(1)
O(1C)	2629(3)	1505(2)	-2749(2)	54(1)
O(2C)	3051(2)	2853(2)	-2974(2)	46(1)
O(3C)	1839(2)	2194(2)	-3864(2)	41(1)
N(1D)	5950(3)	2719(2)	23(2)	34(1)
O(1D)	6704(2)	2688(2)	624(2)	46(1)
O(2D)	5514(2)	2025(2)	-282(2)	49(1)
O(3D)	5618(2)	3447(2)	-265(2)	45(1)
N(11)	-1313(3)	-4334(2)	4687(2)	22(1)
N(12)	-110(3)	-672(2)	2121(2)	26(1)
C(10)	-321(3)	-3988(2)	4761(2)	28(1)
C(11)	-29(3)	-3290(2)	4261(2)	28(1)
C(12)	-803(3)	-2921(2)	3645(2)	23(1)
C(13)	-1839(3)	-3274(2)	3561(2)	31(1)
C(14)	-2053(3)	-3974(2)	4090(2)	31(1)

C(15)	-540(3)	-2153(2)	3109(2)	22(1)
C(16)	214(3)	-1531(2)	3430(2)	27(1)
C(17)	396(3)	-811(2)	2926(2)	29(1)
C(18)	-829(3)	-1265(2)	1817(2)	33(1)
C(19)	-1077(3)	-2007(2)	2275(2)	35(1)
N(21)	-4821(3)	58(2)	-3698(2)	36(1)
N(22)	-973(2)	313(2)	102(2)	23(1)
C(20)	-3952(3)	-466(2)	-3597(2)	41(1)
C(21)	-3169(3)	-442(2)	-2882(2)	36(1)
C(22)	-3265(3)	167(2)	-2219(2)	26(1)
C(23)	-4162(3)	719(3)	-2315(3)	31(1)
C(24)	-4914(4)	629(2)	-3066(3)	36(1)
C(25)	-2460(3)	205(2)	-1417(2)	23(1)
C(26)	-2454(3)	915(2)	-836(2)	32(1)
C(27)	-1725(3)	941(2)	-101(2)	31(1)
C(28)	-965(3)	-361(2)	-466(3)	26(1)
C(29)	-1680(3)	-435(2)	-1220(3)	26(1)
N(31)	6021(2)	2294(2)	5509(2)	28(1)
N(32)	1684(2)	919(2)	2406(2)	24(1)
C(30)	6194(3)	1872(2)	4776(2)	33(1)
C(31)	5369(3)	1570(2)	4172(2)	33(1)
C(32)	4291(3)	1692(2)	4321(2)	23(1)
C(33)	4118(3)	2117(2)	5086(2)	30(1)
C(34)	4990(3)	2403(2)	5654(2)	32(1)
C(35)	3392(3)	1417(2)	3668(2)	23(1)
C(36)	2350(3)	1732(2)	3688(2)	36(1)
C(37)	1536(3)	1466(2)	3042(3)	37(1)
C(38)	2687(4)	598(2)	2396(3)	33(1)
C(39)	3535(3)	833(3)	3010(3)	36(1)
N(41)	-3123(2)	-5880(2)	4362(2)	23(1)
N(42)	-7316(3)	-7359(2)	1204(2)	36(1)
C(40)	-2885(3)	-6268(2)	3620(2)	26(1)
C(41)	-3659(3)	-6521(2)	2953(2)	26(1)
C(42)	-4739(3)	-6378(2)	3042(2)	21(1)
C(43)	-4993(3)	-5970(2)	3802(2)	26(1)
C(44)	-4164(3)	-5742(3)	4440(3)	28(1)
C(45)	-5630(3)	-6686(2)	2370(2)	24(1)
C(46)	-5460(3)	-7367(2)	1805(2)	33(1)

C(47)	-6329(3)	-7684(2)	1246(2)	39(1)
C(48)	-7465(3)	-6679(2)	1724(2)	37(1)
C(49)	-6648(3)	-6318(2)	2307(2)	36(1)
N(51)	3427(2)	-4855(2)	10433(2)	30(1)
N(52)	-429(2)	-5331(2)	6665(2)	23(1)
C(50)	2685(3)	-4229(2)	10198(2)	31(1)
C(51)	1942(3)	-4275(2)	9454(2)	28(1)
C(52)	1922(3)	-5017(2)	8921(2)	21(1)
C(53)	2672(3)	-5668(2)	9175(3)	29(1)
C(54)	3395(4)	-5568(2)	9920(3)	34(1)
C(55)	1126(3)	-5101(2)	8120(2)	23(1)
C(56)	1278(3)	-5707(2)	7471(2)	31(1)
C(57)	487(3)	-5802(2)	6759(2)	29(1)
C(58)	-554(3)	-4726(2)	7267(2)	28(1)
C(59)	204(3)	-4595(2)	7997(3)	28(1)

Table 1. Crystal data and structure refinement for **4**.

Identification code	**4**	
Empirical formula	C60 H136 Br6 N42 O54 Pt7	
Formula weight	4155.20	
Temperature	296(2) K	
Wavelength	0.71073 Å	
Crystal system	Monoclinic	
Space group	P2(1)/c	
Unit cell dimensions	a = 20.648(4) Å	α= 90°.
	b = 16.205(3) Å	β= 111.031(11)°.
	c = 19.397(3) Å	γ = 90°.
Volume	6057.8(18) $Å^3$	
Z	2	
Density (calculated)	2.278 Mg/m^3	
Absorption coefficient	10.134 mm^{-1}	
F(000)	3956	
Crystal size	0.40 x 0.25 x 0.25 mm^3	
Theta range for data collection	1.64 to 25.06°.	
Index ranges	-24<=h<=22, 0<=k<=19, 0<=l<=23	
Reflections collected	10175	
Independent reflections	10175 [R(int) = 0.0000]	
Completeness to theta = 25.06°	94.8 %	
Max. and min. transmission	0.1861 and 0.1066	
Refinement method	Full-matrix least-squares on F^2	
Data / restraints / parameters	10175 / 162 / 800	
Goodness-of-fit on F^2	0.705	
Final R indices [I>2sigma(I)]	R1 = 0.0434, wR2 = 0.1185	
R indices (all data)	R1 = 0.0912, wR2 = 0.1301	
Largest diff. peak and hole	1.998 and -1.561 e.$Å^{-3}$	

Table 2. Atomic coordinates (x 10^4) and equivalent isotropic displacement parameters (Å^{2}x 10^3) for **4**. U(eq) is defined as one third of the trace of the orthogonalized U^{ij} tensor.

	x	y	z	U(eq)
Pt(1)	2933(1)	7627(1)	4229(1)	39(1)
N(7)	2915(2)	11594(2)	7528(2)	38(1)
C(71)	2813(3)	10823(3)	7641(3)	48(2)
C(72)	2823(3)	10189(3)	7173(3)	54(2)
C(73)	3001(3)	10357(3)	6577(3)	46(2)
C(74)	3131(3)	11162(3)	6460(3)	51(2)
C(75)	3094(3)	11746(3)	6942(3)	56(2)
N(6)	1789(2)	12437(2)	7748(2)	39(1)
C(61)	1402(3)	12039(4)	8060(3)	65(2)
C(62)	712(3)	12017(4)	7800(3)	69(2)
C(63)	347(3)	12424(3)	7176(3)	48(2)
C(64)	738(3)	12849(4)	6827(3)	62(2)
C(65)	1441(3)	12829(4)	7153(3)	60(2)
N(4)	1875(2)	7617(2)	3776(2)	40(1)
C(41)	1539(3)	7846(4)	3089(3)	69(2)
C(42)	835(3)	7838(4)	2764(3)	72(2)
C(43)	446(3)	7569(3)	3170(3)	46(2)
C(44)	786(3)	7311(4)	3877(3)	62(2)
C(45)	1498(3)	7344(4)	4161(3)	62(2)
N(3)	2917(2)	8490(2)	4992(2)	39(1)
C(31)	3173(3)	8312(3)	5704(3)	44(2)
C(32)	3223(3)	8903(3)	6237(3)	56(2)
C(33)	2976(2)	9684(3)	6019(3)	41(2)
C(34)	2687(3)	9846(3)	5274(3)	50(2)
C(35)	2693(3)	9228(3)	4789(3)	48(2)
Pt(2)	2830(1)	12487(1)	8213(1)	40(1)
Pt(3)	0	10000	5000	49(1)
N(15)	-556(3)	10478(3)	3983(3)	79(2)
C(151)	-1048(5)	9771(6)	3636(5)	193(5)
C(161)	-1019(5)	9164(4)	3895(4)	109(4)
N(16)	-654(2)	8995(3)	4612(3)	65(2)
Br(7)	837(1)	9414(1)	4521(1)	97(1)
Pt(4)	3081(1)	15032(1)	6223(1)	60(1)

N(11)	3779(2)	15548(4)	6883(3)	153(2)
C(111)	4455(6)	15382(7)	7021(5)	233(7)
C(121)	4481(5)	14759(6)	6533(7)	204(6)
N(12)	3833(3)	14429(4)	6004(3)	132(3)
N(13)	2290(3)	14417(3)	5454(3)	98(3)
C(131)	1647(4)	14601(4)	5594(4)	113(4)
C(141)	1642(4)	15442(4)	5758(4)	98(3)
N(14)	2296(2)	15639(3)	6399(3)	71(2)
Br(5)	3045(1)	16088(1)	5321(1)	100(1)
Br(6)	3086(1)	13993(1)	7137(1)	82(1)
N(2)	3994(2)	7600(3)	4620(2)	51(2)
N(8)	3864(2)	12594(3)	8725(2)	52(2)
N(5)	2809(2)	13380(3)	8953(2)	50(2)
N(1)	3039(2)	6768(3)	3509(2)	51(2)
C(51)	3495(3)	13670(4)	9336(4)	94(3)
C(11)	3744(3)	6695(5)	3535(3)	89(3)
C(81)	4022(4)	13143(5)	9356(4)	117(3)
C(21)	4241(3)	6933(4)	4267(4)	94(3)
N(1S)	4953(3)	9302(3)	3936(8)	330(9)
O(1S)	4612(3)	9902(4)	3859(6)	296(6)
O(2S)	5005(5)	8575(3)	3978(6)	309(7)
O(3S)	5571(2)	9617(5)	4104(5)	298(6)
N(2S)	2031(2)	7265(2)	1549(2)	77(2)
O(21S)	1710(3)	7576(3)	955(2)	104(2)
O(22S)	1872(3)	6605(2)	1756(3)	114(2)
O(23S)	2536(2)	7650(2)	1966(2)	81(2)
N(3S)	1945(2)	12735(2)	10150(2)	69(2)
O(31S)	1778(2)	13410(2)	9875(2)	78(2)
O(32S)	2402(2)	12330(2)	10049(2)	82(2)
O(33S)	1653(2)	12435(3)	10557(2)	103(2)
N(4S)	1720(2)	9829(3)	8619(3)	97(3)
O(41S)	1241(3)	9814(6)	8819(4)	185(5)
O(42S)	2225(3)	10301(4)	8970(3)	148(4)
O(43S)	1768(3)	9363(4)	8149(3)	106(3)
N(4X)	1654(3)	9776(5)	8574(4)	155(18)
O(41X)	1523(6)	10311(5)	8923(5)	192(13)
O(42X)	2233(3)	9626(11)	8561(8)	280(20)
O(43X)	1181(5)	9410(7)	8099(7)	263(18)

N(5S)	1702(2)	10055(3)	2821(2)	95(2)
O(51S)	1556(3)	10537(3)	3222(3)	162(3)
O(52S)	2282(2)	9749(4)	2971(3)	158(3)
O(53S)	1286(4)	9927(5)	2208(3)	197(5)
N(7S)	4150(3)	10716(3)	9376(2)	140(4)
O(71S)	4032(4)	11222(3)	9743(3)	268(6)
O(72S)	4313(3)	10845(5)	8836(3)	194(4)
O(73S)	4001(6)	10088(3)	9563(5)	466(11)
N(8S)	4769(2)	7639(5)	6836(2)	215(5)
O(81S)	4635(4)	7293(5)	6243(2)	266(6)
O(82S)	4391(3)	7489(5)	7224(3)	180(3)
O(83S)	5314(3)	7955(5)	7254(5)	307(6)
O(1W)	5659(3)	7631(4)	8618(3)	150(3)
O(2W)	4465(5)	5702(6)	10084(9)	396(9)
O(3W)	3545(5)	5895(5)	8325(4)	254(5)
O(4W)	30(4)	10754(6)	2941(4)	269(4)
O(5W)	-183(3)	12384(4)	4681(3)	138(3)
O(6W)	67(4)	13779(6)	4222(5)	258(5)

Table 1. Crystal data and structure refinement for $3c{\cdot}(4)_2$.

Identification code	$3c{\cdot}(4)_2$	
Empirical formula	C100 H108 N32 O58 Pd6	
Formula weight	3324.58	
Temperature	293(2) K	
Wavelength	0.71073 Å	
Crystal system	Monoclinic	
Space group	P21/n	
Unit cell dimensions	a = 17.429(3) Å	α= 90°.
	b = 14.785(3) Å	β= 101.555(4)°.
	c = 27.061(5) Å	γ = 90°.
Volume	6832(2) $Å^3$	
Z	2	
Density (calculated)	1.616 Mg/m^3	
Absorption coefficient	0.875 mm^{-1}	
F(000)	3344	
Crystal size	0.20 x 0.15 x 0.15 mm^3	
Theta range for data collection	1.54 to 25.00°.	
Index ranges	-15<=h<=20, -10<=k<=17, -32<=l<=32	
Reflections collected	28290	
Independent reflections	11995 [R(int) = 0.1013]	
Completeness to theta = 25.00°	99.6 %	
Max. and min. transmission	0.8799 and 0.8444	
Refinement method	Full-matrix least-squares on F^2	
Data / restraints / parameters	11995 / 222 / 854	
Goodness-of-fit on F^2	0.797	
Final R indices [I>2sigma(I)]	R1 = 0.0812, wR2 = 0.2110	
R indices (all data)	R1 = 0.2251, wR2 = 0.2490	
Largest diff. peak and hole	1.618 and -0.551 e.$Å^{-3}$	

Table 2. Atomic coordinates (x 10^4) and equivalent isotropic displacement parameters (Å^{2}x 10^3) for **3c·(4)$_2$**. U(eq) is defined as one third of the trace of the orthogonalized U^{ij} tensor.

	x	y	z	U(eq)
Pd(1)	8310(1)	365(1)	1988(1)	76(1)
Pd(2)	6936(1)	1652(1)	-1496(1)	71(1)
Pd(3)	7626(1)	-3704(1)	448(1)	81(1)
N(11A)	7662(7)	-2989(7)	-181(5)	79(3)
C(11A)	7665(8)	-2099(8)	-158(5)	70(4)
C(12A)	7677(7)	-1557(8)	-577(5)	66(3)
C(13A)	7697(9)	-1974(10)	-1033(6)	90(4)
C(14A)	7689(11)	-2904(11)	-1062(7)	109(6)
C(15A)	7665(10)	-3378(10)	-621(7)	99(5)
N(11B)	7361(6)	888(7)	-891(4)	62(3)
C(11B)	7395(7)	-22(9)	-925(5)	63(3)
C(12B)	7681(7)	-551(8)	-511(5)	57(3)
C(13B)	7955(6)	-149(8)	-69(5)	55(3)
C(14B)	7906(6)	792(8)	-5(5)	52(3)
C(15B)	7608(7)	1266(9)	-440(5)	61(3)
N(11C)	8329(6)	1121(7)	1369(4)	67(3)
C(11C)	8123(7)	785(8)	919(5)	55(3)
C(12)	8150(7)	1234(8)	489(5)	56(3)
C(13C)	8404(9)	2123(9)	526(6)	81(4)
C(14C)	8651(10)	2452(10)	993(6)	99(5)
C(15C)	8598(9)	1968(10)	1405(6)	84(4)
N(21A)	7173(6)	587(7)	1955(4)	73(3)
C(21A)	6655(8)	-36(9)	1739(5)	66(3)
C(22A)	5873(8)	25(8)	1701(5)	59(3)
C(23A)	5566(9)	746(10)	1896(6)	90(4)
C(24A)	6087(11)	1397(10)	2133(7)	113(6)
C(25A)	6873(10)	1287(10)	2155(6)	96(5)
N(21B)	4151(6)	-1517(7)	1359(4)	65(3)
C(21B)	4418(8)	-2115(9)	1043(5)	67(3)
C(22B)	5142(7)	-2054(8)	919(5)	56(3)
C(23B)	5602(7)	-1351(8)	1121(4)	54(3)
C(24B)	5365(7)	-738(8)	1443(4)	54(3)
C(25B)	4617(7)	-850(9)	1550(4)	59(3)

N(21C)	6468(7)	-3496(6)	349(4)	69(3)
C(21C)	6197(8)	-2895(7)	633(5)	60(3)
C(22C)	5415(8)	-2709(8)	586(5)	60(3)
C(23C)	4896(8)	-3224(9)	235(5)	72(3)
C(24C)	5186(10)	-3855(9)	-36(6)	86(4)
C(25C)	5980(9)	-3975(9)	20(6)	78(4)
O(10A)	5902(11)	3189(10)	1181(6)	169(6)
O(10B)	4711(10)	3018(10)	1255(6)	170(6)
C(101)	5201(7)	1920(5)	787(3)	87(4)
C(102)	4470(5)	1526(7)	623(4)	105(5)
C(103)	4396(4)	771(7)	310(4)	99(5)
C(104)	5051(6)	411(5)	163(3)	68(3)
C(105)	5782(5)	805(7)	328(4)	94(5)
C(106)	5857(5)	1559(7)	640(4)	99(5)
C(107)	5301(13)	2752(15)	1105(7)	119(6)
O(20A)	9383(11)	-1410(15)	-1952(9)	279(10)
O(20B)	9360(11)	-2607(17)	-1528(11)	290(12)
C(201)	9569(12)	-1282(17)	-1075(8)	236(13)
C(202)	9625(13)	-344(17)	-1069(8)	300(20)
C(203)	9803(13)	115(12)	-612(11)	217(13)
C(204)	9926(14)	-363(19)	-161(8)	239(16)
C(205)	9871(14)	-1301(18)	-167(8)	249(13)
C(206)	9692(11)	-1760(11)	-623(11)	300(20)
C(207)	9590(50)	-1820(20)	-1548(12)	960(110)
N(1AN)	8359(9)	-416(9)	2582(5)	113(4)
N(2AN)	9436(8)	-13(10)	2027(5)	120(5)
C(1AN)	9066(15)	-1000(16)	2624(8)	162(9)
C(2AN)	9733(15)	-510(20)	2507(9)	206(13)
N(1BN)	7986(7)	1817(9)	-1663(5)	102(4)
N(2BN)	6562(7)	2438(9)	-2106(5)	110(5)
C(1BN)	7957(11)	2536(17)	-2026(9)	176(10)
C(2BN)	7191(13)	2520(20)	-2367(8)	195(13)
N(1CN)	7660(7)	-4393(8)	1092(5)	104(4)
N(2CN)	8777(8)	-3932(9)	593(7)	137(6)
C(1CN)	8457(11)	-4562(15)	1372(10)	157(9)
C(2CN)	8952(14)	-4580(20)	1002(11)	209(15)
N(300)	8189(12)	-1640(11)	1221(7)	129(6)
O(301)	8149(13)	-2176(14)	1560(7)	243(9)

O(302)	8746(10)	-1424(14)	1097(8)	216(9)
O(303)	7523(7)	-1320(7)	978(5)	103(3)
N(200)	7248(19)	3775(16)	-451(12)	310(17)
O(201)	7476(18)	4514(15)	-292(12)	363(16)
O(202)	7032(12)	3263(11)	-209(10)	245(10)
O(203)	6980(40)	3740(30)	-951(11)	630(50)
N(400)	9490(30)	2770(80)	-660(20)	1230(110)
O(401)	9887(19)	2810(30)	-1000(13)	463(18)
O(402)	8840(20)	2620(30)	-776(13)	450(30)
O(403)	9790(20)	3210(40)	-234(17)	570(40)
N(100)	3300(20)	5040(20)	2834(12)	300(30)
O(101)	2630(20)	5040(40)	2901(18)	590(30)
O(102)	3800(20)	5140(60)	3172(15)	1000(100)
O(103)	3380(20)	4430(30)	2478(14)	540(20)
O(1W)	5450(30)	1130(30)	-4030(20)	560(40)
O(2W)	6550(20)	-3620(20)	1756(8)	343(17)
O(3W)	6580(30)	-70(30)	-3300(40)	920(90)
O(4W)	9590(20)	-3690(30)	-2220(12)	410(20)
O(5W)	7001(11)	3902(12)	782(9)	243(9)
O(6W)	10720(30)	-190(30)	-3705(16)	530(30)
O(7W)	9340(20)	179(18)	-3770(9)	368(18)
O(8W)	4162(12)	2422(14)	2086(7)	238(10)
O(9W)	700(20)	5550(30)	2143(13)	430(20)
O(10W)	1499(10)	5734(13)	2920(6)	195(7)
O(11W)	9380(20)	-4690(30)	-370(20)	510(30)
O(12W)	6587(17)	-1683(17)	2509(8)	402(19)
O(13W)	4956(14)	2550(30)	3078(13)	520(30)

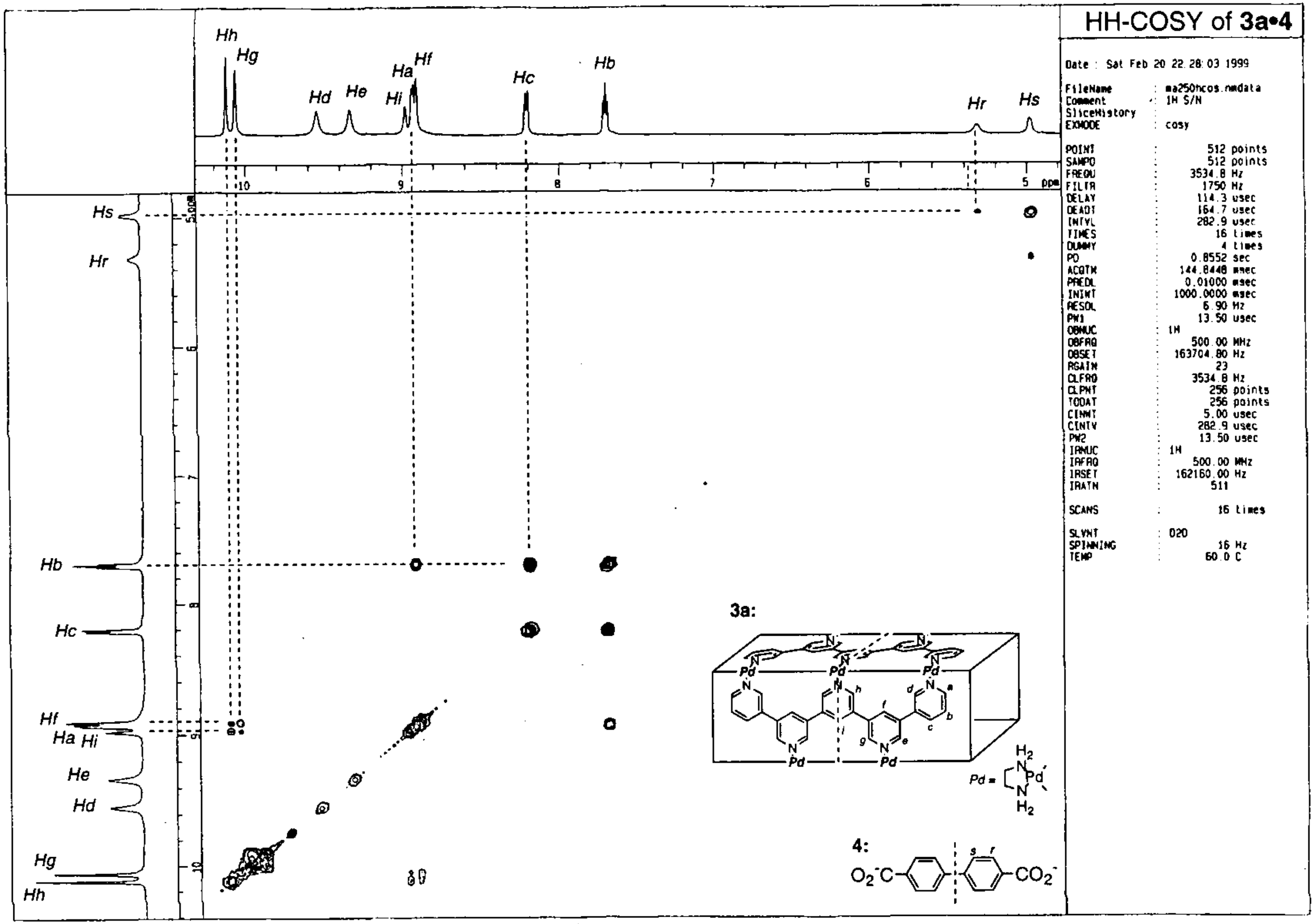
HH-COSY of 3a•4
Hh
Hg
Hd
He
Hi
Ha
Hf
Hc
Hb
Hr
Hs
10
9
8
7
6
5
ppm
Date : Sat Feb 20 22 28 03 1999
FileName : ma250hcos.nmdata
Comment : 1H S/N
SliceHistory :
EXMODE : cosy
POINT : 512 points
SAMPO : 512 points
FREQU : 3534.8 Hz
FILTR : 1750 Hz
DELAY : 114.3 usec
DEADT : 164.7 usec
INTVL : 282.9 usec
TIMES : 16 times
DUMMY : 4 times
PD : 0.8552 sec
ACQTM : 144.8448 msec
PREDL : 0.01000 msec
INIWT : 1000.0000 msec
RESOL : 6.90 Hz
PW1 : 13.50 usec
OBNUC : 1H
OBFRQ : 500.00 MHz
OBSET : 163704.80 Hz
RGAIN : 23
CLFRQ : 3534.8 Hz
CLPNT : 256 points
TODAT : 256 points
CINWT : 5.00 usec
CINTV : 282.9 usec
PW2 : 13.50 usec
IRNUC : 1H
IRFRQ : 500.00 MHz
IRSET : 162160.00 Hz
IRATN : 511
SCANS : 16 times
SLVNT : D2O
SPINNING : 16 Hz
TEMP : 60.0 C
3a:
Pd
N
a
b
c
d
e
f
g
h
i
Pd =
4:
s
r
O_2^-C
CO_2^-

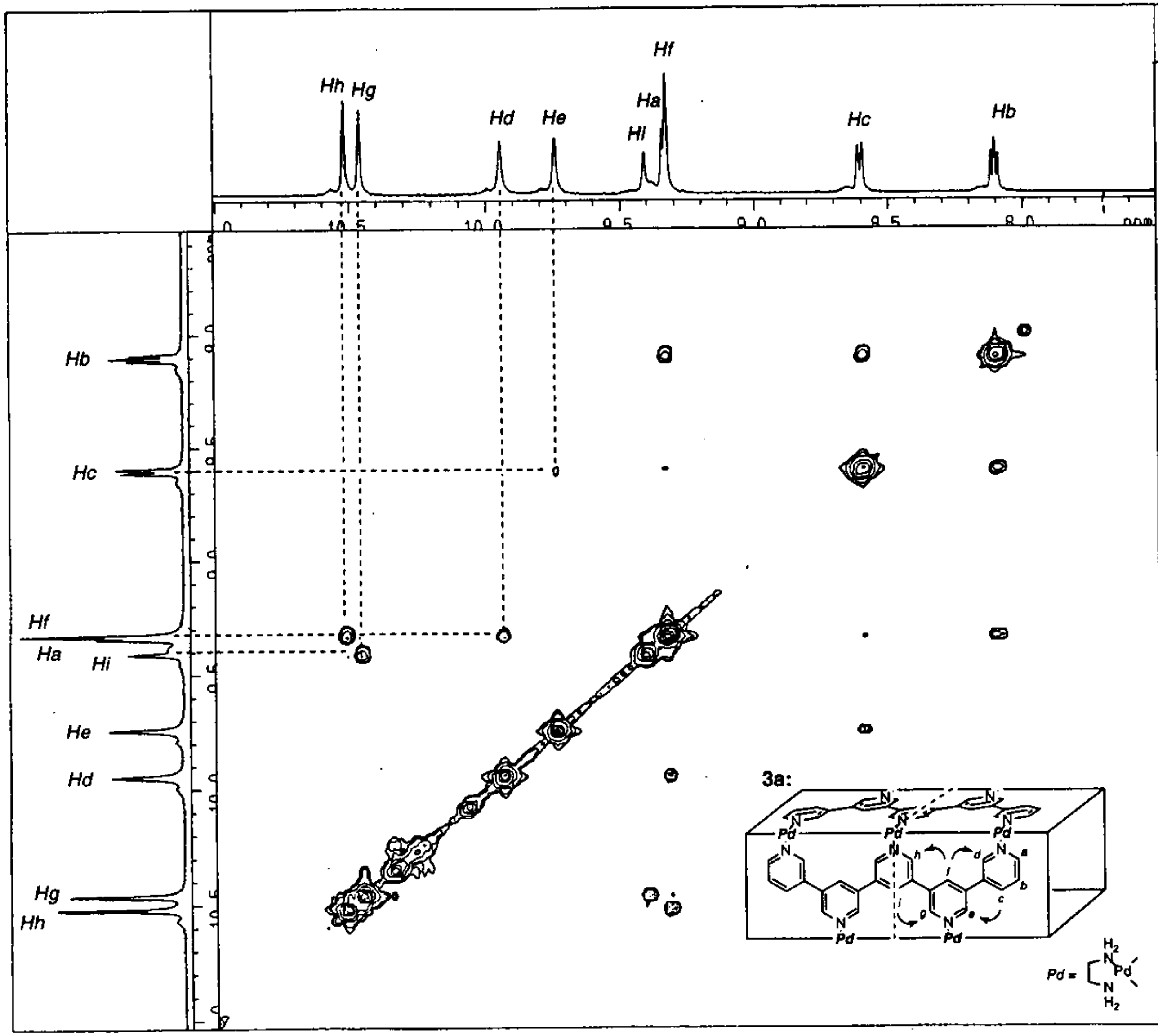

NOESY of **3a•4**

Date : Mon Nov 16 05:24:48 1998

FileName	:	ma217noesy.nmdata
Comment	:	1H S/N
SliceHistory	:	
EXMODE	:	noesy
POINT	:	512 points
SAMPO	:	512 points
FREQU	:	3501.4 Hz
FILTR	:	1750 Hz
DELAY	:	114.3 usec
DEADT	:	164.7 usec
INTVL	:	285.6 usec
TIMES	:	64 times
DUMMY	:	4 times
PD	:	1.0000 sec
ACQTM	:	146.2272 msec
PREDL	:	0.01000 msec
INIWT	:	1000.0000 msec
RESOL	:	6.84 Hz
PW1	:	13.50 usec
OBNUC	:	1H
OBFRQ	:	500.00 MHz
OBSET	:	163919.64 Hz
RGAIN	:	19
CLFRQ	:	3501.4 Hz
CLPNT	:	256 points
TODAT	:	256 points
CINWT	:	5.00 usec
CINTV	:	285.6 usec
PI1	:	500.000 msec
IRNUC	:	1H
IRFRQ	:	500.00 MHz
IRSET	:	162410.00 Hz
IRATN	:	511
SCANS	:	64 times
SLVNT	:	D2O
SPINNING	:	15 Hz
TEMP	:	70.0 C

CH-COSY of **3a•4.**

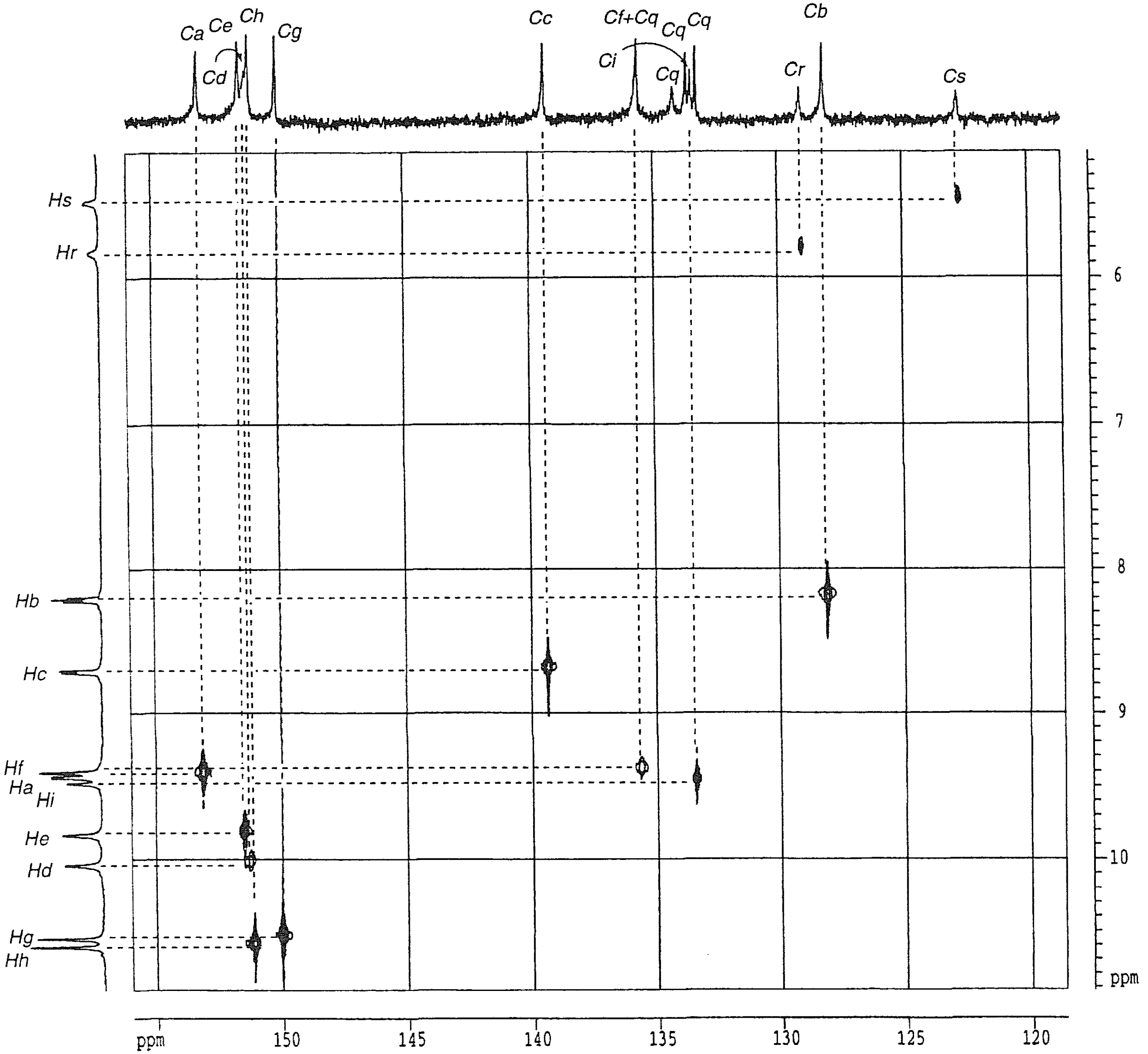

Current Data Parameters	
NAME	aoyagiCHCO1
EXPNO	1
PROCNO	2

F2 - Acquisition Parameters	
Date_	990205
Time	20.04
INSTRUM	drx500
PROBHD	5 mm BBO BB-1
PULPROG	hxco
TD	4096
SOLVENT	D2O
NS	512
DS	4
SWH	4699.248 Hz
FIDRES	1.147277 Hz
AQ	0.4358644 sec
RG	16384
DW	106.400 usec
DE	6.00 usec
TE	300.0 K
P1	6.45 usec
p2	12.90 usec
d0	0.00000300 sec
CNST2	145.0000000
d2	0.00344828 sec
CNST11	3.0000000
d3	0.00229885 sec
d11	0.03000000 sec
d12	0.00002000 sec
D1	2.00000000 sec
PL2	-4.00 dB
P3	8.40 usec
SFO2	500.2340156 MHz
NUC2	1H
SFO1	125.8001545 MHz
NUC1	13C
PL1	2.00 dB
PL12	16.00 dB
CPDPRG2	waltz16
PCPD2	81.00 usec
IN0	0.00017280 sec

F1 - Acquisition parameters	
ND0	2
TD	128
SFO1	500.234 MHz
FIDRES	22.605614 Hz
SW	5.784 ppm

F2 - Processing parameters	
SI	2048
SF	125.7828840 MHz
WDW	GM
SSB	0
LB	-5.00 Hz
GB	0.1
PC	1.40

F1 - Processing parameters	
SI	1024
MC2	QF
SF	500.2300000 MHz
WDW	GM
SSB	0
LB	-5.00 Hz
GB	0.1

2D NMR plot parameters	
CX2	17.00 cm
CX1	15.00 cm
F2PLO	155.984 ppm
F2LO	19620.15 Hz
F2PHI	118.624 ppm
F2HI	14920.91 Hz
F1PLO	10.920 ppm
F1LO	5462.33 Hz
F1PHI	5.135 ppm
F1HI	2568.81 Hz
F2PPMCM	2.19765 ppm/cm
F2HZCM	276.42639 Hz/cm
F1PPMCM	0.38563 ppm/cm
F1HZCM	192.90123 Hz/cm

3a:

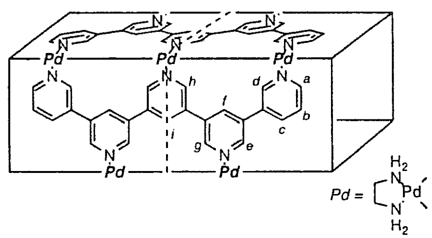

4:

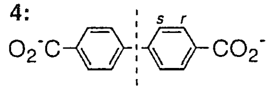

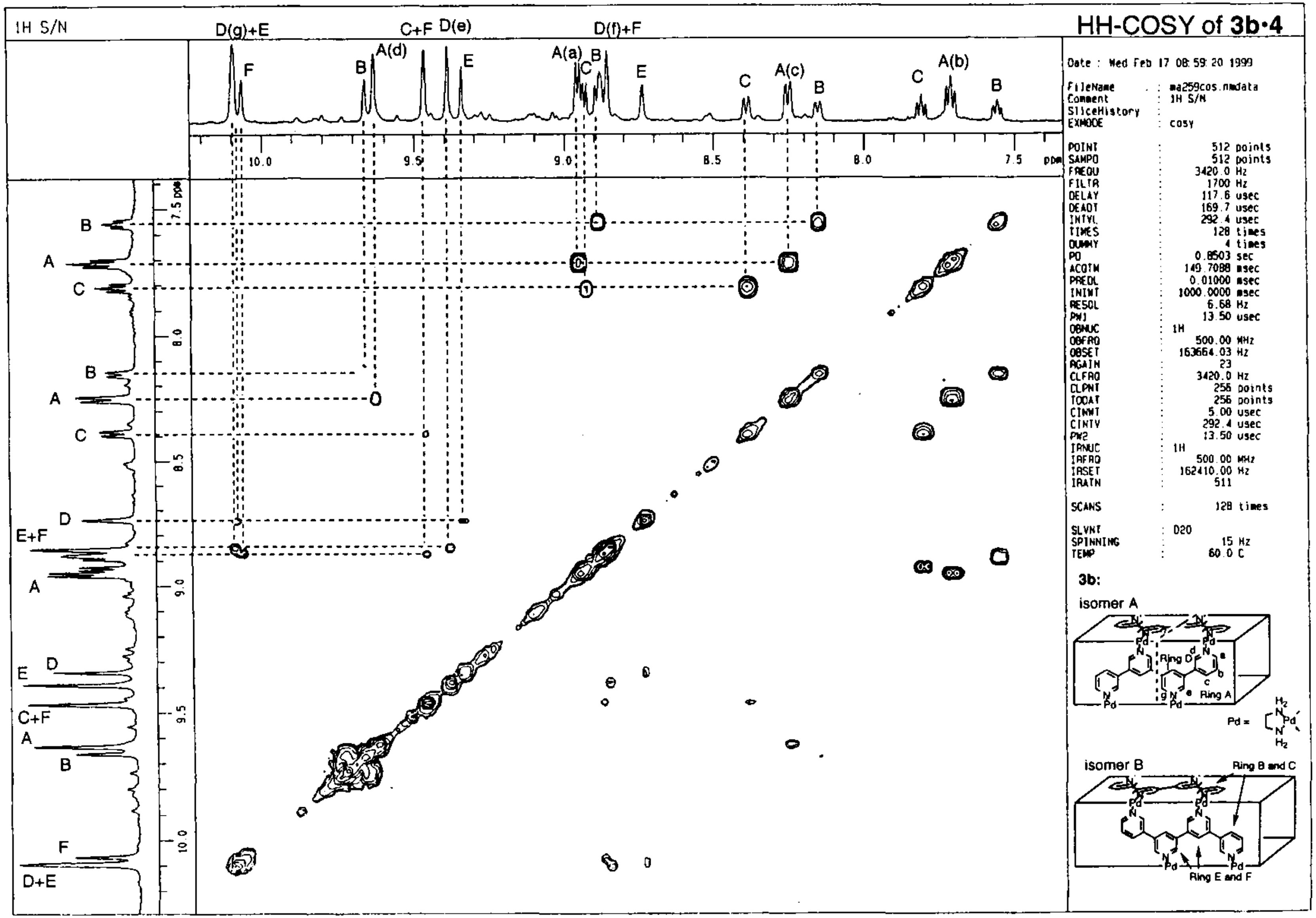
HH-COSY of 3b·4
1H S/N
D(g)+E
F
B
A(d)
C+F
D(e)
E
A(a)
C
B
D(f)+F
E
C
A(c)
B
C
A(b)
B
10.0
9.5
9.0
8.5
8.0
7.5
ppm
E+F
D+E
C+F
Date : Wed Feb 17 08:59:20 1999
FileName : ma259cos.nmdata
Comment : 1H S/N
SliceHistory :
EXMODE : cosy
POINT : 512 points
SAMPO : 512 points
FREQU : 3420.0 Hz
FILTR : 1700 Hz
DELAY : 117.6 usec
DEADT : 169.7 usec
INTVL : 292.4 usec
TIMES : 128 times
DUMMY : 4 times
PD : 0.8503 sec
ACQTM : 149.7088 msec
PREDL : 0.01000 msec
ININT : 1000.0000 msec
RESOL : 6.68 Hz
PW1 : 13.50 usec
OBNUC : 1H
OBFRQ : 500.00 MHz
OBSET : 163664.03 Hz
RGAIN : 23
CLFRQ : 3420.0 Hz
CLPNT : 256 points
TODAT : 256 points
CINWT : 5.00 usec
CINTV : 292.4 usec
PW2 : 13.50 usec
IRNUC : 1H
IRFRQ : 500.00 MHz
IRSET : 162410.00 Hz
IRATN : 511
SCANS : 128 times
SLVNT : D2O
SPINNING : 15 Hz
TEMP : 60.0 C
3b:
isomer A
Ring D
Ring A
Pd =
isomer B
Ring B and C
Ring E and F

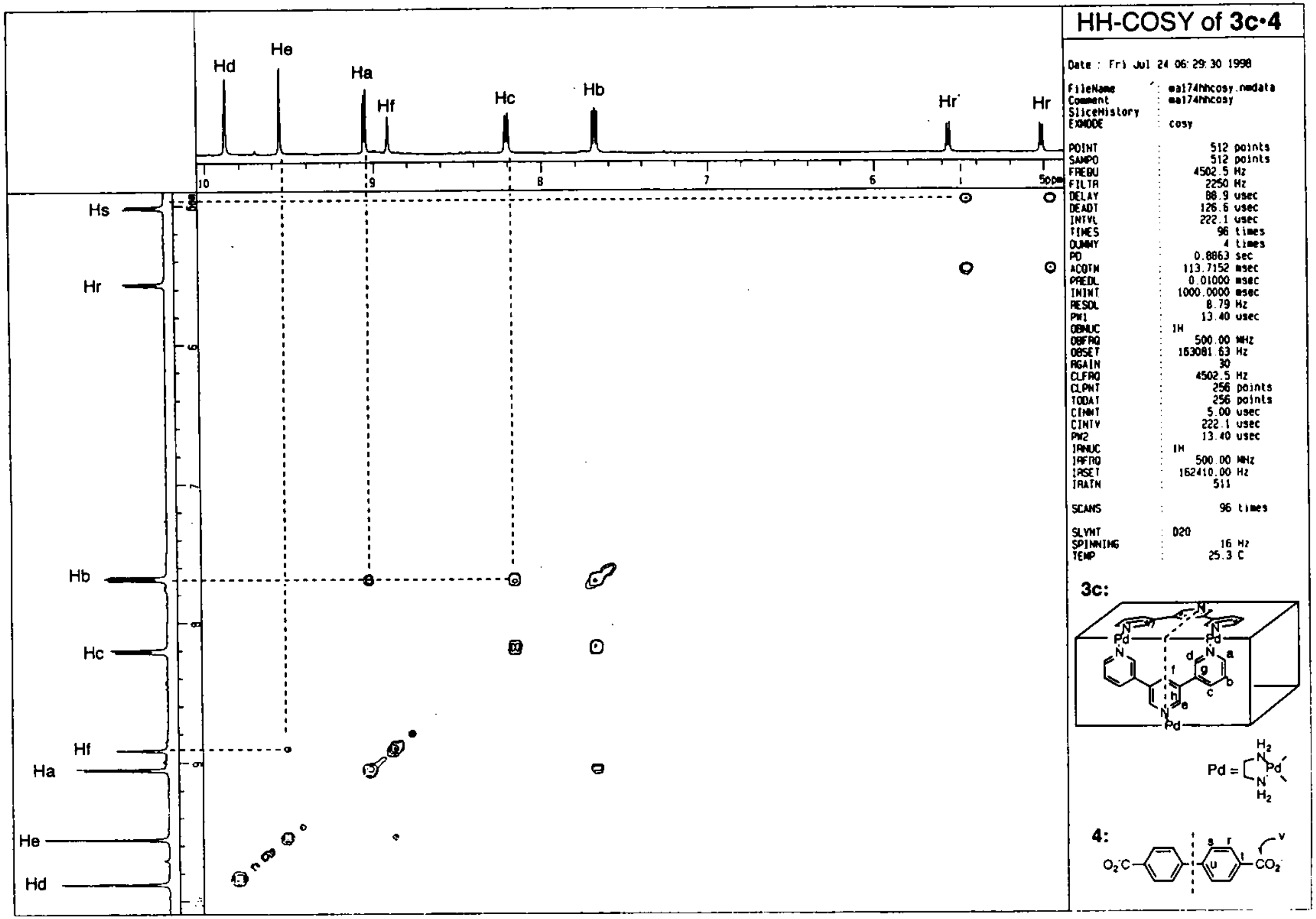
HH-COSY of 3c•4
Date : Fri Jul 24 06:29:30 1998
FileName : ma174hhcosy.nmdata
Comment : ma174hhcosy
SliceHistory :
EXMODE : cosy
POINT : 512 points
SAMPO : 512 points
FREQU : 4502.5 Hz
FILTR : 2250 Hz
DELAY : 88.9 usec
DEADT : 126.6 usec
INTVL : 222.1 usec
TIMES : 96 times
DUMMY : 4 times
PD : 0.8863 sec
ACQTM : 113.7152 msec
PREDL : 0.01000 msec
INIWT : 1000.0000 msec
RESOL : 8.79 Hz
PW1 : 13.40 usec
OBNUC : 1H
OBFRQ : 500.00 MHz
OBSET : 163081.63 Hz
RGAIN : 30
CLFRQ : 4502.5 Hz
CLPNT : 256 points
TODAT : 256 points
CINWT : 5.00 usec
CINTV : 222.1 usec
PW2 : 13.40 usec
IRNUC : 1H
IRFRQ : 500.00 MHz
IRSET : 162410.00 Hz
IRATN : 511
SCANS : 96 times
SLVNT : D2O
SPINNING : 16 Hz
TEMP : 25.3 C
Hd
He
Ha
Hf
Hc
Hb
Hr'
Hr
Hs
10
9
8
7
6
5ppm
3c:
Pd
N
a
b
c
d
e
f
g
h
Pd =
H2
4:
s
r
t
u
v
O2C
CO2

CH-COSY of 3c•4

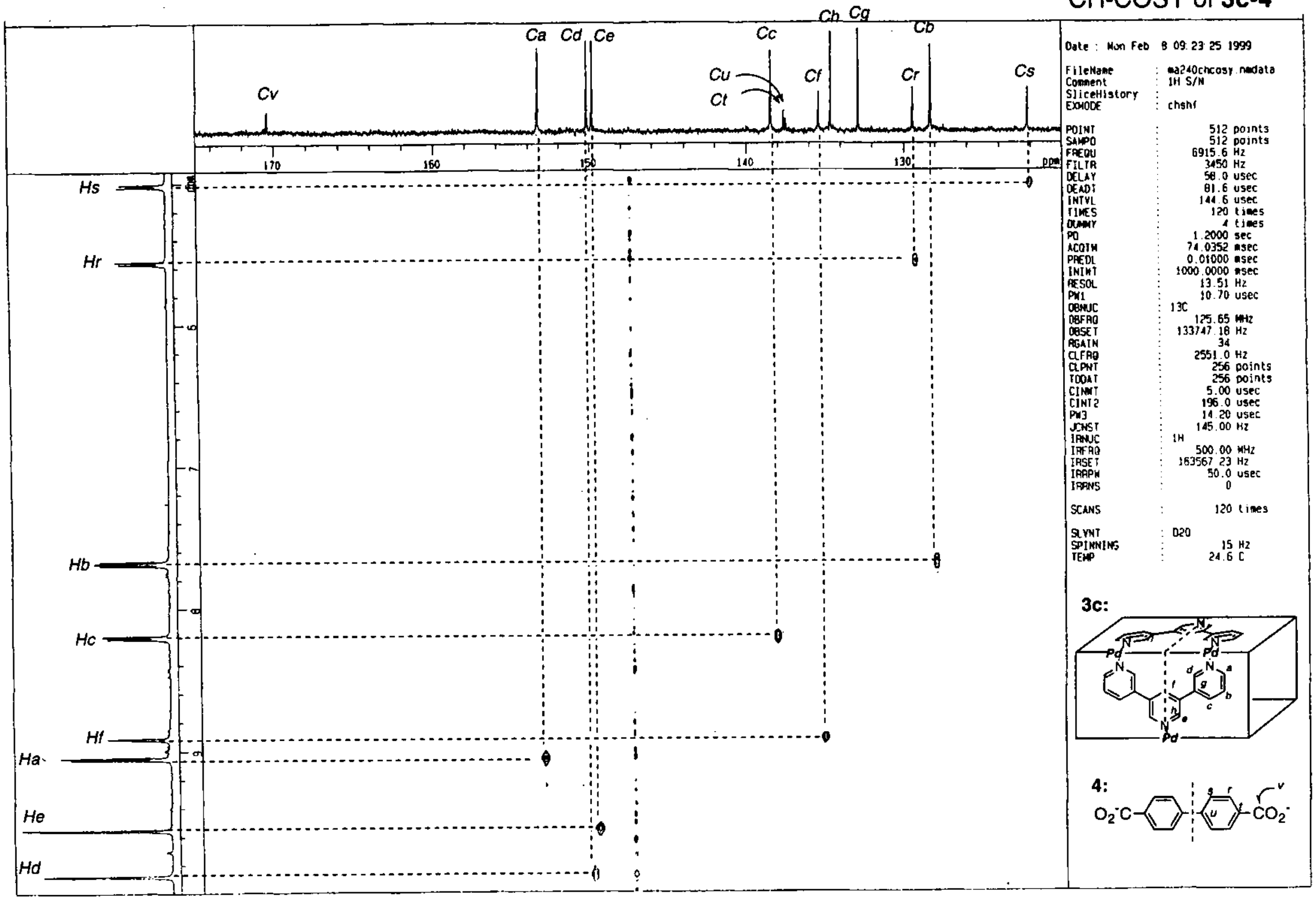

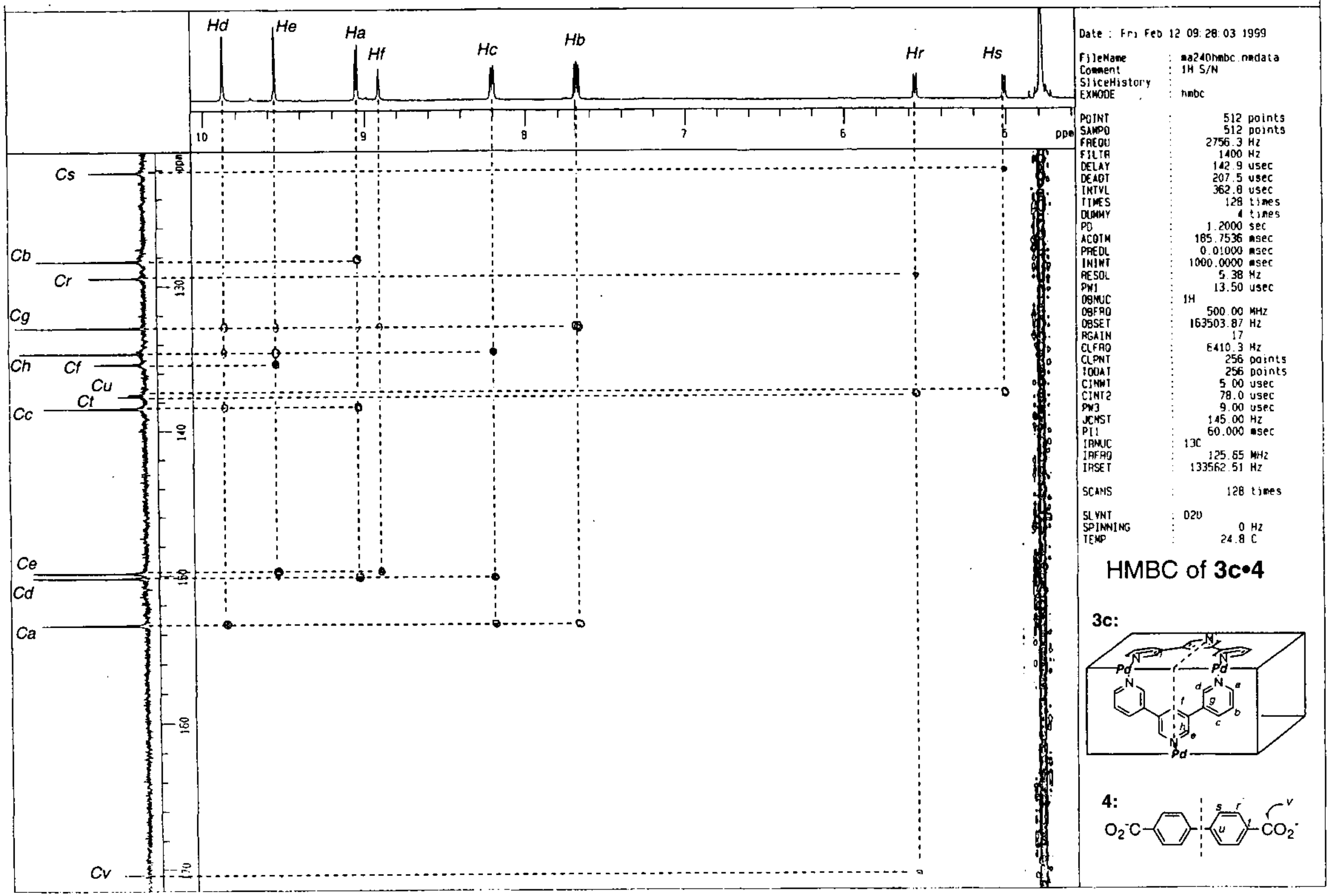
Hd
He
Ha
Hf
Hc
Hb
Hr
Hs
10
9
8
7
6
5
ppm
Cs
Cb
Cr
Cg
Ch
Cf
Cu
Ct
Cc
Ce
Cd
Ca
Cv
130
140
150
160
170
Date : Fri Feb 12 09:28:03 1999
FileName : ma240hmbc.nmdata
Comment : 1H S/N
SliceHistory :
EXMODE : hmbc
POINT : 512 points
SAMPO : 512 points
FREQU : 2756.3 Hz
FILTR : 1400 Hz
DELAY : 142.9 usec
DEADT : 207.5 usec
INTVL : 362.8 usec
TIMES : 128 times
DUMMY : 4 times
PD : 1.2000 sec
ACQTM : 185.7536 msec
PREDL : 0.01000 msec
INIWT : 1000.0000 msec
RESOL : 5.38 Hz
PW1 : 13.50 usec
OBNUC : 1H
OBFRQ : 500.00 MHz
OBSET : 163503.87 Hz
RGAIN : 17
CLFRQ : 6410.3 Hz
CLPNT : 256 points
TODAT : 256 points
CINWT : 5.00 usec
CINT2 : 78.0 usec
PW3 : 9.00 usec
JCNST : 145.00 Hz
PI1 : 60.000 msec
IRNUC : 13C
IRFRQ : 125.65 MHz
IRSET : 133562.51 Hz
SCANS : 128 times
SLVNT : D2O
SPINNING : 0 Hz
TEMP : 24.8 C
HMBC of 3c•4
3c:
Pd
N
4:
O_2C
CO_2^-

Table 1. Crystal data and structure refinement for **2b•(3a)**$_2$.

Identification code	**2b•(3a)**$_2$
Empirical formula	C124 H216 N47 O93 Pd8
Formula weight	4704.64
Temperature	153(2) K
Wavelength	0.71073 Å
Crystal system	Triclinic
Space group	P-1
Unit cell dimensions	a = 17.549(2) Å a= 107.271(3)°.
	b = 20.344(3) Å b= 91.243(3)°.
	c = 29.840(4) Å g = 114.438(3)°.
Volume	9133(2) Å3
Z	2
Density (calculated)	1.711 Mg/m3
Absorption coefficient	0.884 mm-1
F(000)	4802
Crystal size	0.15 x 0.15 x 0.15 mm3
Theta range for data collection	1.31 to 25.00°.
Index ranges	-20<=h<=15, -16<=k<=24, -35<=l<=32
Reflections collected	48058
Independent reflections	31565 [R(int) = 0.0653]
Completeness to theta = 25.00°	98.1 %
Absorption correction	None
Max. and min. transmission	0.8788 and 0.8788
Refinement method	Full-matrix-block least-squares on F2
Data / restraints / parameters	31565 / 470 / 2529
Goodness-of-fit on F2	1.924
Final R indices [I>2sigma(I)]	R1 = 0.1299, wR2 = 0.3168
R indices (all data)	R1 = 0.1805, wR2 = 0.3307
Largest diff. peak and hole	5.444 and -4.933 e.Å-3

Table 2. Atomic coordinates (x 104) and equivalent isotropic displacement parameters (Å2x 103) for **2b•(3a)$_2$**. U(eq) is defined as one third of the trace of the orthogonalized Uij tensor.

	x	y	z	U(eq)
Pd(1)	-445(1)	-545(1)	-2565(1)	31(1)
Pd(2)	-2644(1)	1239(1)	197(1)	29(1)
Pd(3)	4560(1)	19279(1)	2394(1)	30(1)
Pd(4)	6841(1)	17459(1)	3664(1)	31(1)
Pd(5)	8338(1)	22646(1)	5302(1)	28(1)
Pd(6)	3632(1)	15564(1)	5788(1)	33(1)
Pd(7)	2828(1)	3172(1)	-709(1)	39(1)
Pd(8)	983(1)	5070(1)	2049(1)	64(1)
N(11A)	-1238(8)	-645(7)	-2090(4)	32(3)
C(11A)	-1976(9)	-1278(8)	-2181(5)	33(3)
C(12A)	-2519(10)	-1408(9)	-1846(5)	41(4)
C(13A)	-2292(10)	-796(8)	-1407(5)	38(4)
C(14A)	-1553(9)	-156(7)	-1309(5)	31(3)
C(15A)	-1048(9)	-82(8)	-1660(5)	33(3)
N(21A)	-1722(7)	1133(7)	-179(4)	32(3)
C(21A)	-1890(10)	576(8)	-573(5)	34(3)
C(22A)	-1294(10)	500(8)	-830(5)	35(4)
C(23A)	-452(9)	1021(7)	-673(4)	27(3)
C(24A)	-233(11)	1620(8)	-239(5)	40(4)
C(25A)	-897(10)	1677(8)	-5(5)	36(4)
N(31A)	2044(8)	2932(7)	-225(4)	41(3)
C(31A)	1248(10)	2381(8)	-361(5)	41(4)
C(32A)	659(10)	2239(8)	-47(5)	38(4)
C(33A)	918(10)	2724(9)	424(5)	41(4)
C(34A)	1740(11)	3313(9)	573(6)	52(5)
C(35A)	2275(11)	3382(9)	228(6)	50(5)
N(41A)	1786(11)	4665(8)	1740(5)	67(5)
C(41A)	1508(12)	4134(9)	1287(7)	58(5)
C(42A)	2064(13)	3862(10)	1061(7)	68(6)
C(43A)	2883(11)	4152(10)	1282(6)	67(6)
C(44A)	3139(13)	4685(12)	1721(7)	70(6)
C(45A)	2600(14)	4953(11)	1937(7)	81(8)
N(11B)	4792(7)	16261(6)	5705(4)	27(3)

C(11B)	4848(9)	16576(7)	5377(4)	24(3)
C(12B)	5603(8)	17031(8)	5257(4)	27(3)
C(13B)	6380(10)	17143(7)	5513(4)	30(3)
C(14B)	6291(10)	16814(8)	5868(5)	38(4)
C(15B)	5514(10)	16376(8)	5960(5)	41(4)
N(21B)	6066(7)	17544(7)	4149(4)	32(3)
C(21B)	6140(9)	17349(8)	4541(5)	30(3)
C(22B)	5591(9)	17326(8)	4870(5)	30(3)
C(23B)	4946(9)	17519(7)	4772(4)	27(3)
C(24B)	4823(9)	17696(8)	4374(5)	31(3)
C(25B)	5410(10)	17723(8)	4076(5)	31(3)
N(31B)	2733(7)	17757(6)	4419(4)	24(2)
C(31B)	3393(9)	17612(8)	4482(4)	27(3)
C(32B)	4114(9)	17890(8)	4284(4)	27(3)
C(33B)	4112(9)	18293(7)	3989(4)	27(3)
C(34B)	3421(9)	18431(8)	3902(5)	29(3)
C(35B)	2756(8)	18155(8)	4131(5)	28(3)
N(41B)	3833(7)	19267(6)	2915(3)	27(3)
C(41B)	3874(10)	18912(8)	3216(5)	33(3)
C(42B)	3388(9)	18861(7)	3580(4)	25(3)
C(43B)	2830(10)	19188(9)	3606(6)	42(4)
C(44B)	2764(10)	19545(8)	3289(5)	36(4)
C(45B)	3302(10)	19593(8)	2956(5)	38(4)
N(11C)	7722(7)	18566(7)	4003(4)	35(3)
C(11C)	7535(9)	19136(7)	4014(4)	26(3)
C(12C)	8126(9)	19905(8)	4251(4)	26(3)
C(13C)	8908(11)	20065(10)	4458(5)	43(4)
C(14C)	9096(10)	19451(9)	4424(5)	41(4)
C(15C)	8524(10)	18719(9)	4215(5)	36(4)
N(21C)	7876(7)	21694(6)	4701(4)	26(3)
C(21C)	8118(9)	21138(8)	4675(5)	30(3)
C(22C)	7877(7)	20505(7)	4255(4)	21(3)
C(23C)	7363(9)	20472(8)	3867(5)	32(3)
C(24C)	7115(8)	21050(7)	3910(4)	25(3)
C(25C)	7380(8)	21654(7)	4343(5)	26(3)
N(31C)	5494(7)	20323(7)	2825(4)	31(3)
C(31C)	5982(9)	20327(8)	3181(4)	29(3)
C(32C)	6577(9)	21044(8)	3524(4)	28(3)

C(33C)	6584(9)	21703(8)	3485(5)	29(3)
C(34C)	6079(9)	21687(7)	3131(4)	23(3)
C(35C)	5510(9)	20973(7)	2794(4)	27(3)
N(41C)	6260(7)	23685(6)	3567(4)	28(3)
C(41C)	6158(9)	22970(8)	3528(5)	32(3)
C(42C)	6077(9)	22435(8)	3111(5)	28(3)
C(43C)	6027(9)	22575(8)	2679(5)	33(3)
C(44C)	6113(10)	23287(9)	2722(5)	39(4)
C(45C)	6211(9)	23816(9)	3141(5)	36(4)
N(11D)	-751(9)	-4412(7)	-2467(4)	49(4)
C(11D)	-455(10)	-3656(8)	-2287(5)	40(4)
C(12D)	-330(10)	-3185(9)	-2549(5)	38(4)
C(13D)	-547(10)	-3525(9)	-3050(6)	45(4)
C(14D)	-846(12)	-4315(10)	-3242(6)	54(5)
C(15D)	-938(11)	-4743(8)	-2951(6)	49(4)
N(21D)	-14(7)	-1161(6)	-2311(4)	31(3)
C(21D)	-260(9)	-1904(8)	-2497(5)	35(4)
C(22D)	-13(8)	-2344(7)	-2331(5)	30(3)
C(23D)	640(9)	-1943(8)	-1917(5)	33(3)
C(24D)	965(8)	-1169(7)	-1715(4)	30(3)
C(25D)	611(8)	-799(8)	-1919(4)	26(3)
N(31D)	2428(7)	-696(6)	-627(4)	27(3)
C(31D)	1802(9)	-1070(8)	-1004(5)	31(3)
C(32D)	1653(9)	-711(8)	-1305(5)	32(3)
C(33D)	2150(8)	55(8)	-1202(4)	28(3)
C(34D)	2782(9)	472(7)	-791(4)	29(3)
C(35D)	2876(9)	54(8)	-524(5)	36(4)
N(41D)	3363(7)	2535(7)	-582(4)	39(3)
C(41D)	2967(9)	1764(7)	-731(5)	30(3)
C(42D)	3317(9)	1311(8)	-656(4)	29(3)
C(43D)	4147(10)	1682(8)	-401(5)	38(4)
C(44D)	4551(11)	2431(9)	-247(5)	44(4)
C(45D)	4191(11)	2870(9)	-350(5)	42(4)
O(11E)	4369(7)	1512(7)	3780(4)	48(3)
O(12E)	3197(7)	1172(6)	4087(4)	42(3)
C(11E)	4226(9)	876(8)	4340(5)	33(3)
C(12E)	3799(10)	598(9)	4672(5)	38(4)
C(13E)	4109(11)	266(10)	4927(6)	50(5)

C(14E)	4843(9)	184(8)	4862(5)	34(3)
C(15E)	5234(11)	450(11)	4525(6)	52(5)
C(16E)	4985(11)	810(10)	4277(6)	48(4)
C(17E)	3903(10)	1224(8)	4040(5)	35(4)
O(11F)	2209(8)	20311(7)	7257(4)	57(3)
O(12F)	3104(7)	20707(6)	7935(4)	46(3)
C(11F)	2373(10)	19374(8)	7498(5)	35(3)
C(12F)	1804(9)	18785(9)	7112(5)	36(4)
C(13F)	1618(9)	18024(8)	7028(5)	37(4)
C(14F)	2003(9)	17832(8)	7349(5)	33(3)
C(15F)	2579(10)	18440(9)	7745(5)	39(4)
C(16F)	2751(10)	19154(9)	7811(6)	41(4)
C(17F)	2568(10)	20181(9)	7558(5)	39(4)
O(21F)	1434(10)	14437(6)	7294(4)	67(4)
O(22F)	1683(8)	14397(7)	6563(4)	55(3)
C(21F)	1637(10)	15523(8)	7067(5)	36(3)
C(22F)	1731(10)	15994(9)	7532(6)	42(4)
C(23F)	1865(10)	16725(9)	7631(5)	40(4)
C(24F)	1822(9)	17055(8)	7269(5)	33(3)
C(25F)	1693(9)	16536(9)	6783(6)	39(4)
C(26F)	1596(9)	15784(9)	6687(6)	43(4)
C(27F)	1576(11)	14722(8)	6980(5)	42(4)
O(11G)	-3354(9)	-2488(8)	-679(5)	90(5)
O(12G)	-2793(9)	-2646(8)	-1357(4)	77(4)
C(11G)	-1868(11)	-1616(10)	-645(6)	51(4)
C(12G)	-1203(12)	-1454(12)	-866(6)	59(5)
C(13G)	-447(11)	-806(10)	-603(6)	54(5)
C(14G)	-384(11)	-359(10)	-148(6)	50(4)
C(15G)	-1134(12)	-563(12)	53(7)	72(7)
C(16G)	-1828(15)	-1167(13)	-202(7)	85(8)
C(17G)	-2738(14)	-2289(11)	-917(7)	68(6)
N(11)	-878(10)	46(10)	-2847(5)	48(4)
N(12)	344(9)	-421(10)	-3063(4)	45(4)
C(11)	-234(17)	463(14)	-3100(8)	73(7)
C(12)	65(18)	-130(17)	-3408(8)	80(7)
N(21)	-3547(9)	1408(9)	548(4)	39(3)
N(22)	-2983(9)	1703(8)	-226(4)	35(3)
C(21)	-3971(13)	1723(12)	294(6)	51(5)

C(22)	-3376(13)	2176(10)	44(7)	52(5)
N(31)	3632(9)	18237(8)	1955(4)	41(3)
N(32)	5233(9)	19166(7)	1842(5)	36(3)
C(31)	3879(12)	18085(10)	1475(6)	50(5)
C(32)	4821(12)	18344(10)	1545(5)	44(4)
N(41)	6014(10)	16357(8)	3301(6)	49(4)
N(42)	7556(9)	17306(8)	3153(5)	42(3)
C(41)	6505(14)	15989(11)	2990(7)	56(5)
C(42)	7052(15)	16560(12)	2776(6)	59(5)
N(51)	9453(8)	23086(8)	5094(5)	44(3)
N(52)	8846(10)	23609(8)	5884(5)	48(4)
C(51)	9932(15)	23916(15)	5355(13)	110(12)
C(52)	9765(17)	24028(14)	5848(8)	100(10)
N(61)	3473(10)	14793(8)	5133(5)	49(4)
N(62)	2433(9)	14827(7)	5776(5)	41(3)
C(61)	2591(12)	14216(9)	4998(6)	47(4)
C(62)	2247(12)	14044(9)	5405(7)	52(5)
N(71)	2362(16)	3877(13)	-813(10)	94(8)
N(72)	3528(11)	3420(8)	-1219(5)	49(4)
C(71)	3020(20)	4373(17)	-1070(14)	121(12)
C(72)	3100(20)	3780(14)	-1469(9)	104(11)
N(81)	195(12)	5523(10)	2313(6)	56(4)
N(82)	1345(19)	5800(11)	1694(9)	106(10)
C(81)	70(20)	5901(16)	2007(10)	95(9)
C(82)	940(50)	6350(20)	1910(20)	250(40)
N(100)	4787(9)	14447(7)	5839(5)	66(5)
O(101)	5289(9)	14365(10)	6089(6)	94(5)
O(102)	5013(10)	14636(7)	5491(4)	76(4)
O(103)	4111(10)	14387(11)	5963(8)	126(9)
N(200)	-985(9)	3214(7)	1173(5)	59(4)
O(201)	-680(12)	3916(7)	1377(6)	112(7)
O(202)	-1758(9)	2836(9)	1095(8)	132(9)
O(203)	-536(7)	2883(6)	1144(4)	57(3)
N(300)	7836(13)	23684(9)	4505(7)	145(15)
O(301)	7161(12)	23387(11)	4651(6)	126(9)
O(302)	8201(10)	23301(10)	4305(7)	149(10)
O(303)	8222(18)	24384(8)	4644(8)	231(18)
N(400)	5645(8)	18298(7)	3003(4)	44(3)

O(401)	6049(9)	17915(7)	2945(4)	66(4)
O(402)	5202(10)	18254(9)	2652(4)	81(5)
O(403)	5740(7)	18774(6)	3395(3)	41(3)
N(500)	4916(8)	137(7)	-904(4)	52(4)
O(501)	5429(10)	755(8)	-932(5)	95(6)
O(502)	4277(8)	-275(8)	-1219(5)	84(5)
O(503)	4998(11)	-58(8)	-565(5)	92(5)
N(600)	284(18)	3600(13)	-132(7)	260(30)
O(601)	-166(17)	3534(18)	186(9)	192(14)
O(602)	1017(15)	4130(19)	-48(11)	290(20)
O(603)	-20(20)	3108(16)	-531(9)	241(18)
N(700)	1156(9)	1372(7)	-1645(4)	54(4)
O(701)	719(16)	1040(11)	-2046(6)	170(12)
O(702)	1760(11)	1998(8)	-1588(6)	117(7)
O(703)	1071(7)	1012(6)	-1373(3)	47(3)
N(800)	7610(30)	912(16)	-1721(14)	250(20)
O(801)	7090(30)	680(20)	-1464(18)	380(30)
O(802)	7770(20)	468(15)	-2058(11)	212(13)
O(803)	7873(15)	1560(12)	-1731(8)	135(7)
N(900)	2948(13)	16596(13)	3144(8)	220(20)
O(901)	3700(13)	16740(20)	3102(12)	400(40)
O(902)	2633(11)	16374(12)	3475(8)	212(17)
O(903)	2550(20)	16760(30)	2891(10)	280(20)
N(110)	31(13)	17691(10)	6037(5)	92(7)
O(111)	-157(12)	17936(13)	6427(7)	157(10)
O(112)	-380(20)	16991(12)	5821(8)	270(20)
O(113)	676(12)	18079(18)	5945(6)	230(20)
N(120)	-1300(20)	18705(17)	5450(20)	1180(90)
O(121)	-1599(19)	17992(15)	5253(11)	195(14)
O(122)	-1620(30)	19160(20)	5563(17)	320(20)
O(123)	-570(20)	18850(20)	5376(15)	286(18)
N(130)	9111(14)	21316(12)	5847(7)	120(12)
O(131)	9580(20)	21221(16)	6125(12)	300(20)
O(132)	9166(15)	21973(14)	5958(10)	239(19)
O(133)	8550(20)	20756(15)	5572(10)	250(20)
N(140)	5549(17)	4814(13)	-529(7)	230(20)
O(141)	5139(15)	4908(12)	-831(11)	209(15)
O(142)	5950(17)	5364(14)	-163(10)	244(19)

O(143)	5590(19)	4202(12)	-660(15)	420(40)
O(1W)	1953(9)	21556(8)	7293(5)	68(4)
O(2W)	2391(7)	1263(7)	3358(4)	55(3)
O(3W)	4836(9)	3797(9)	881(5)	82(5)
O(4W)	6349(8)	17778(6)	1942(4)	56(3)
O(5W)	10315(11)	22225(9)	5267(7)	113(7)
O(6W)	3865(8)	1712(8)	2978(4)	65(4)
O(7W)	4280(10)	3119(9)	1934(5)	95(5)
O(8W)	6041(10)	16976(8)	7153(5)	78(4)
O(9W)	4493(13)	15471(10)	8126(5)	123(8)
O(10W)	8882(12)	23287(8)	6775(5)	95(5)
O(11W)	6246(10)	3631(8)	598(5)	90(5)
O(12W)	1275(15)	12917(9)	6192(6)	132(9)
O(13W)	3217(10)	16800(9)	2097(7)	105(6)
O(14W)	1806(13)	2911(14)	1991(8)	135(8)
O(15W)	2842(15)	15127(12)	8026(6)	134(8)
O(16W)	5371(13)	23406(10)	8250(11)	169(11)
O(17W)	860(20)	12723(15)	8029(11)	184(12)
O(18W)	5312(12)	-1896(13)	-1497(7)	131(8)
O(19W)	6934(16)	4465(15)	-10(12)	185(11)
O(20W)	486(17)	5018(16)	730(8)	160(10)
O(21W)	5953(14)	-827(15)	-2009(7)	139(9)
O(22W)	-1742(11)	17733(13)	6556(7)	120(7)
O(23W)	3604(13)	-2260(18)	-1516(5)	178(13)
O(24W)	2576(12)	3268(15)	3032(7)	130(8)
O(25W)	2493(17)	16142(14)	8765(7)	200(15)
O(26W)	6170(11)	-915(14)	-580(5)	155(11)
O(27W)	-1762(12)	2524(12)	-759(7)	120(7)
O(28W)	8339(17)	24660(14)	5596(8)	157(9)
O(29W)	869(12)	12939(10)	7197(8)	126(7)
O(32W)	-950(20)	4848(17)	713(10)	246(17)
O(30W)	-2270(30)	3630(50)	-1030(30)	710(80)
O(31W)	-70(50)	2160(40)	-1300(30)	600(60)
O(33W)	-1017(18)	11545(16)	7627(11)	238(18)
O(34W)	-784(18)	12104(13)	6845(14)	260(20)
O(35W)	-1760(20)	3940(20)	-310(19)	320(20)
O(36W)	3020(20)	4360(30)	3160(18)	530(50)
O(37W)	6592(17)	14410(20)	5620(10)	240(17)

O(38W)	9900(20)	25789(17)	5698(11)	209(14)
O(39W)	790(20)	3610(30)	-1221(13)	268(18)
O(40W)	4700(20)	16111(18)	2605(13)	290(20)

VT-NMR of **2a•3b** ([H]/[G]=1/2).

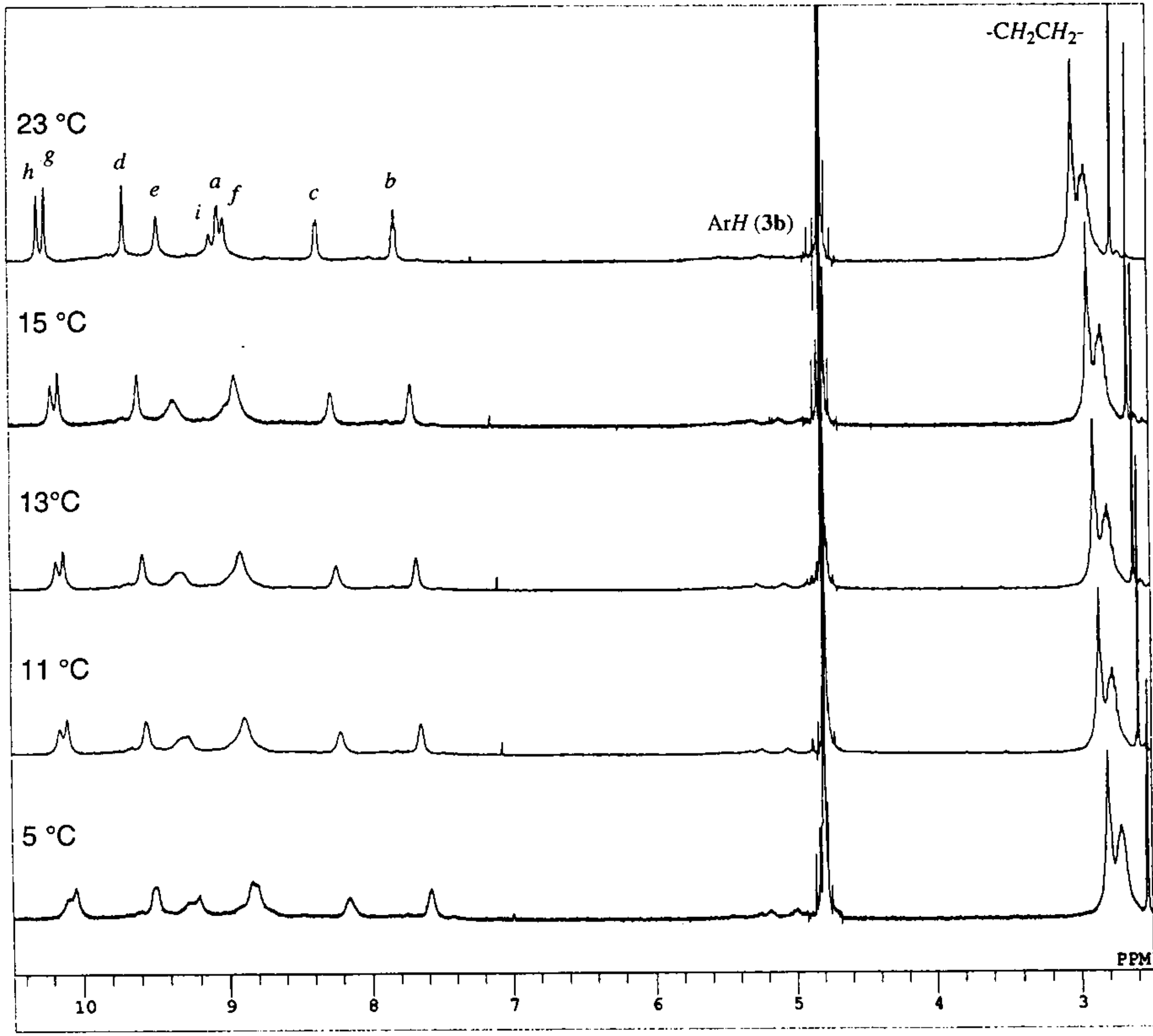


```
DATIM   Tue Jul 20 10:51:38 1999
OBNUC   1H
EXMOD   non
OBFRQ          500.00 MHz
OBSET          160.00 KHz
OBFIN          2410.0 Hz
POINT           32768
FREQU          8000.0 Hz
SCANS              32
ACQTM           4.096 sec
PD              2.904 sec
PW1               6.8 us
IRNUC   1H
CTEMP             5.0 c
SLVNT   D2O
EXREF            0.00 ppm
BF               0.05 Hz
RGAIN              24
```

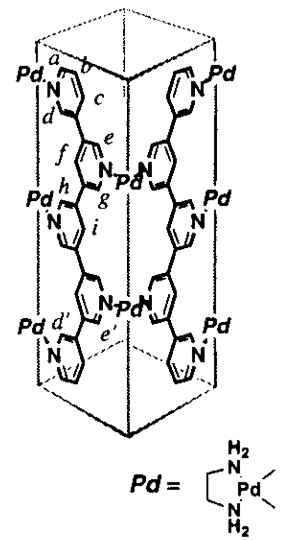

HH-COSY of **2b•3a** (isomer **A**).

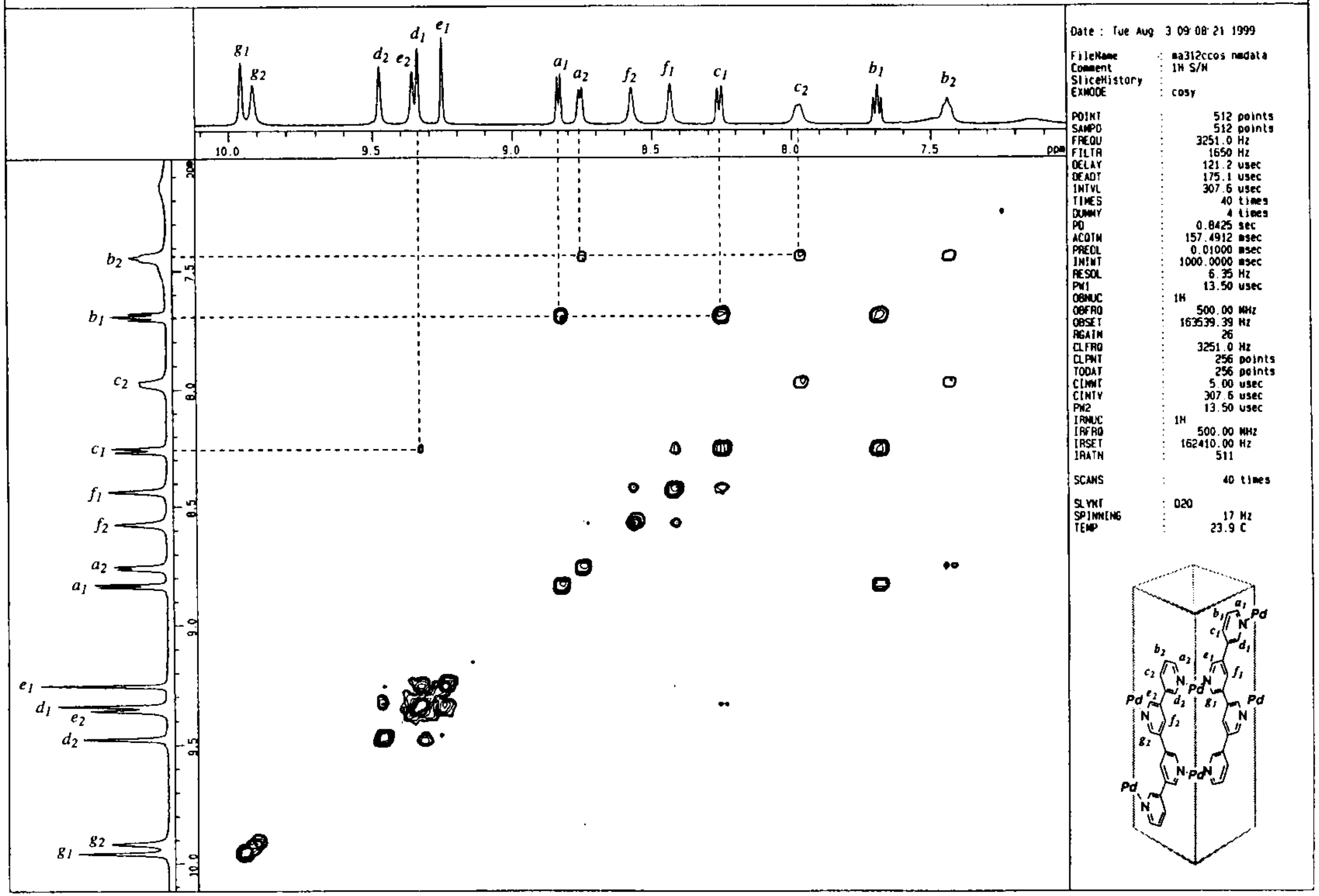

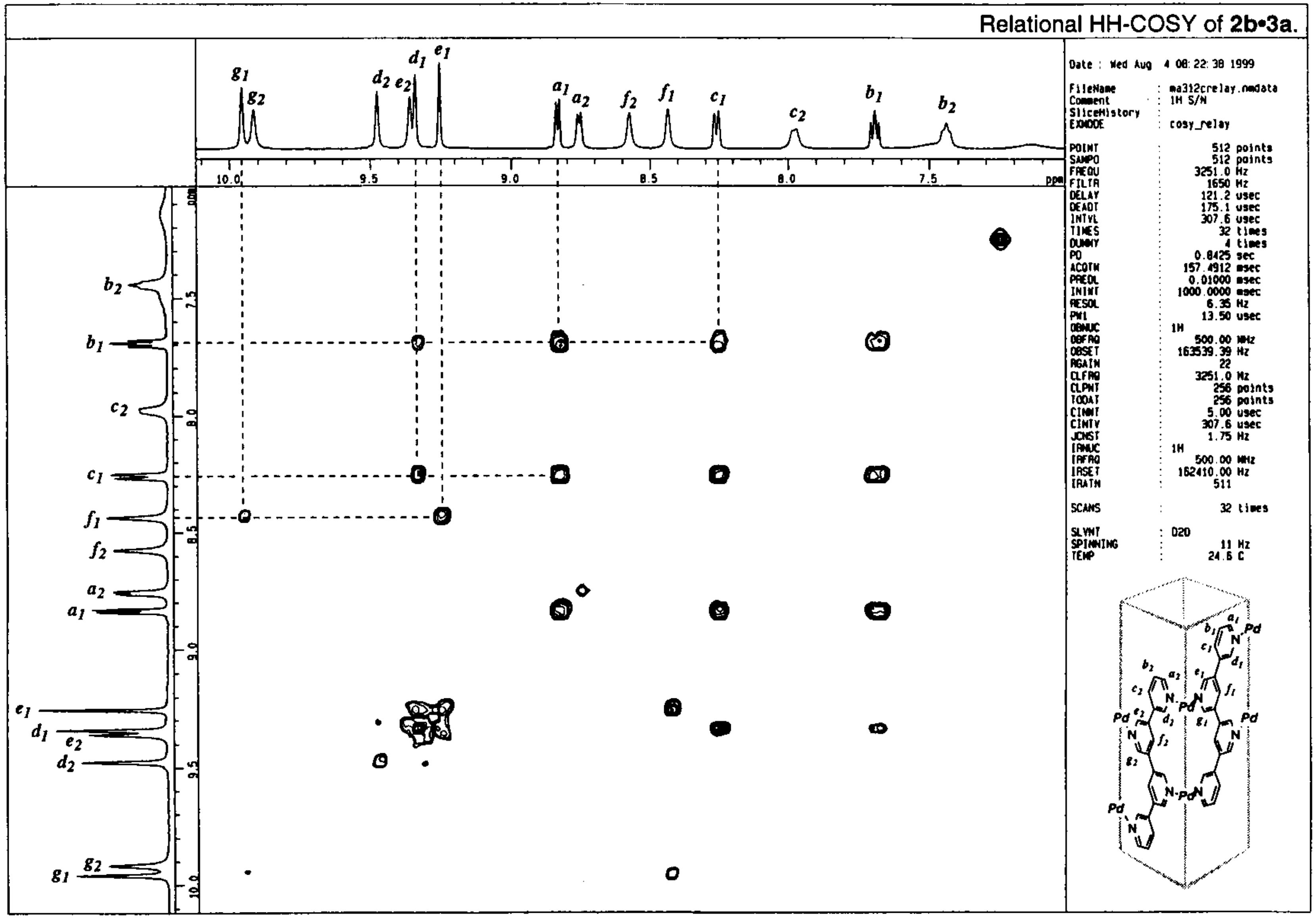
Relational HH-COSY of 2b•3a.
g1 g2 d2 e2 d1 e1 a1 a2 f2 f1 c1 c2 b1 b2
10.0 9.5 9.0 8.5 8.0 7.5 ppm
Date : Wed Aug 4 08:22:38 1999
FileName : ma312crelay.nmdata
Comment : 1H S/N
SliceHistory :
EXMODE : cosy_relay
POINT : 512 points
SAMPO : 512 points
FREQU : 3251.0 Hz
FILTR : 1650 Hz
DELAY : 121.2 usec
DEADT : 175.1 usec
INTVL : 307.6 usec
TIMES : 32 times
DUMMY : 4 times
PD : 0.8425 sec
ACQTM : 157.4912 msec
PREDL : 0.01000 msec
INIWT : 1000.0000 msec
RESOL : 6.35 Hz
PW1 : 13.50 usec
OBNUC : 1H
OBFRQ : 500.00 MHz
OBSET : 163539.39 Hz
RGAIN : 22
CLFRQ : 3251.0 Hz
CLPNT : 256 points
TODAT : 256 points
CINWT : 5.00 usec
CINTV : 307.6 usec
JCNST : 1.75 Hz
IRNUC : 1H
IRFRQ : 500.00 MHz
IRSET : 162410.00 Hz
IRATN : 511
SCANS : 32 times
SLVNT : D2O
SPINNING : 11 Hz
TEMP : 24.6 C
Pd
N

NOESY of **2b•3a.**

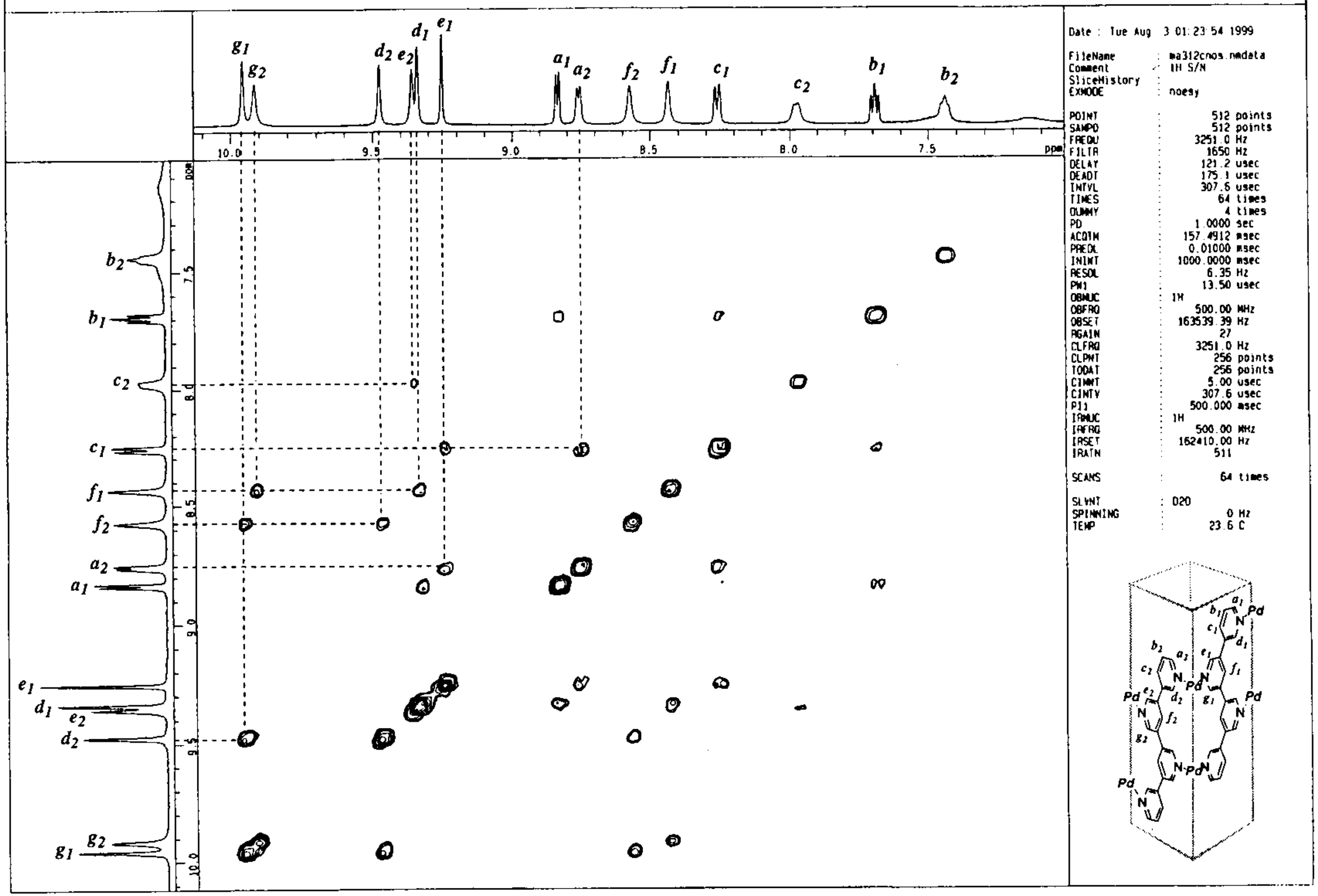

HH-COSY of **2c•3b**.

Solvent: D2O
Ambient temperature.
INOVA-500 "varian2"
PULSE SEQUENCE: relayh
Relax. delay 1.000 sec
COSY 90-90
Acq. time 0.159 sec
Width 3212.5 Hz
2D Width 3212.5 Hz
128 repetitions
256 increments
OBSERVE H1, 500.1472037 MHz
DATA PROCESSING
Sine bell 0.080 sec
F1 DATA PROCESSING
Sine bell 0.040 sec
FT size 1024 x 1024
Total time 10.9 hours

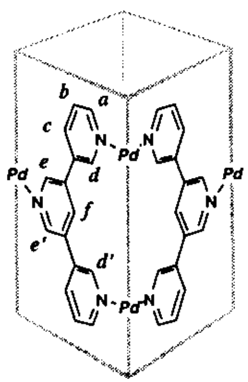

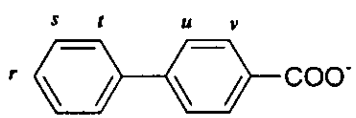

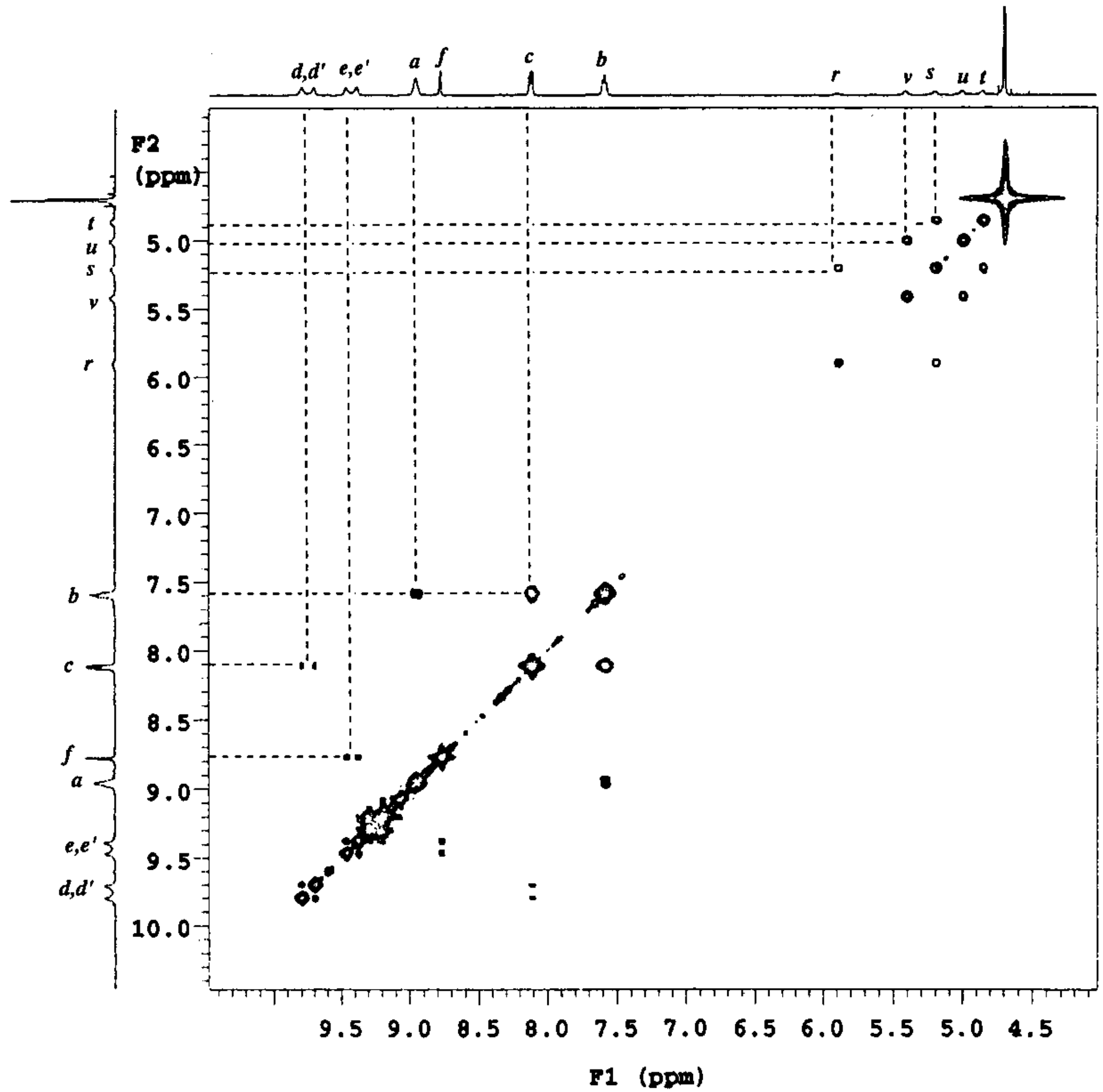

CH-COSY of **2c•3b**.

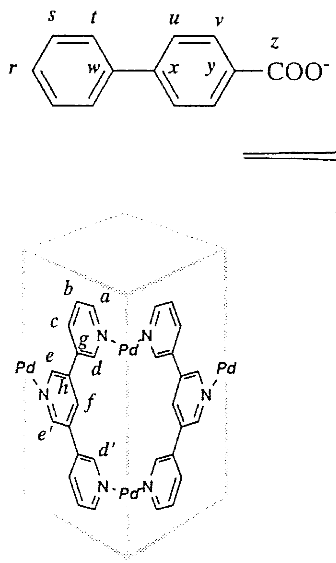

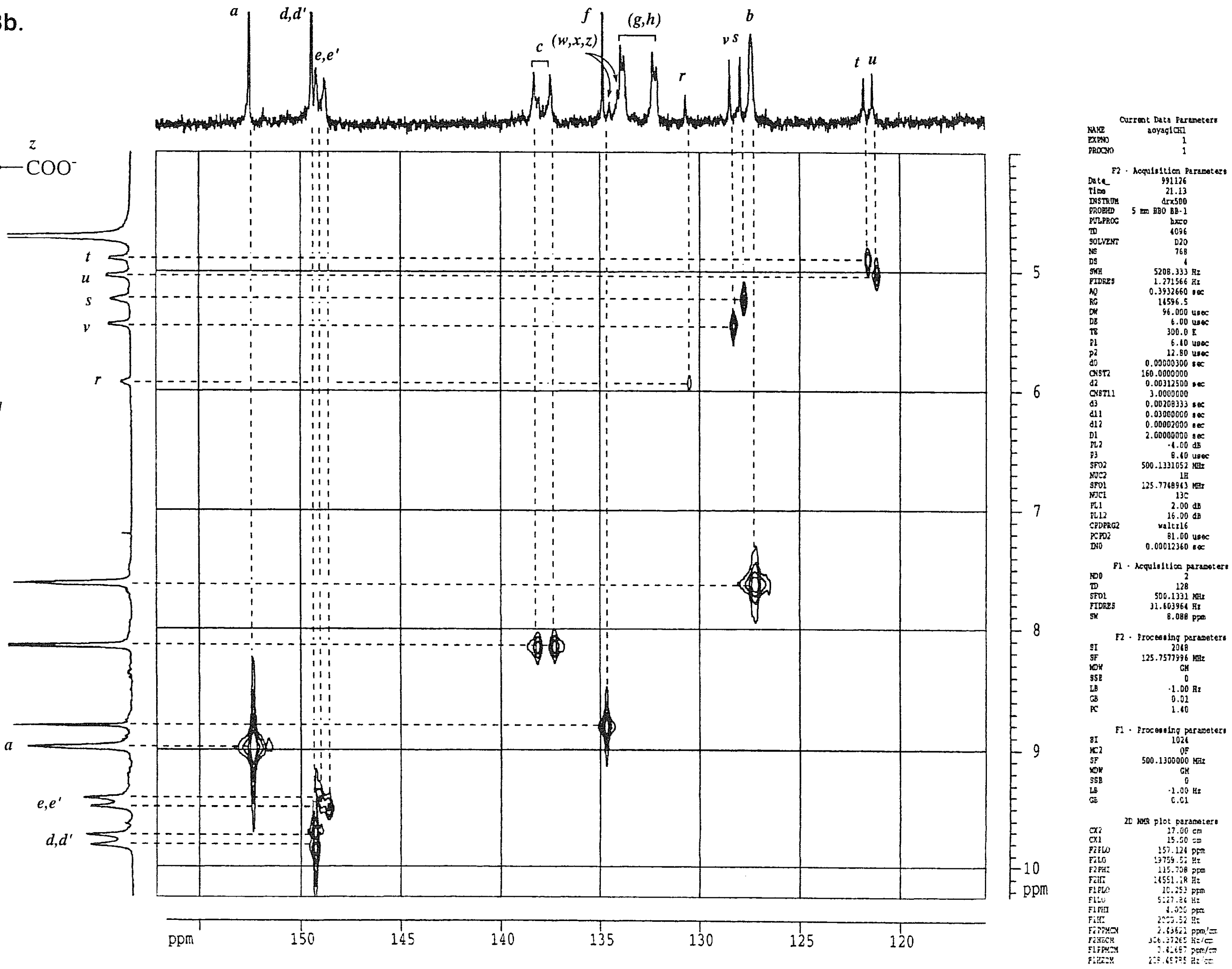

VT ^{1}H NMR of **2c•3b.**

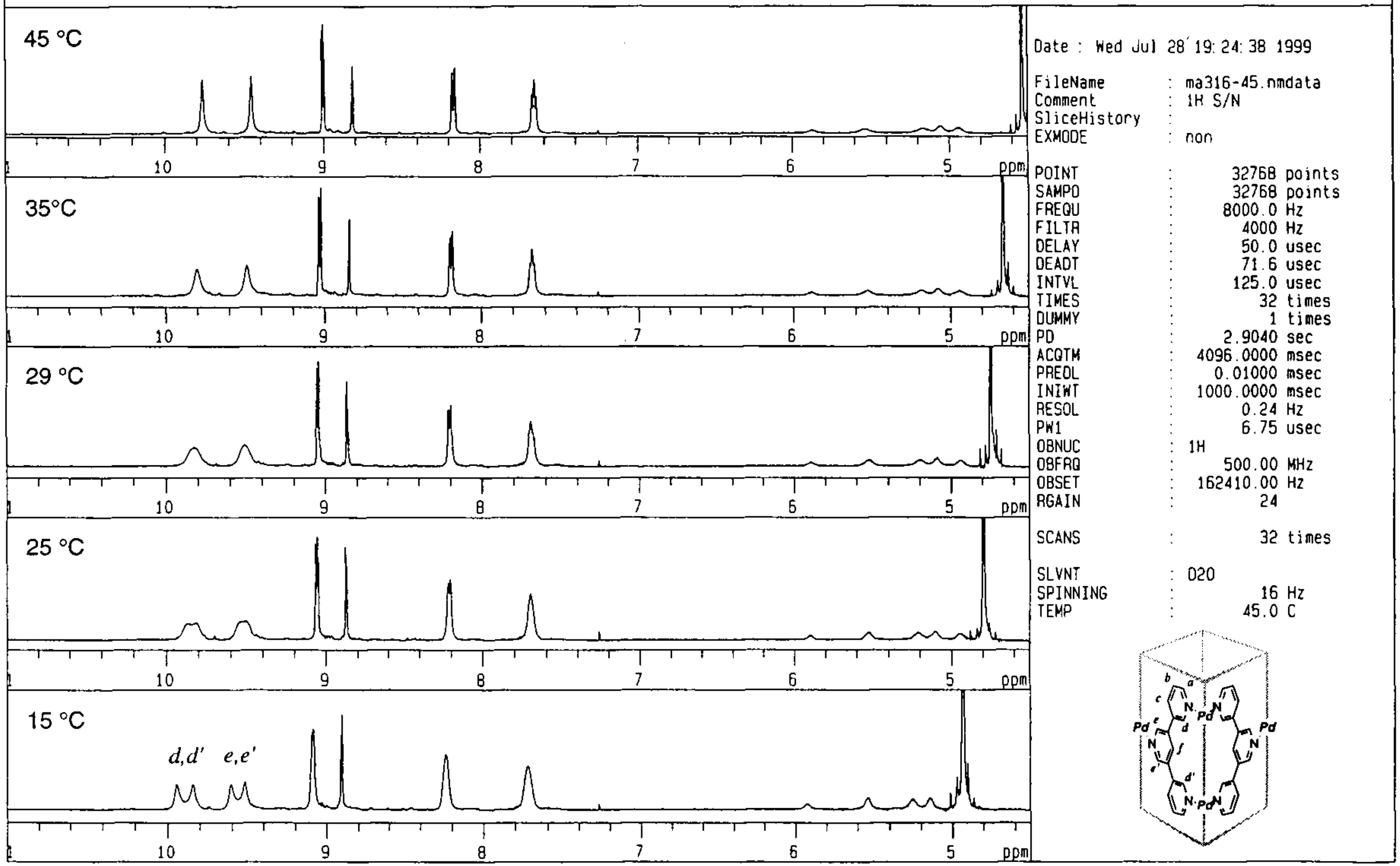

List of Publications

1) Fujita, M.; Aoyagi, M.; Ogura, K. "*Macro cyclic dinuclear complexes self-assembled from (en)Pd(NO_3)$_2$ and pyridine-based bridging ligands*" *Inorg. Chem. Acta* **1996**, *246*, 53- 57.

2) Fujita, M.; Aoyagi, M.; Ibukuro, F.; Ogura, K.; Yamaguchi, K. "*Made-to-Order Assembling of [2]Catenanes from Palladium(II)-Linked Rectangular Molecular Boxes*" *J. Am. Chem. Soc.* **1998**, *120*, 611-612.

3) Fujita, M.; Aoyagi, M.; Ogura, K. "*Coordination Polymers Self-Assembling from Cadmium(II) Ion and Flexible Pyridine-Based Bridging Ligands*" *Bull. Chem. Soc. J.* **1998**, *71*, 1799-1804.

4) Aoyagi, M.; Biradha, K.; Fujita, M. "*Quantitative Formation of Coordination Nanotubes Templated by Rod-like Guests*" *J. Am. Chem. Soc.* **1999**, *121*, 7457-7458.

5) Aoyagi, M; Biradha, K.; Fujita, M. "*Pd(II) and Pt(II)-linked Tetranuclear Complex as an Assembly Unit into Higher Ordered Structures*" *Bull. Chem. Soc. J.* **1999**, *72*, 2603-2606.

6) Kasai, K.; Aoyagi, M.; Fujita, M.; Yamaguchi, K. "*Flexible Coordination Networks with Fluorinated Backbornes. Remarkable Ability for Induced-Fit Enclathration of Organic Molecules*" *J. Am. Chem. Soc.* **2000**, *122*, 2140-2141.

7) Biradha, K.; Aoyagi, M.; Fujita, M. "*Coordination Polytubes with the Affinity for Guest Inclusion*" *J. Am. Chem. Soc.* **2000**, *122*, 2397-2398.

8) Aoyagi, M; Biradha, K.; Fujita, M. "*Formation of Two, One, and Zero-Dimensional Coordination Assemblies from Cd(II) Ion and 4,4'-Bipyridine*" *Bull. Chem. Soc. J.* in press.

Acknowledgment

The present author is sincerely grateful to his supervisor, Professor Makoto Fujita of Nagoya University, for his valuable discussion, useful suggestion, and encouragement throughout this study. He is grateful to Dr. Takahiro Kusukawa of Nagoya University for his help and useful suggestion. He is also grateful to Professor Koji Tanaka of Institute for Molecular Science for his continuing interest and encouragement.

He is indebted to Dr. Kumar Biradha of Nagoya University who supported the present study. Thanks are due to Professor Kentaro Yamaguchi and Mr. Shigeru Sakamoto of Chiba University for the mass spectrum analyses, and Ms. Sachiyo Nomura of Institute for Molecular Science for the micro analyses.

He thanks all the members of Coordination Chemistry Laboratories at Institute for Molecular Science and Prodessor Fujita's laboratory of Nagoya University for their kind encouragement during this study. Finally, he thanks JSPS for financial support.

Masaru Aoyagi

Masaru Aoyagi